LAWRENCE
LIVERMORE
NATIONAL
LABORATORY

UCRL-TR-224558

Analyses in Support of Z-Pinch IFE and Actinide Transmutation - LLNL Progress Report for FY-06

W. R. Meier, R. W. Moir

September 20, 2006

This work was performed under the auspices of the U.S. Department of Energy by University of California, Lawrence Livermore National Laboratory under Contract W-7405-Eng-48.

UCRL-TR-xxxxxx

Analyses in Support of Z-Pinch IFE and Actinide Transmutation - LLNL Progress Report for FY-06

W.R. Meier, R.W. Moir, R.P. Abbott

September 19, 2006

This work was performed under the auspices of the U.S. Department of Energy by University of California, Lawrence Livermore National Laboratory under Contract W-7405-ENG-48.

Contents

1. Introduction

This report documents results of LLNL's work in support of two studies being conducted by Sandia National Laboratories (SNL): the development of the Z-pinch driven inertial fusion energy (Z-IFE), and the use of Z-pinch driven inertial fusion as a neutron source to destroy actinides from fission reactor spent fuel.[1,2]

LLNL's efforts in FY06 included:

- Development of a systems code for Z-IFE and use of the code to examine the operating parameter space in terms of design variables such as the Z-pinch driver energy, the chamber pulse repetition rate, the number of chambers making up the power plant, and the total net electric power of the plant. This is covered in Section 3 with full documentation of the model in Appendix A.
- Continued development of innovative concepts for the design and operation of the recyclable transmission line (RTL) and chamber for Z-IFE. The work, which builds on our FY04 and FY05 contributions,[3-5] emphasizes design features that are likely to lead to a more attractive power plant including: liquid jets to protect all structures from direct exposure to neutrons, rapid insertion of the RTL to maximize the potential chamber rep-rate, and use of cast flibe for the RTL to reduce recycling and remanufacturing costs and power needs. See Section 4 and Appendix B.
- Description of potential figures of merit (FOMs) for actinide transmutation technologies and a discussion of how these FOMs apply and can be used in the ongoing evaluation of the Z-pinch actinide burner, referred to as the In-Zinerator. See Section 5.
- A critique of, and suggested improvements to, the In-Zinerator chamber design in response to the SNL design team's request for feedback on its preliminary design. This is covered in Section 6.

A summary of findings and conclusions is given in Section 2. References are given at the end of each section.

References for Section 1

1. C. Olson et al., "Development Path for Z-Pinch IFE," *Fusion Science and Technology*, **47** 633-640 (2005).
2. B.B. Cipiti, "Fusion Transmutation of Waste and the Role of the In-Zinerator in the Nuclear Fuel Cycle," SAND2006-3522, June 2006
3. W.R. Meier, R.P. Abbott, J.F. Latkowski, R.W. Moir, S. Reyes, R.C. Schmitt, **"**Analyses in Support of ZIFE: LLNL Progress Report for FY-04," LLNL Report UCRL-TR-207101 (Sept. 2004).
4. R.W. Moir, R.P. Abbott, J.F. Latkowski, W.R. Meier, S. Reyes, "Analyses in Support of Z-IFE LLNL Progress Report for FY-05," LLNL Report UCRL-TR-216327 (Sept. 2005).
5. W.R. Meier, R.C. Schmitt, R.P. Abbott, J.F. Latkowski, S. Reyes, "Nuclear Design Considerations for Z-IFE Chambers, Fusion Engineering and Design, **81**, 1661 (2006).

2. Summary of Findings and Conclusions

Systems Modeling for Z-IFE

An update and more comprehensive systems model for a Z-IFE electric power plant was completed this year. The code is written is Mathcad®, which makes it easy to read and easy for even novice users to exercise. The complete model is given in Appendix A. All assumptions and the bases for the physics, engineering and cost scaling relationships are documented in the code and are given in Appendix A. The results of our analyses with this more detailed Z-IFE power plant systems code confirm and quantify previous findings.[1,2] The key conclusion is the that Z-IFE power plant configurations with few chambers (perhaps 1-3) operating at as high a pulse rate at possible (perhaps up to 0.5 Hz) have the most attractive economics in terms of COE. The COE for the single chamber plant operating at 0.5 Hz is slightly better than the most recent result for laser-driven IFE.[3] As with all fusion systems, plants with larger total net electric power, e.g., 2 GWe instead of the nominal 1 GWe, are more competitive. We note that this Z-IFE systems code is a "first generation" model and as such would benefit for careful critique and further refinement. In particular, a more detailed and documented cost and performance model is needed for the driver. The code should also be updated as progress is made and new information is developed on target performance. Finally, a future version should examine the impact of fast ignition targets, which could significantly reduce the driver energy (and associated cost) needed to achieve the very high target yields that are compatible with the inherently low rep-rate and desire to minimize the number of chambers for a given net electric power.

RTL and Chamber Design Progress for Z-IFE

Design alternatives are suggested to improve feasibility and economics of the Z-IFE power plant. The work in this area focused on redesign of the RTL and its injection system to address issue with the previous version. A solid RTL made of frozen flibe greatly eases its recycle and lowers its cost. We developed a new method of providing liquid jet shielding directly above the RTL that eliminates the need for solid shielding, which can have a significant energy cost. Pulsed injection of liquid above the RTL protects the upper chamber structures so that from the point of view of neutron damage these structures could be considered life of the plant components. All structures are protected by 1 m of flibe equivalent. A time motion study results in an estimated 1.9 s between pulses. This rapid pulse rate should improve economics by allowing one chamber and one driver to power the entire plant rather than needing up to ten chambers and ten power supplies for the same total power. The chamber is kept under vacuum during the operation so as to keep non-condensable gases in the transmission line and RTL below the limiting value that will short out the transmission line. We recommend against tungsten for the high-Z components in the target in order to ease recovery and recycle and lower cost. The chamber material is steel. Carbon composite materials, while not practical today, might be developed in the foreseeable future allowing much higher operating temperature with its substantially increased efficiency of conversion of thermal energy to electricity or to other uses.

Potential Figures of Merit for Transmutation Technologies

As noted in the introduction, several figures of merit (FOM) that can be use to evaluate the performance and attractiveness of a Z-pinch based fusion reactor for actinide transmutation are discussed. Section 5 is LLNL's contribution to SNL's progress report on the study of actinide transmutation in the Z-pinch fusion device called the In-Zinerator.[4] The list of potential FOMs (or so called comparative measures) is taken from a National Academies study[5] that compared several non-fusion-based transmutation technologies. They include:

1) Rate and time for various percentage reductions in the transuranic (TRU) inventory
2) Flexibility and rate for reducing key fission product inventories
3) Safety issues for the reactor, fuel materials, and supporting fuel cycle
4) Development time, cost, feasibility, and risk through complete demonstration
5) Estimated time scale and costs for complete deployment, including overall fuel cycle economics; and
6) Comparative thermal and electrical efficiencies per net amount of waste transmuted.

In Section 5, each potential FOM is discussed in terms of its applicability to the In-Zinerator. At this point in the development of the concept, transmutation rates (1 and 2) and efficiencies (6) can easily be determined from the neutronics and plant design studies being carried out by SNL and other study team members. Some estimates of the economic aspects can also made. For example, we show that an In-Zinerator that burns the waste from four light water fission reactors (LWR) and also produces electricity itself, can cost up to 50% more than an LWR and only increase the COE by 10%.

Suggested Improvements and Calculations for the In-Zinerator

The In-Zinerator conceptual design is still preliminary and several critical issues remain to be addressed in continued R&D. In Section 6, we note several issues and propose design modifications to improve the current design. In particular, we recommend the use of a wetted-wall chamber design (instead of a gas-protected dry-wall) to protect the first structural wall from x-rays, ions and hopefully target debris. The thermal stress in the 5-cm-thick first wall is ~ 120 MPa if cooled from only one side, which is high but likely acceptable. It can be reduced by two-sided cooling (i.e., using a wetted wall) and/or by providing internal cooling channels or subdividing the wall with a cooling channel between the layers. We also propose a redesign of the RTL insertion region that provides liquid protection and tritium breeding at the top of the chapter; the current design has none. The concept of using liquid jets above the incoming RTL is developed fully in Section 4, our work on Z-IFE. We also propose adding a pool at the bottom for better neutron economy. We note that pulse heating and the resulting isochoric pressure pulse ($\Delta T \sim 1000k$, P = 4.8 GPa) in the actinide blanket present significant design challenges.

References for Section 2

1. W.R. Meier, R.P. Abbott, J.F. Latkowski, R.W. Moir, S. Reyes, R.C. Schmitt, **"**Analyses in Support of ZIFE: LLNL Progress Report for FY-04," LLNL Report UCRL-TR-207101 (Sept. 2004).

2. R.W. Moir, R.P. Abbott, J.F. Latkowski, W.R. Meier, S. Reyes, "Analyses in Support of Z-IFE LLNL Progress Report for FY-05," LLNL Report UCRL-TR-216327 (Sept. 2005).
3. W.R. Meier, "Systems Modeling and Analyses – Progress Update and Recent Results," HAPL Project Meeting (ORNL, March 21-22, 2006), LLNL document UCRL-PRES-219894.
4. B.B. Cipiti, "Fusion Transmutation of Waste and the Role of the In-Zinerator in the Nuclear Fuel Cycle," SAND2006-3522, June 2006.
5. *Nuclear Wastes: Technologies for Separations and Transmutation*, National Academy Press, Washington DC, ISBN: 0-309-56195-7 (1996).

3. Systems Modeling for Z-IFE

3.1 Introduction

An update and more comprehensive systems model for a Z-IFE electric power plant was completed this year. The code is written is Mathcad®, which makes it easy to read and easy for even novice users to exercise. The complete model is given in Appendix A. All assumptions and the bases for the physics, engineering and cost scaling relationships are documented in the code and are not reproduced in detail as part of this text. Many example results in the form of graphs and tables are also given in Appendix A. In this section, we highlight some of the key assumptions and present important results and findings.

3.2 Target Gain and Yield

A fundamental relationship for any IFE concept is the target gain as a function of driver energy. For Z-IFE this relationship was determined based on reported results for target yield for the dynamic hohlraum.[1,2] Figure 3.1 shows the target yield as a function of the z-pinch energy, i.e., the energy delivered to the pinch.

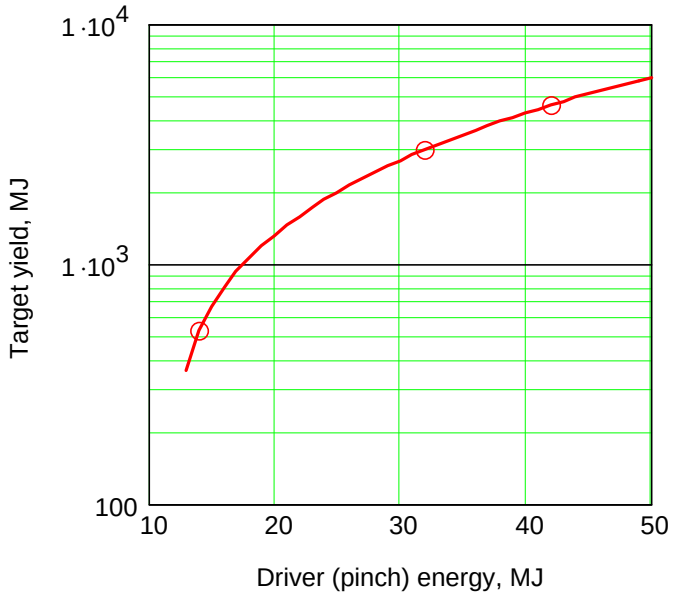

Figure 3.1: Target yield versus driver energy.
Fit through three calculated cases is shown.

The fit through the three reported cases was used to determine the target gain versus driver energy as

$$G = 30.15 \cdot (E-12.2)^{0.38} .$$

This is plotted in Fig. 3.2.

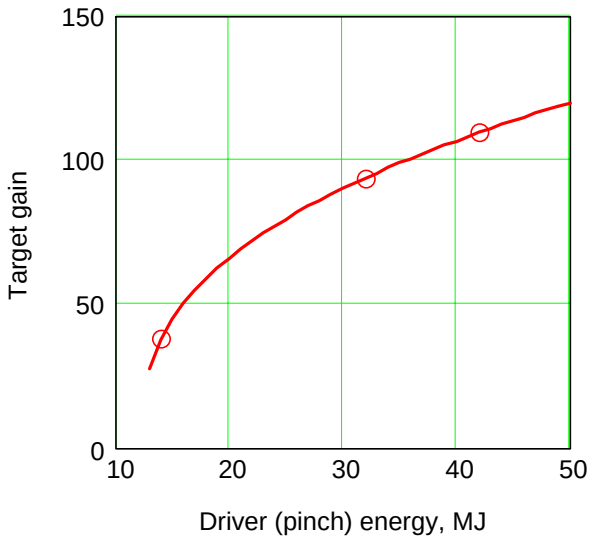

Fig. 3.2: Dynamic hohlraum target gain versus driver energy

3.3 Driver Efficiency and Cost

The Z-IFE systems code does not have a detailed model for the pulsed power driver. At this point the driver cost is simply given as the product of the energy delivered to the pinch (J) times a unit cost expressed in $/J. The driver unit cost is a variable in the cost of electricity calculation, so the user may examine the sensitivity of the results to driver cost. At the time of this report, we had not received a good unit cost estimate, but have taken $15/J as the reference case value. This is based on statements by SNL researchers that current pulsed power machines cost ~$30/J and the linear transformer driver (LTD) should be a factor of two lower. The driver efficiency is assumed to be 60% based on material presented at the August 2005 Z-IFE workshop for the LTD.[3]

3.4 Chamber and Power Plant

The cost scaling relationship for the chamber and power plant are based on the thick liquid wall chamber using flibe as the working fluid. The chamber is costed on a $/J of structure basis. Two options are given: a chamber in the geometry of a flattened ellipsoid (original SNL design) and the more cylindrical chamber developed by LLNL and reported in FY05. The based case structure is low activation ferritic steel, but the code includes the option to use carbon-carbon composite for chamber structures, a high performance option proposed by LLNL.

The balance of plant facilities and equipment models are based on the Osiris cost scaling relationships, but escalated from 1991 dollars to 2005 dollars.[4,5] Many of the Osiris models were based on previous design studies and for the most part are consistent with those used for HYLIFE-II.[6] The plant power conversion efficiency (total thermal to gross electric) is 42% for the steel chamber and 50% for the carbon-composite chamber.

An important design variable in the systems model is the number of chambers in the power plant. The original SNL reference design for a Z-IFE power plant consisted of ten chambers each producing ~100 MWe net power for a total plant power of ~1000 MWe, a typical standard power for this type of study. Our previous preliminary economic systems analyses indicated that power plant with many small chambers is not competitive with a plant with fewer chambers operating at higher yield and pulse repetition rate (rep-rate). As shown in the following results, those preliminary findings are confirmed and better quantified by this year's work.

Consistent previous SNL conceptual designs, we assume that each chamber has an independent driver, heat transfer system and power conversion system. Only the heat rejection system (e.g., cooling towers) is shared in chamber plants.

3.5 RTL and Target Factory

The cost and power consumption of the factory needed to produce the recyclable transmission lines (RTLs) was developed and reported by SNL for two cases: steel RTLs and RTLs made of flibe.[7] The systems code includes options for both cases, but due to the significant cost and power advantages of using cast flibe RTLs, flibe is the base case in our analyses.

We also account for the cost of the fuel capsule and hohlraum that must be mated to the RTL. The capsule cost and cost scaling with yield and production rate are based on a detailed study completed by General Atomics for direct-drive laser IFE.[8] To account for the added cost of the dynamic hohlraum components of the target, the capsule factory cost is simply doubled. That is, the Z-IFE capsule plus hohlraum is twice the cost of laser IFE capsule (for a given yield).

We assume that the RTL and target factories service the entire power plant, i.e., all chambers.

3.6 Total Capital Cost and Cost of Electricity

The total capital cost of the Z-IFE power plant is calculated from the sum of the direct capital costs of the driver, chamber, balance of plant, RTL and target factory using in indirect costs equal to 93.6% of the total direct capital cost. Annual capital charges are based on a fixed charge rate of 9.66%. These capital cost factors are consistent with other fusion economic studies. Annual operation and maintenance costs are included for the power plant and target factory. The cost of electricity (COE) is then the sum annual costs divided by the annual net energy produced. The net energy is the produce of the plant net electric power time the hours of operation per year (plant capacity factor = 85%). The net electric power is equal to the gross electric power produced minus the power recirculated to 1) the driver, 2) the RTL factory, 3) plant pumping for creating the thick liquid wall and for the heat transfer system, and 4) other auxiliary power requirements (taken as 4% of the gross electric power). See Appendix A for more details on the COE calculation.

3.7 Key Results

Several key results of the systems analyses are given below. The basic plant design variables are the driver energy, chamber rep-rate, and number of chamber per plant. The net electric power of

the plant can be allowed to vary with these parameters, or more instructively, fixed (e.g., at 1000 MWe) in order to compare plants that deliver the same product.

Figure 3.3 gives the driver energy required to produce a fixed net power of 1000 MWe as a function of the chamber rep-rate. Results are shown for plants consisting of 1, 3, 5 or 10 chambers. Remember this is the driver energy required by each chamber. At a given rep-rate, plants with fewer chambers require higher yield per pulse and thus higher driver energy. Clearly pushing the rep-rate higher than the original SNL base case of 0.1 Hz is attractive if it is technically feasible. In Section 4 of this report, we estimate that a rep-rate of 0.5 Hz might be possible. This is higher than the 0.3 Hz quoted by SNL as a "stretch" case. At 0.5 Hz the single chamber plant require a driver energy of ~ 42 MJ correspond to a target yield of ~4600 MJ.

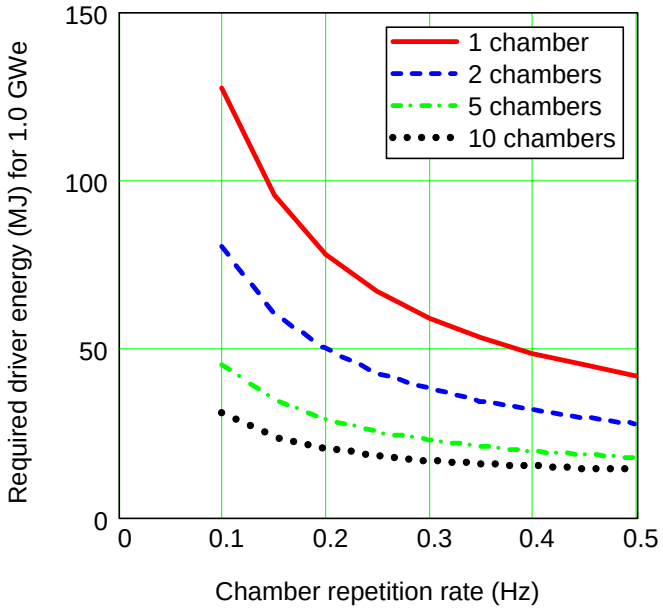

Figure 3.3: Driver energy per chamber required to achieve a net plant power of 1000 MWe versus chamber rep-rate.

The resulting COE as a function chamber rep-rate for 1000 MWe plant with various numbers of chamber is shown in Fig. 3.4. This figure quantifies the economic advantages of configuring the Z-IFE power plant with few chambers and pushing the chamber pulse rate as high as possible. Only the 1 and 3-chamber plants reach a COE less than 10 ¢/kWeh. For comparison, recent MFE and IFE studies quote COEs of 7-9 ¢/kWeh. Even at that it will be hard to compete with advanced fission reactors at 4-6 ¢/kWeh (depending on size). The single chamber Z-IFE plant operating at 0.5 Hz, has a COE of 7.0 ¢/kWeh, roughly the same as the most recent direct-driver laser IFE result of 7.2 ¢/kWeh.[9] The 10 unit, 0.1 Hz plant has a COE of ~20 ¢/kWeh, which is a factor of 2-3 higher than needed to compete with other fusion concepts.

Another way to display these results to show the range of driver energies needed is shown in Figure 3.5. Here we limit the plot range to COEs less than 10 ¢/kWeh and chamber rep-rates less than 0.5 Hz. The single chamber plant needs a driver energy > 42 MJ for a chamber rep-rate < 0.5 Hz, and at 60 MJ, the rep-rate is down to 0.29 Hz. The 3-chamber plant has a chamber rep-rate < 0.5 Hz for driver energies > 22.5 MJ and is down to 0.3 Hz at E ~ 30 MJ. The minimum

COEs occur at 20 MJ for the 1 chamber case and 16 MJ for the 3-chamber plant, but the required rep-rates of 1.8 and 1.0 Hz, respectively, are beyond the reach of the replaceable RTL concept.

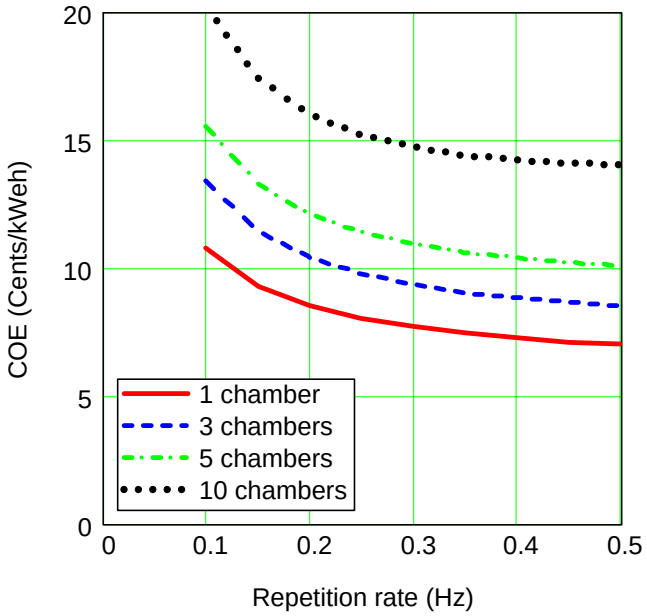

Figure 3.4: COE versus chamber rep-rate for 1000 MWe plants with 1-10 chambers per plant.

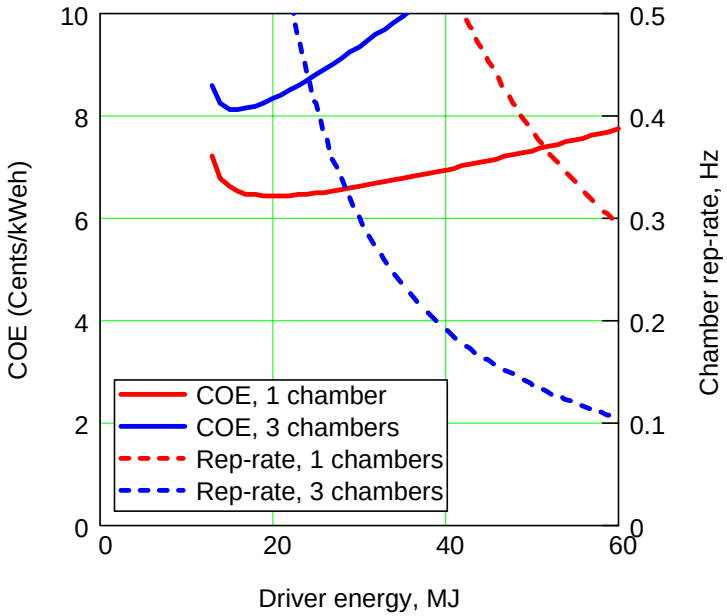

Figure 3.5: COE and chamber rep-rate versus driver energy for 1000 MWe plants with 1 or 3 chambers.

One final result highlights the dependence of the COE on the net electric power of the plant. Figure 3.6 gives the COE as a function of rep-rate for two-chamber power plants with total net powers of 500, 1000 and 2000 MWe. The 500 MWe plant has a COE > 10 ¢/kWeh over the entire range of rep-rates considered (up to 0.5 Hz). The 2000 MWe case shows the favorable economies and benefits of sharing of the single RTL and target factory; the COE is down to 5.7 ¢/kWeh at 0.5 Hz. Note that the COE for the 2-chamber, 1000 MWe case is only 10% higher than for the single-chamber plant discussed previously (i.e., 7.7 ¢/kWeh instead of 7.0 ¢/kWeh at 0.5 Hz).

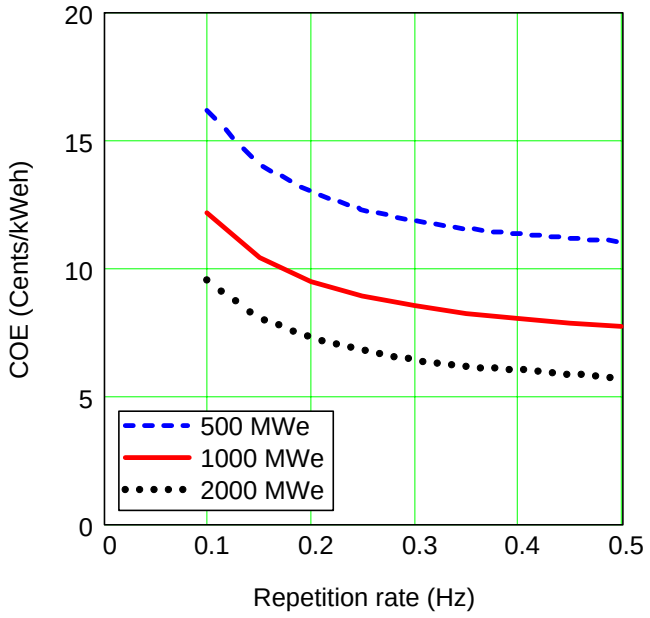

Figure 3.6: COE versus rep-rate for two-chamber plants with various net electric powers.

Note again that there are many additional plots and results reported in Appendix A that not included here in the main text.

3.8 Conclusions and Recommendations

In summary, the results of the more detailed Z-IFE power plant systems code indicate that power plant configurations with few chambers (perhaps 1-3) operating at as high a pulse rate at possible (perhaps up to 0.5 Hz) have the most attractive economics in terms of COE. The COE for the single chamber plant operating at 0.5 Hz is slightly better than the most recent result for laser-driven IFE. We note that this Z-IFE systems code is a "first generation" model and as such would benefit for careful critique and further refinement. In particular, a more detailed and documented cost and performance model is needed for the driver. The code should also be updated as progress is made and new information is developed on target performance. Finally, a future version should examine the impact of fast ignition targets, which could significantly reduce the driver energy (and associated cost) needed to achieve the very high target yields that are compatible with the inherently low rep-rate and desire to minimize the number of chambers for a given net electric power.

References for Section 3

1. C. Olson, "Target Physics Scaling for Z-Pinch Inertial Fusion Energy," *Fusion Science and Technology*, **47** 1147-1151 (2005).
2. R. Vesey, "Multi-GJ Indirect-Drive Targets for Z-IFE Using the Double Ended Hohlraum," Z-IFE Workshop, SNL (Aug. 2005).
3. T. Melhourn, "Overview of Targets for IFE," Z-IFE Workshop, SNL (Aug. 2005).
4. W.R. Meier et al., "OSIRIS and SOMBRERO Inertial Fusion Power Plant Designs," WJSA report WJSA-92-01, DOE/ER/54100-1 (March 1992).
5. W.R. Meier, R. L. Bieri, "Economic Modeling and Parametric Studies for Osiris - An HIF-Driven IFE Power Plant," *Fusion Technol.,* **121,** 1547 (1992).
6. R. W. Moir et al, "HYLIFE-II progress report," LLNL Report UCID-211816 (1991).
7. G. Rochau, "Power Plant Utilizing Z-Pinch Fusion Technology," Z-IFE Workshop, SNL (Aug. 2005)
8. W. Rickman and D. Goodin, "Cost Modeling for Fabrication of Direct Drive Inertial Fusion Energy Targets," *Fusion Science and Technology*, **43**, 353 (2003).
9. W.R. Meier, "Systems Modeling and Analyses – Progress Update and Recent Results," HAPL Project Meeting (ORNL, March 21-22, 2006), LLNL document UCRL-PRES-219894.

4. Recyclable Transmission Line (RTL) and Chamber Design for Z-IFE

4.1 Introduction

This section discusses progress on the third year of contributions by LLNL to the Z-IFE power plant study for Sandia National Laboratory. Sandia has had considerable success delivering pulse power to a load through a coaxial magnetically insulated transmission line (MITL).[1] The goal is to deliver 90 MA at 9 MV to a wire array in ~0.1 μs making 30 MJ of x rays in a few ns to drive an ICF capsule with a yield of 3 GJ (gain = 100) of fusion energy. In the present work we design a chamber that can withstand the effects of this yield and rapidly recover and reload for follow-on shots at pulse rates of approximately 0.5 Hz. This would result in a power of 1 GWe per chamber and its pulse power unit. At LLNL we have considerable experience analyzing and designing similar chambers called HYLIFE-I and II.

4.2 Chamber and RTL Design

The main features of our proposed Z-IFE chamber are shown in Fig. 4.1. The 3.5-m-tall, 2.2-m-diameter (13.3 m^3) pocket protects the chamber walls by containing the x rays and target debris generated by the fusion shot so as to delay their effect on the wall. Note that all structures are protected against neutrons, x rays, and target debris by 1 m of the molten salt flibe, which also serves as the primary coolant and tritium breeder.

The Recyclable Transmission Line (RTL) is made of frozen flibe. It is shown in more detail in Fig. 4.2. This RTL material is frangible meaning it shatters following a shot and quickly becomes part of the coolant. The cost advantages of the frangible flibe RTL compared to that of steel, of the rapid pulse rate of 1.9 s compared to 10 s resulting in only one chamber and power supply needed, and the liquid protection of all structures making them lifetime components should greatly enhance economics.

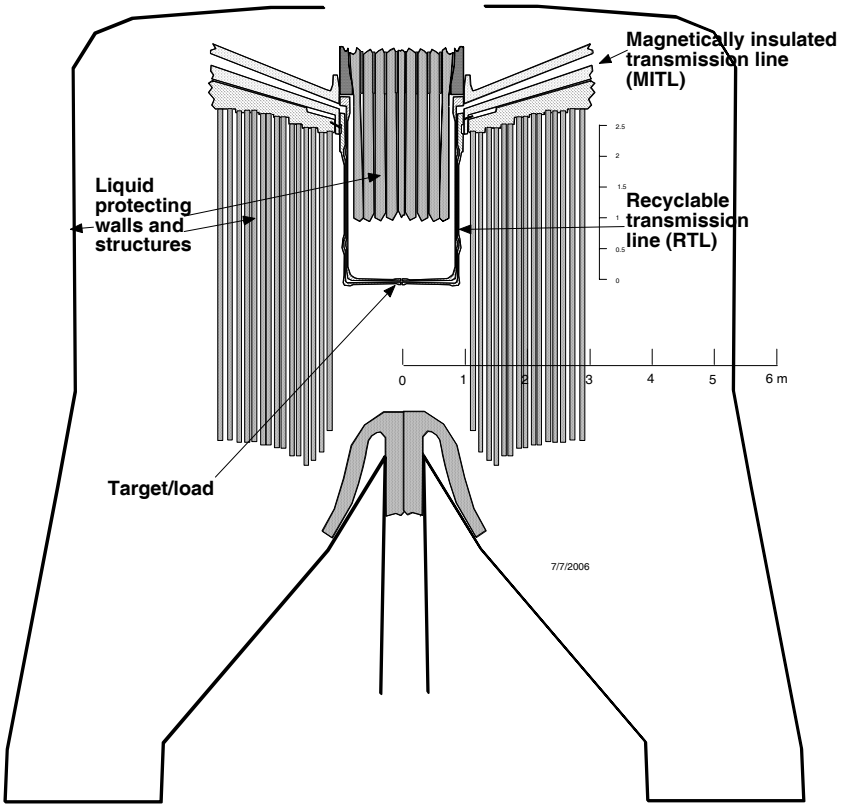

Figure 4.1: The ZIFE chamber and 3 m RTL design are shown With full neutron and blast protection of structures.

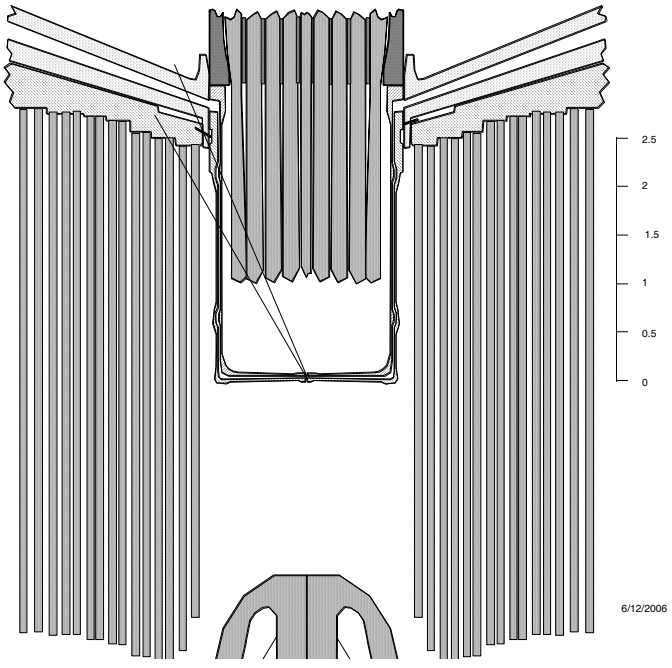

Figure 4.2: The inductance of the RTL is 15 nH out to a radius of 2 m to include some of the MITL.

4.3 Inserter Design

Figure 4.3 shows the 3-m RTL shortly before shot time with the MITL covered and the inner and outer RTL cones still separated. About 0.5 m (0.05 s) before reaching the shot position and shot time, the downward acceleration is increased from 1 g to 2 g's; which is just enough to make the inner cone close the gap to 1.5 mm at the shot position and time as shown in the next figure. The downward acceleration must be increased quickly enough so as to decisively overcome the friction that can hold the two cones together but not so rapidly as to cause the RTL to prematurely shatter. Too slow an application of force will result in jitter in the time and place of closure of the gap. We anticipate being able to measure in real time the gap (possibly by radar techniques) so as to time the pulsed power system to fire when the gap is attained.

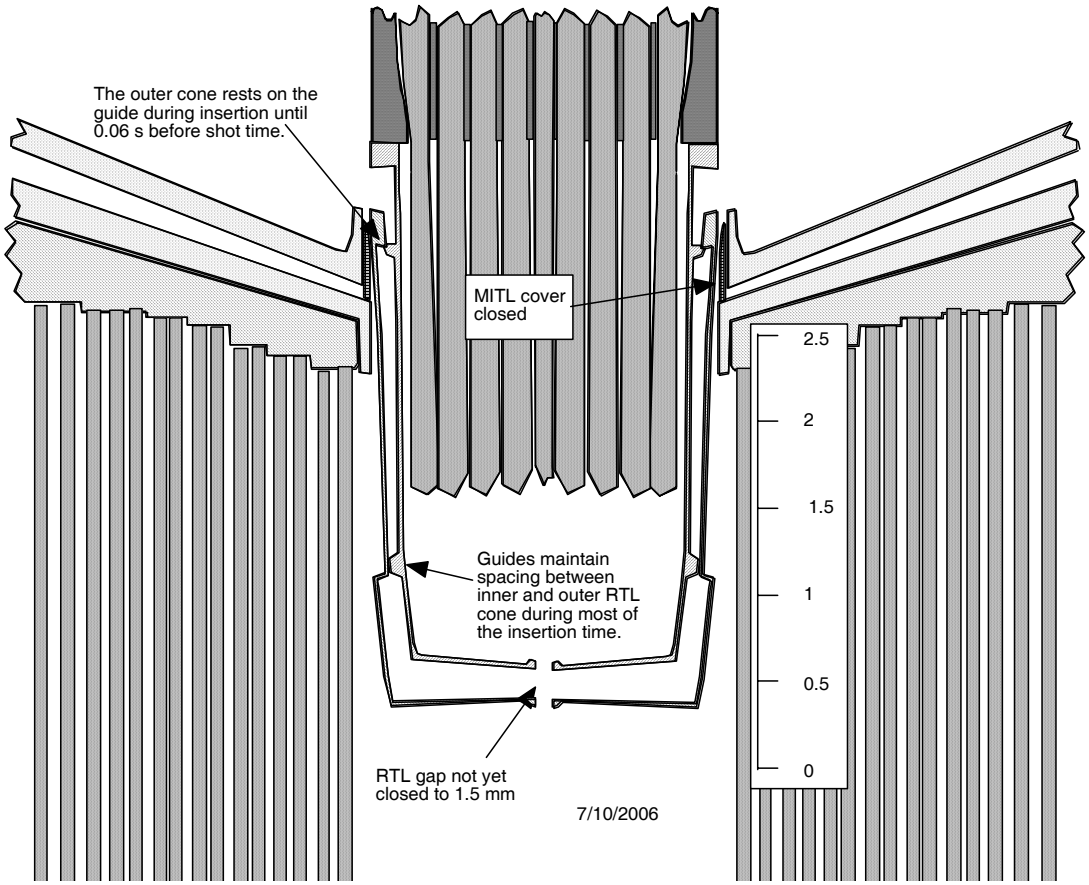

Figure 4.3: The 3 m long recyclable transmission line (RTL) is shown shortly before shot time with its inner and outer cones still separated.

Figure 4.4 shows the RTL at shot time with the MITL uncovered. When the inner and outer RTL separation becomes 1.5 mm at the target/load, the transmission line is triggered. The RTL is traveling downward at 10 m/s and the jets at 15 m/s. The gap in the MITL and RTL varies from 15 mm at r=1 m to 1.5 mm near the target and is shown exaggerated for illustration purposes.

The pressure of the flibe vapor on the outer RTL cone would be 2 Pa at 700 °C (base case) and 5,000 Pa at 1100 °C (high efficiency design). The resulting stress in the walls of the RTL for the 1 mm thick wall case would be 6 kPa for 700 °C and 16 MPa for 1100 °C. The stress for the 700 °C case is negligible. For 1100 °C, the stress could cause failure and thicker walls would likely be needed. In both cases, as discussed in last year's report, the thermal shock is an important design consideration.

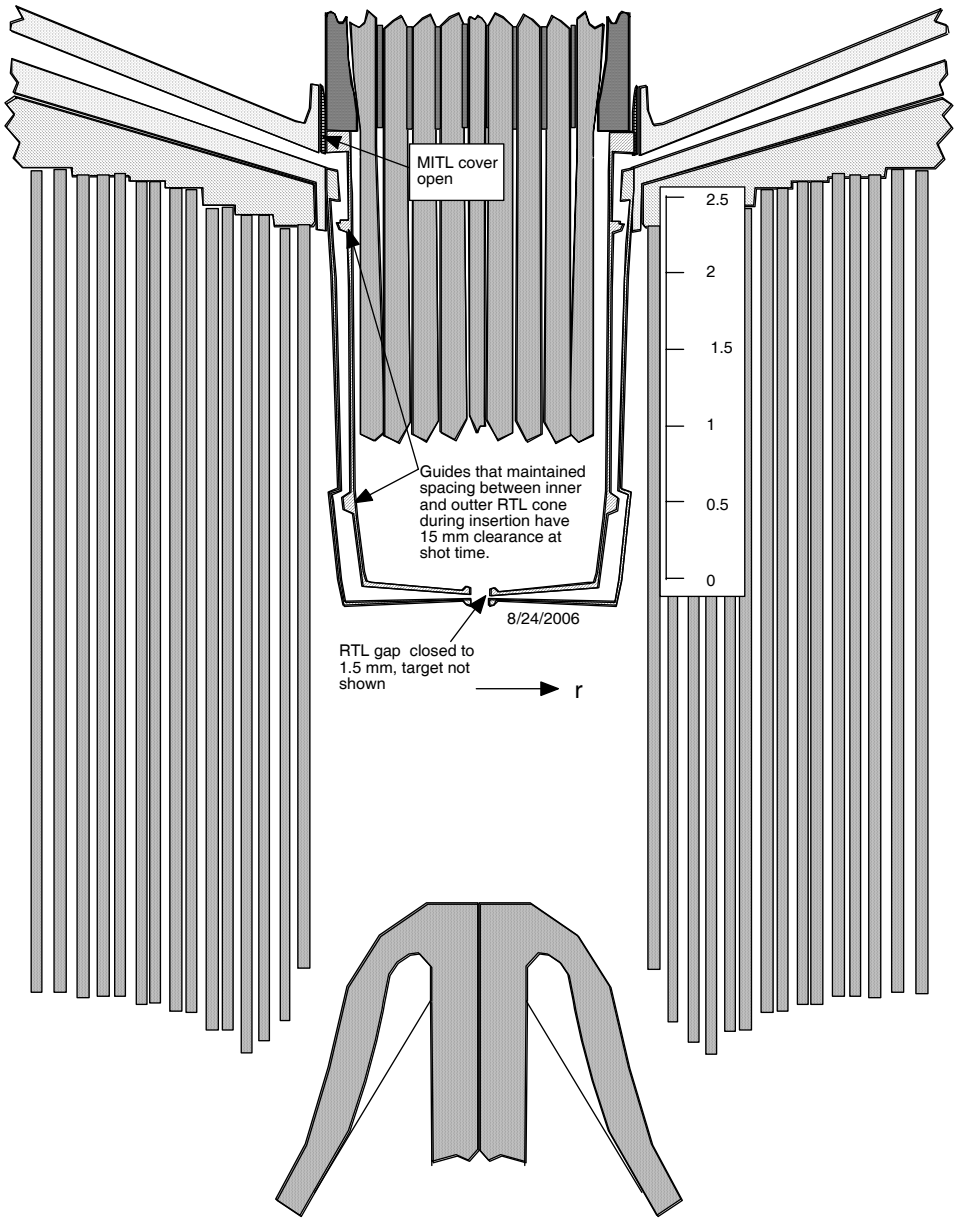

Figure 4.4: RTL at shot time with the MITL uncovered.

Figures 4.1-4.4 show a 2-m-high pulsed column of flibe above the shot. Figure 4.5 shows the design with only 1-m-high column (3 m^3) of flibe. For overcoming upward impulse due to the shot and for neutron protection, 1 m would be quite sufficient and ease injection and filling of the inserter during insertion (see Fig 4.12). The fill time will be about 1 s, which gives a required fill rate of 3 m^3/s. If the flow speed in the fill pipes is kept to a reasonably low 5 m/s then the area of the fill pipes is 0.6 m^2. There would be 76 pipes of 0.1 m diameter, which would represent only a small percentage of the available area on the injection cylinder wall.

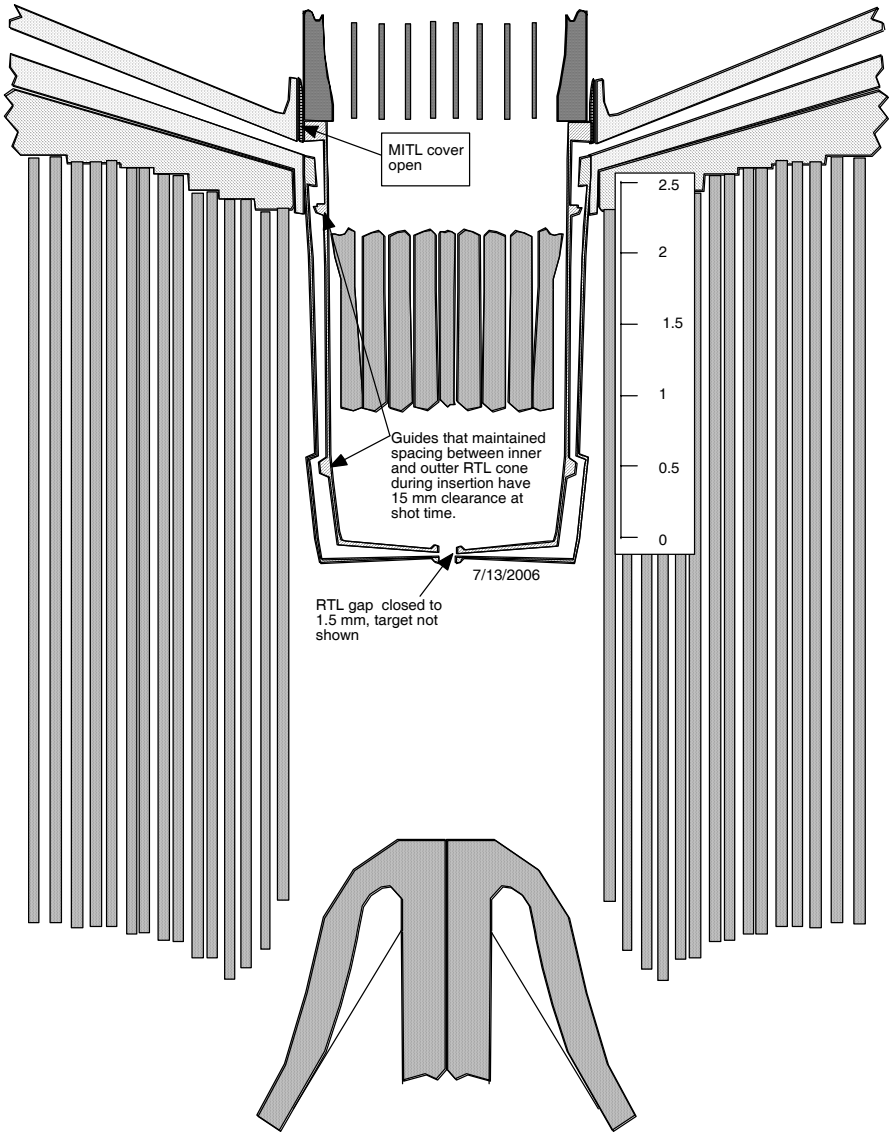

Figure 4.5: The vertical thickness of the pulsed jets above the shot point only needs to be 1 m as shown here rather than the over 2 m shown in prior figures.

4.4 RTL Detail

Details of the RTL are shown in Figs. 4.6 and 4.7. Notice the outer cone in Fig. 4.6 rests on the inner cone and is centered by the inner cone. The outer cone is guided by the injection tube. The estimated mass in the two 1-mm-thick RTL cones is 90 kg plus the thicker regions of 40 kg for a total of 130 kg. A 2-mm-thick RTL set would have a mass of 220 kg.

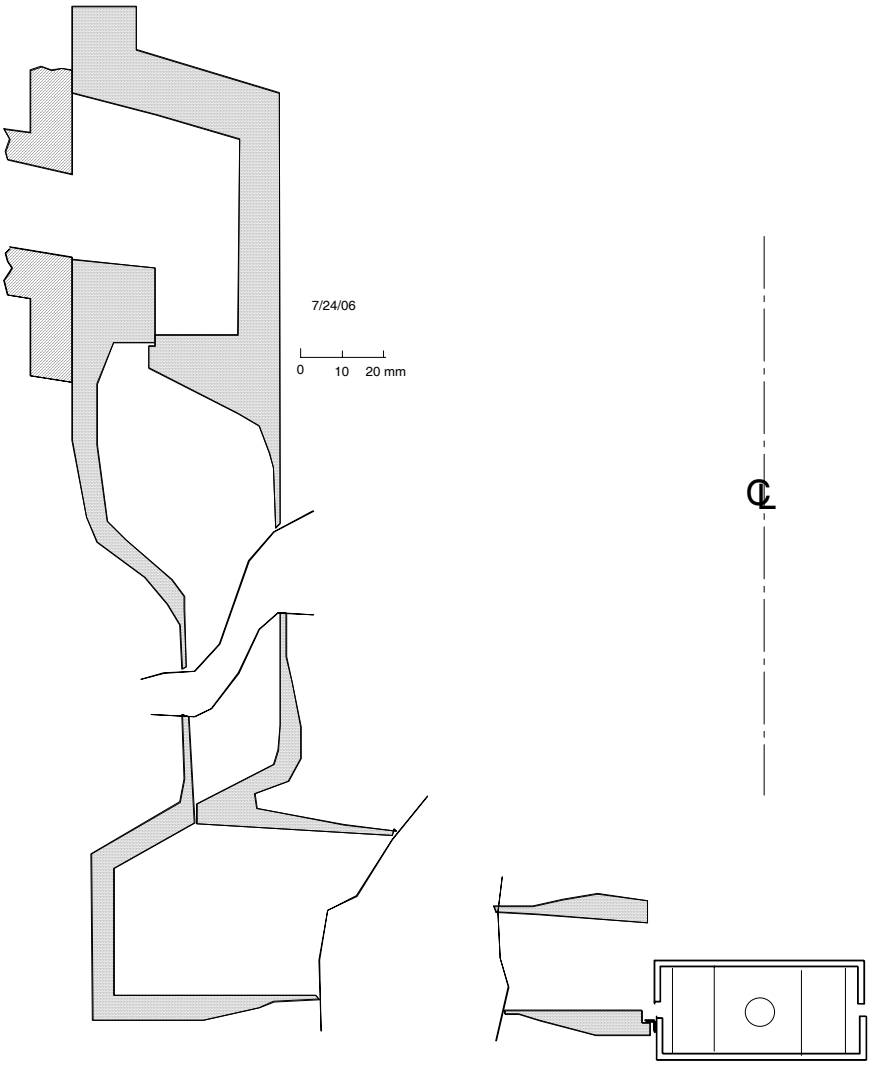

Figure 4.6: RTL before shot during insertion.

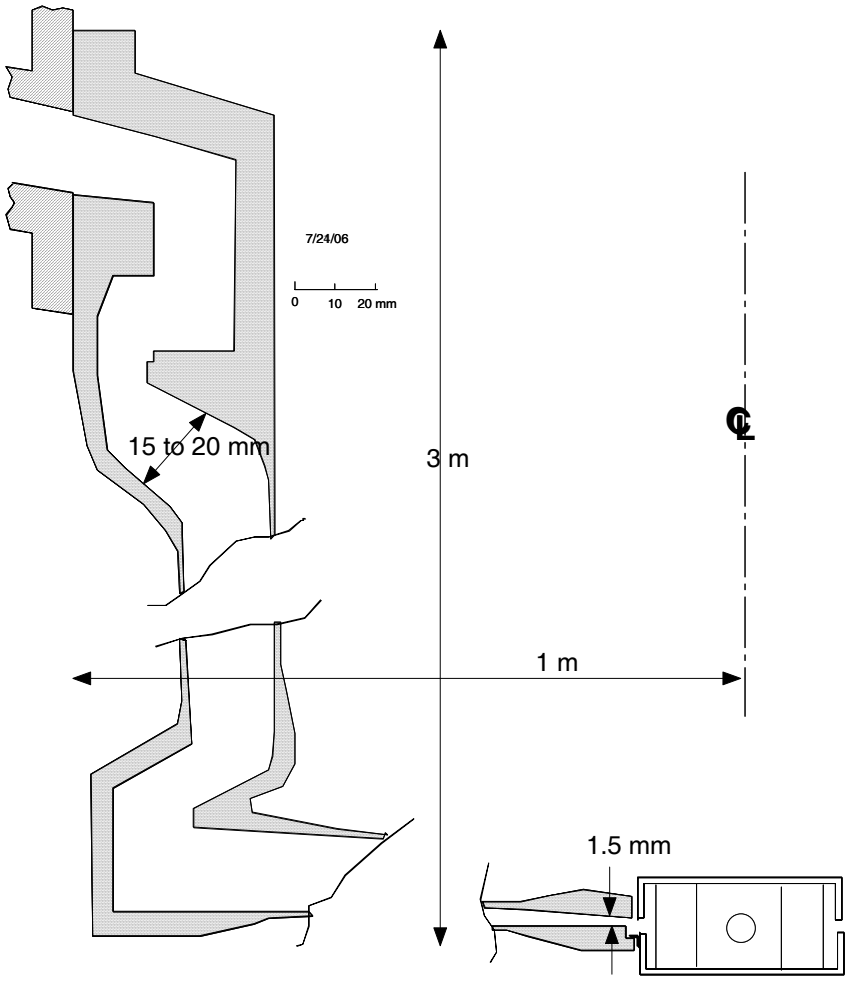

Figure 4.7: RTL at shot time.

4.5 Target Design

The dynamic hohlraum target design is shown schematically in Fig. 4.8. When the current flows in the thin wires a magnetic field is generated that applies a pressure to accelerate the wires as depicted in the sequence shown in Fig. 4.9. The moving wires are accelerated in ~0.1 μs, collide with the foil and thermalize to emit x rays in a few ns. The x rays fill the hohlraum and are absorbed in the capsule filled with D-T. The magnetic field must not be allowed to leak out of the space between the target and the anode because this would greatly increase the inductance and reduce the power delivered to the load. Interlocking fingers could prevent this or a spring like filler material could be used.

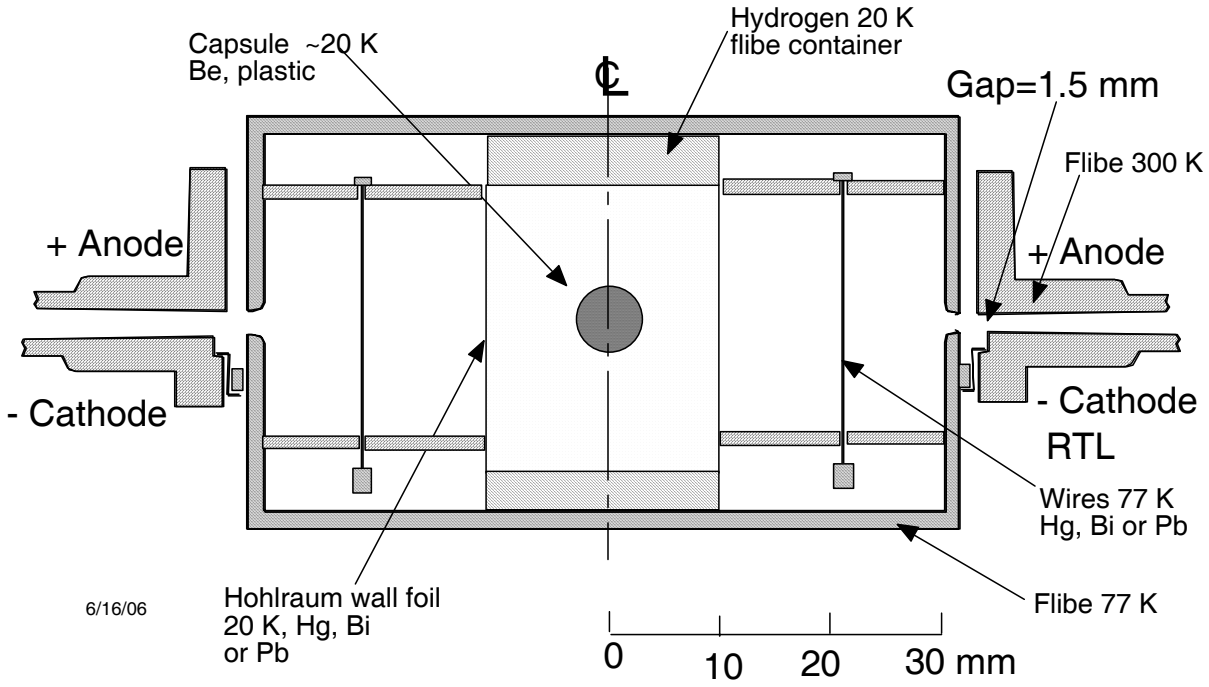

Figure 4.8: Example of targets/loads being studied is the dynamic hohlraum assembly shown attached to the lower RTL cone. The inductance of this target is ~ 2 nH.

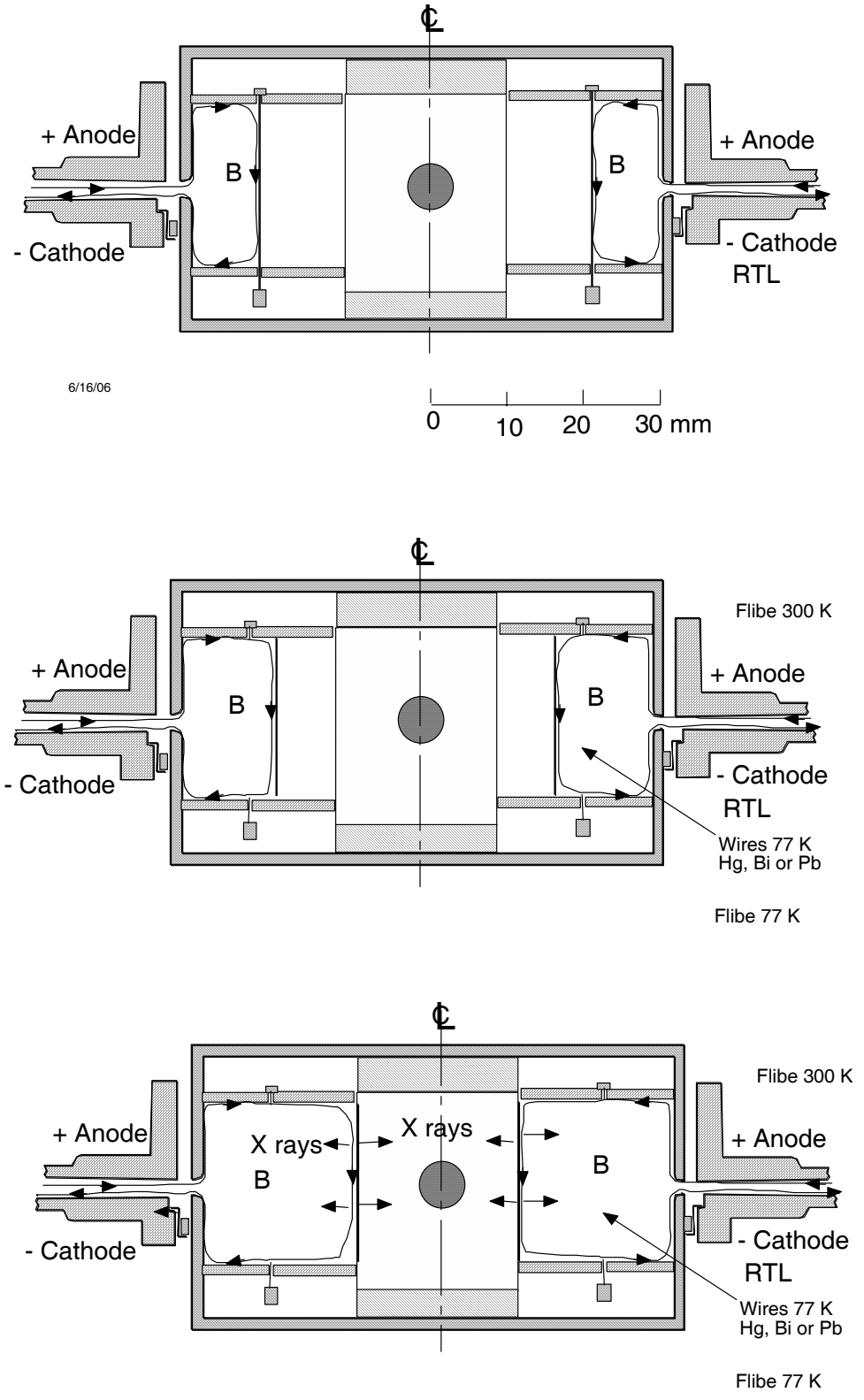

Figure 4.9: Sequence showing wires being accelerated to make x rays.

4.6 Injection Sequence

The equipment shown in Fig. 4.10 inserts an RTL and target every two seconds. Notice there are two coaxial plungers: one to insert the RTL and the other to inject the liquid jets.

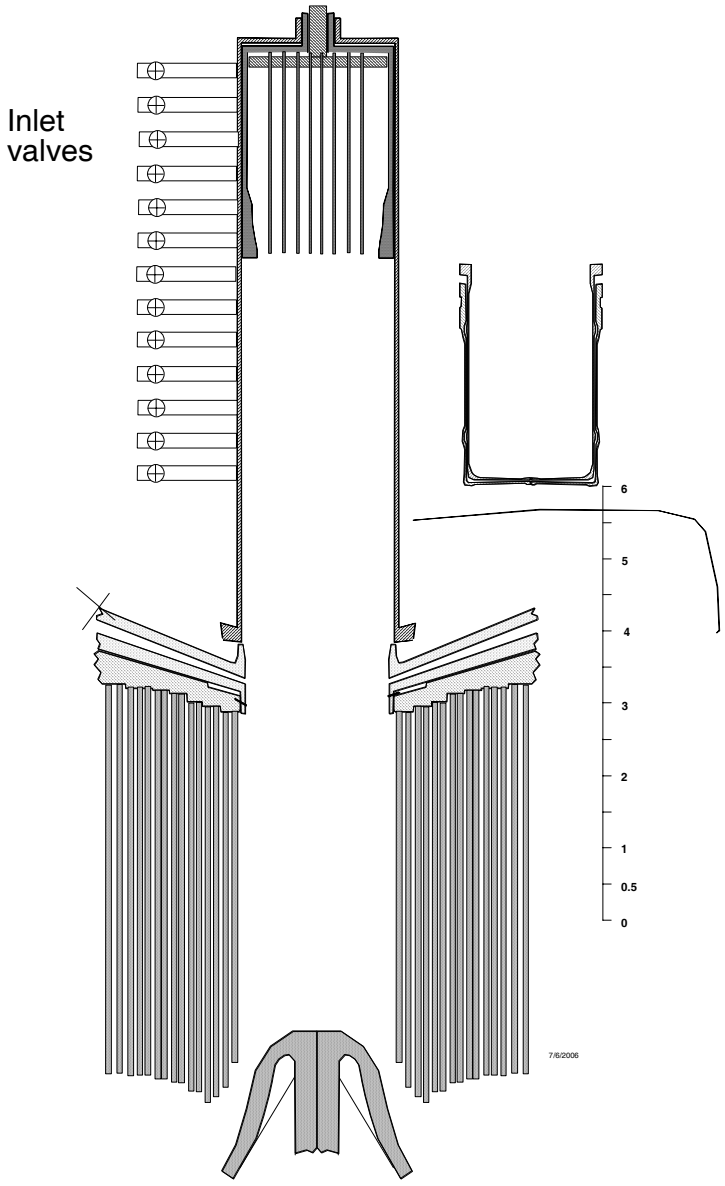

Figure 4.10: Equipment used to insert RTL.

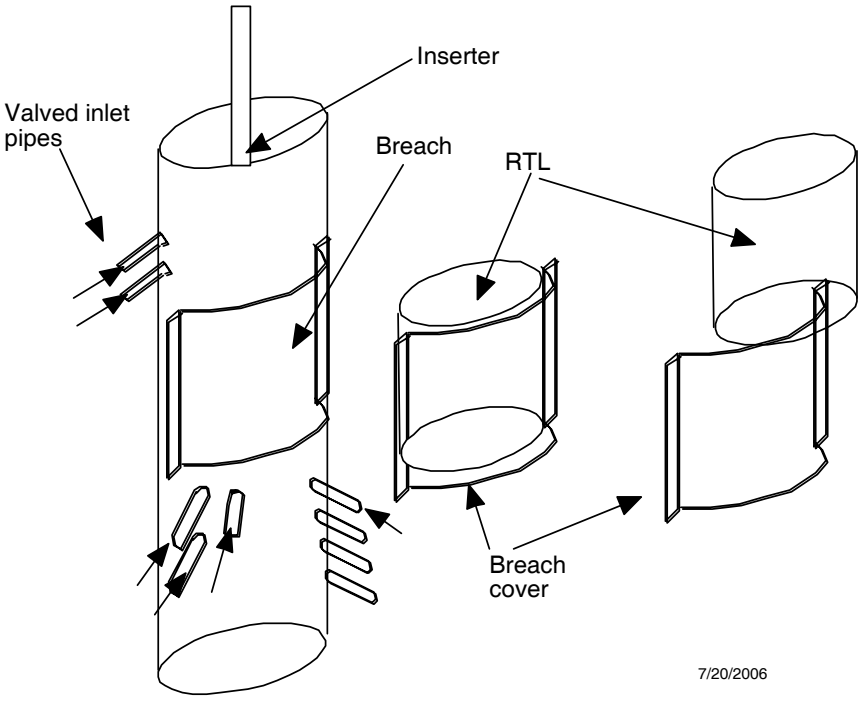

Figure 4.11: The method to load the RTL through a breach is illustrated.

The breach RTL loading system is shown in Fig. 4.11 along with the breach cover and pipes shown for pulse injection of the liquid during the shot time. The liquid fill is done in "free-fall" at 1 g downward or in other words "free-fall." However, the liquid must be accelerated once injected and the liquid surface also is accelerated. Considerable turbulence can be expected during fill. The fluid dynamics will require considerable study and experimentation.

The following shows the sequence of loading the RTL, moving it into place for firing a DT shot and injecting the liquid that protects the upper structures. The plunger to inject liquid is not shown in this sequence as it is in Fig. 4.10.

The RTL inserter and nozzle system is shown in Figs. 4.12.1 to 4.12.9 in a series of nine sequential positions. We do not show the latest RTL design modifications of Figs. 4.3 through 4.7 nor the MITL closure device.

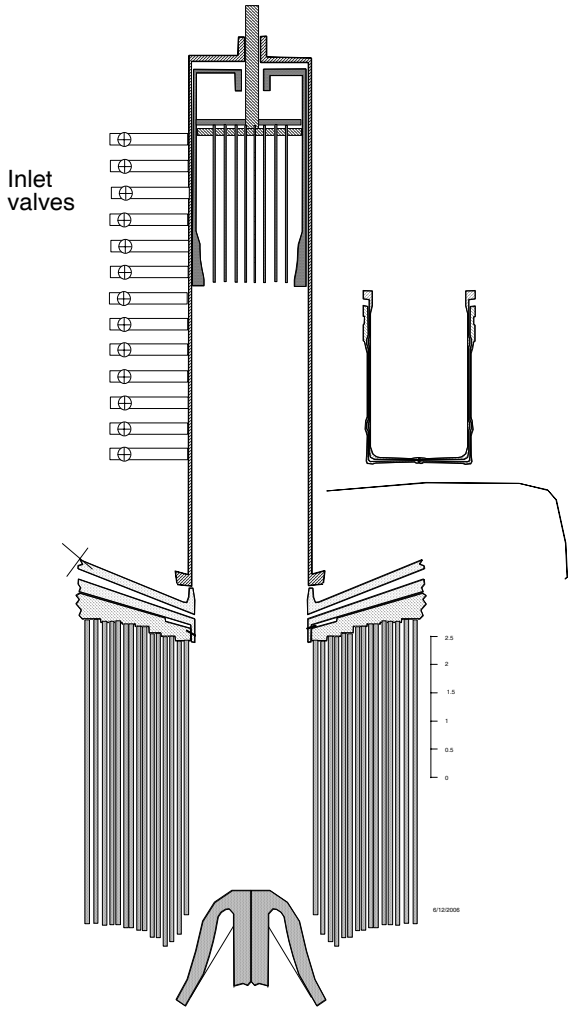

Figure 4.12.1: The new RTL is moving towards the breach of the inserter and is decelerated at -1g.

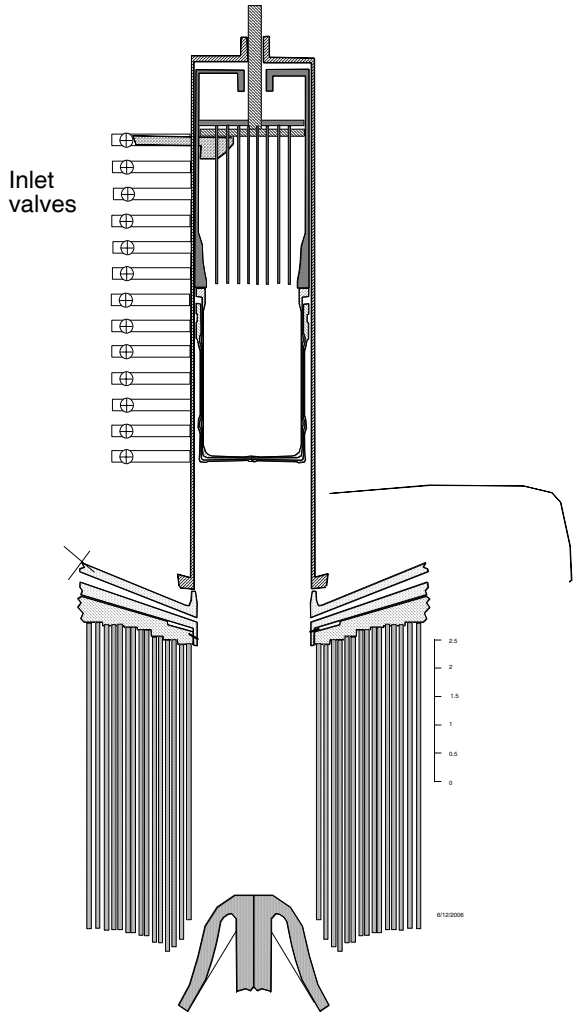

Figure 4.12.2: The RTL is attached to the inserter, inlet valves open to begin injecting liquid, and the inserter begins downward acceleration at 1 g (guided free fall).

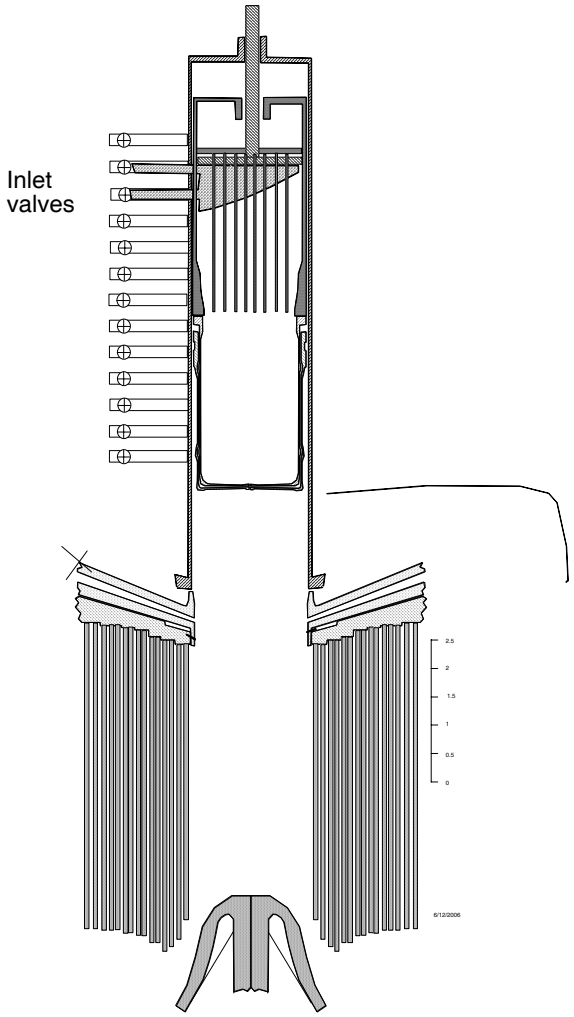

Figure 4.12.3: The RTL is accelerated downward and the inlet valves continue sequentially injecting liquid.

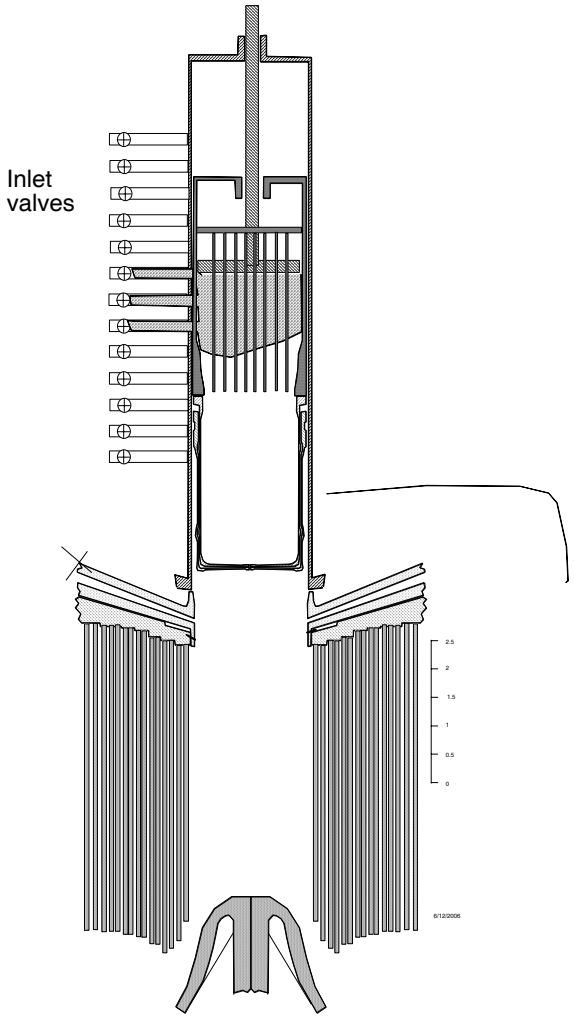

Figure 4.12.4: More liquid is injected during the 1 g free fall of the RTL.

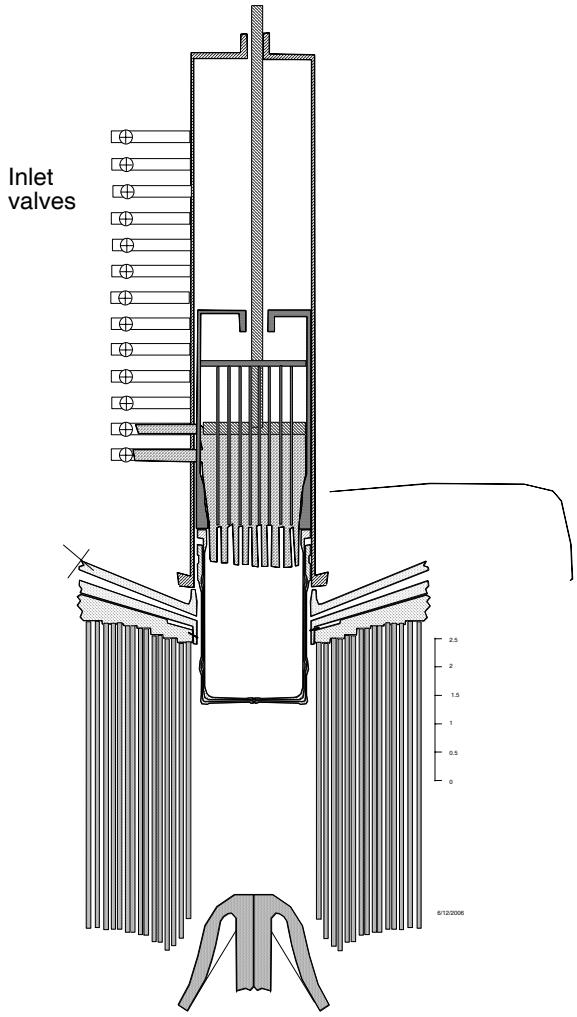

Figure 4.12.5: The last liquid is injected, the inner RTL cone starts accelerating at 2 g while the outer cone continues to free fall.

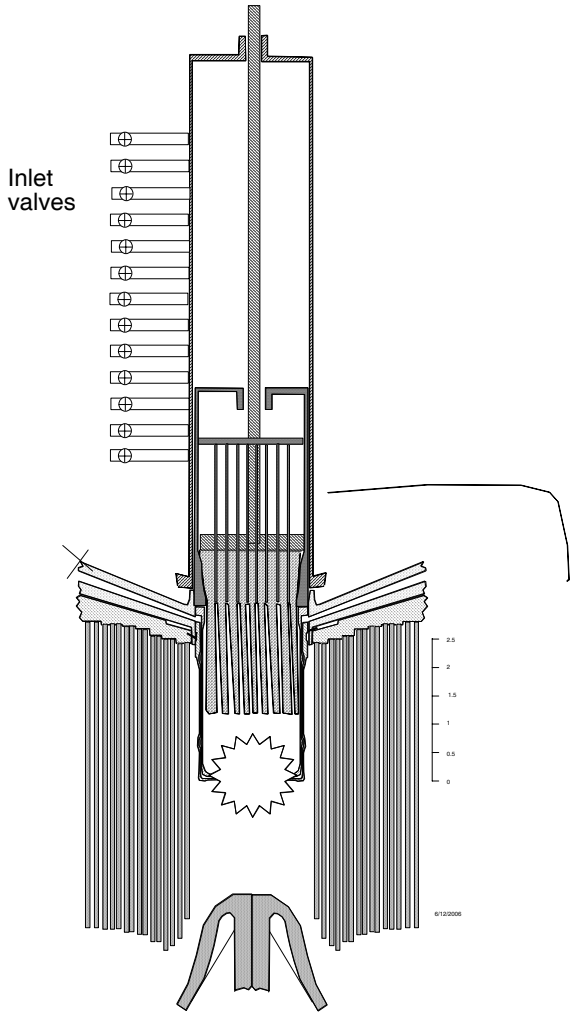

Figure 4.12.6: The RTL mates with the MITL, the gap is closed to 1.5 mm between RLT cones and the shot is fired. The RTL continues moving downward at 10 m/s. The RTL shatters with debris driven into the liquid jets.

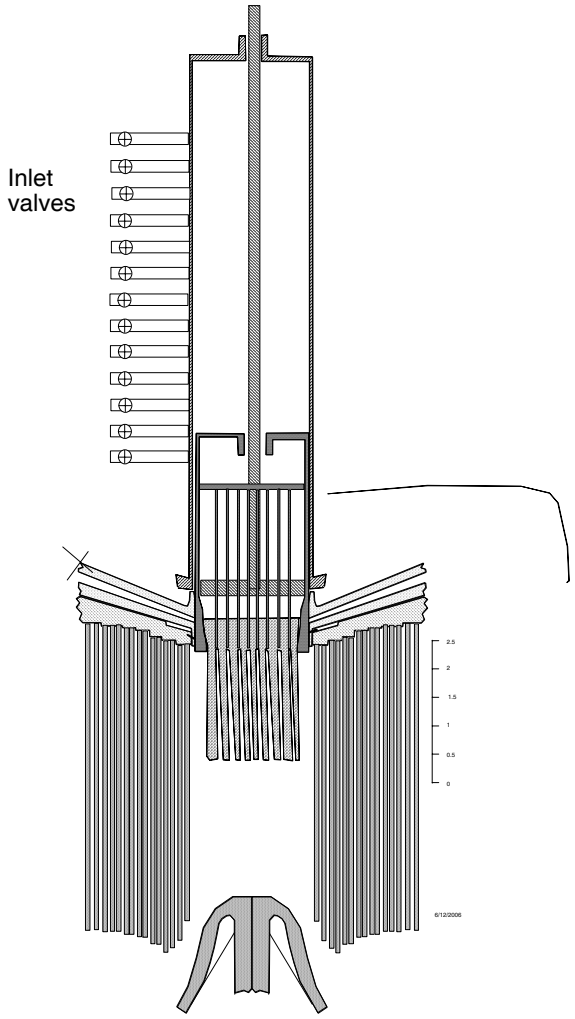

Figure 4.12.7: The liquid above the shot continues to enter the chamber. The RTL inserter covers the open MITL in 1.5 ms and cleans off the face of the MITL as it passes moving at 10 m/s but accelerating upward by now at 20 g.

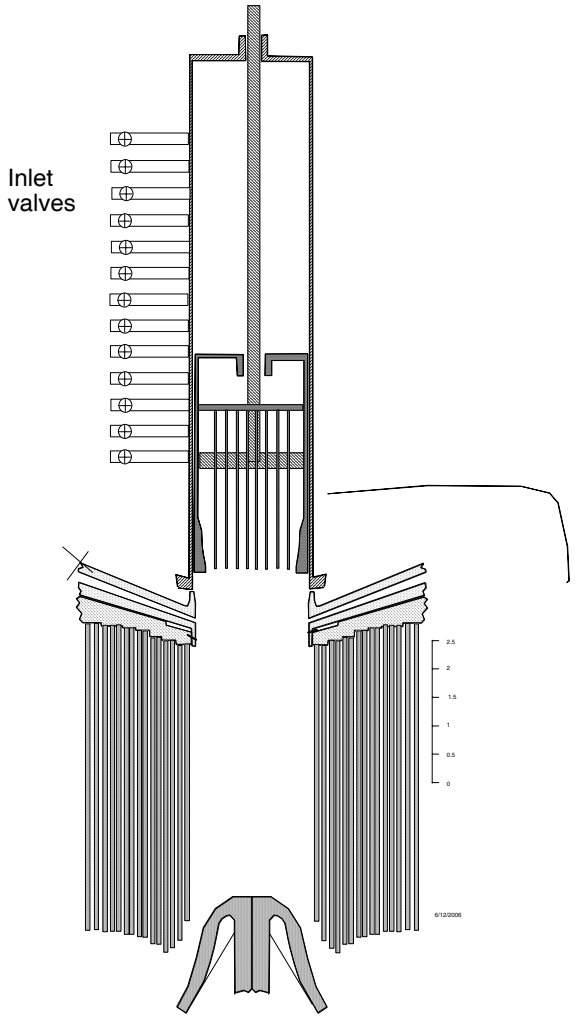

Figure 4.12.8: The inserter, free of liquid, is moving upward towards the starting point.

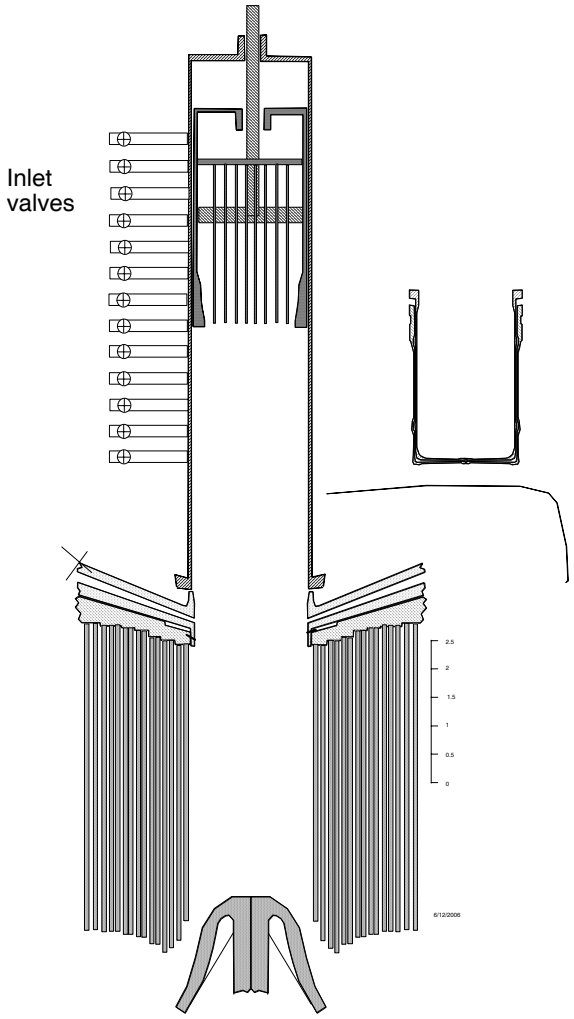

Figure 4.12.9: The inserter is decelerated at 21 g and moves to its starting position and the next RTL is moving towards the breach to be loaded.

4.7 Time-Motion Study

A time-motion analysis determines the time between shots. The following is a list of separate events that each contribute to the time elapsed between shots.

1. The RTL is translated into the breach of the injector tube and the breach cover is closed.
2. The inserter is mated to the RTL.
3. Downward motion:
   a. The inserter is accelerated downward at 1 g until a distance of about 0.53 m before the shot position.
   b. The acceleration is increased to 2 g to cause the inner RTL cone to catch up to the outer cone to within 1.5 mm at shot time.
   c. Simultaneously the cover over the MITL opening is slide upward or opened.
   d. Simultaneously the liquid is injected through a sequence of valves into the inserter cavity.
   e. Simultaneously the plunger ejects the liquid at 15 m/s (5 m/s relative to the inserter speed of ~10 m/s).
   f. The inserter is accelerated upward at 20 g but continues its downward motion until the turn around point.
4. Upward motion:
   a. The inserter is accelerated upward at 20 g to a certain point.
   b. Then the inserter is decelerated at 21 g until it comes to rest at the top.
   c. Simultaneously the breach cover is removed.
   d. Simultaneously the MITL faces are inspected by optical techniques for damage and possibly cleaned off with a broaching tool. This step might add time to the sequence.

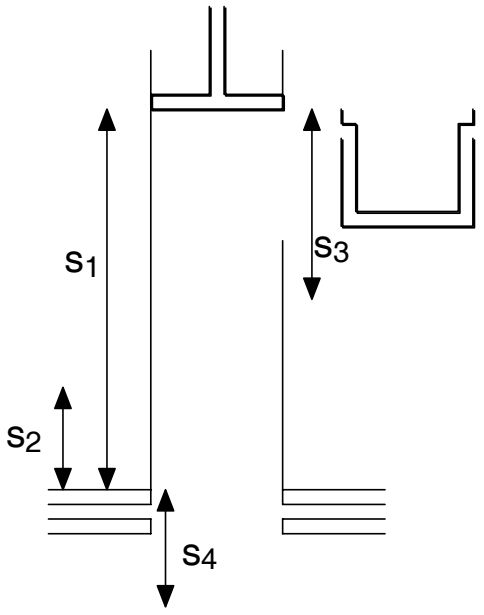

Figure 4.13: Illustration of injection sequence.

We now go into detail to estimate the time needed for each operation. Definitions are given in the Fig. 4.13 above.

1. The RTL is translated into the breach of the injector tube and the breach cover is closed.

   s = distance for deceleration,
   t = time for deceleration,
   a = deceleration rate,
   v = translation speed to the breach.
   Example, s = 0.5 m, a = 1 g,

   $$t = \sqrt{\frac{2s}{a}} = \sqrt{\frac{2 \times 0.5\,m}{10\,m/s^2}} = 0.32\,s$$

   $$v = at = 10\,m/s^2 \times 0.32\,s = 3.2\,m/s$$

2. The inserter is mated to the RTL

   Time assumed to be 0.1 s.

3. Downward motion.
   a. The inserter is accelerated downward at 1 g until a distance of about s_2= 0.6 m before the shot position. This downward motion is guided free fall. The outer cone is resting on the inner cone.

      The time for the outer cone to reach the shot point is

      $$t = \sqrt{\frac{2s_1}{a}} = \sqrt{\frac{2 \times 6\,m}{10\,m/s^2}} = 1.1\,s$$

      $v = at = 10\,m/s^2 \times 1.1\,s = 10.1\,m/s$ = speed of the RTL at shot time.

   b. The acceleration is increased to 2 g to cause the inner RTL cone to catch up to the outer cone to within 1.5 mm at shot time assuming a starting gap of 15 mm.

      $$t = \sqrt{\frac{2s}{a}} = \sqrt{\frac{2 \times (0.015\,m - 0.0015\,m)}{10\,m/s^2}} = 0.052\,s$$ = time to close the gap.

      $\Delta v = at = 10\,m/s^2 \times 0.052\,s = 0.52\,m/s$ = change in speed of the inner cone relative to the outer cone.

      $s_2 \approx vt = 10.1\,m/s \times 0.052\,s = 0.53\,m$ = starting point for increased acceleration.

   c. Simultaneously the cover over the MITL opening is slide upward or opened.

d. Simultaneously the liquid is injected through a sequence of valves into the inserter cavity.
e. Simultaneously the plunger ejects the liquid at 15 m/s (5 m/s relative to the inserter).
f. The inserter is accelerated upward at 20 g but continues its downward motion until the turn around point.

The time to bring the inserter to 3 m from its starting position is

$$t = \frac{v + \sqrt{v^2 + 2as_2}}{a} = \frac{10.1 m/s + 0.52 m/s + \sqrt{10.62^2 + 2 \times 20 \times 10 m/s^2 \times 3m}}{20 \times 10 m/s^2}$$

$= 0.23$ s.

The time to turn-around is 0.053 s and the distance is

$$s_4 = \tfrac{1}{2} at^2 = 0.5 \times 20 \times 10 m/s^2 \times (0.053 s)^2 = 0.28 m$$

4. Upward motion.

a. The inserter is accelerated upward at 20 g to a certain point 3 m from the starting point in 0.23 s.

The upward speed at 3 m from the starting position is

$$v = at - v_{down} = 20 \times 10 m/s^2 \times 0.23 s - 10.62 m/s = 35.4 m/s$$

b. Then the inserter is decelerated at 21 g until it comes to rest at the top.

$$a = \frac{v^2}{2s_3} = \frac{(35.4 m/s)^2}{2 \times 3m} = 209 m/s^2 = 21 g$$

$$t = \frac{v}{a} = \frac{35.4 m/s}{209 m/s^2} = 0.17 s = \text{time to bring inserter to rest.}$$

c. Simultaneously the breach cover is removed.

d. Simultaneously the MITL faces are inspected and possibly cleaned off.

Table 4.1: Summary of RTL cycle times

	g force	Time, s
Load the breach	-1 sideways	0.32
Mate inserter/RTL	0	0.1
Accelerate to shot point	1 downward	1.1
Accelerate upward	20 upward	0.23
Decelerate	21 downward	0.17
Total time		1.92

The time for the various steps is tallied in Table 4.1 for a total estimated cycle time of 1.9 s. The most delicate operation occurs during loading the RTL in the breach of the inserter tube where the sideways force is 1 g. The 1 g downward motion is a force-free operation (except for the 1-2 g jerk) taking the most time. The high g force operations are without the RTL during return of the inserter to the starting point. The cycle time allows a fusion power of 3 GJ/1.9 s = 1.6 GW from one chamber.

4.8 Features of the RTL and Chamber Design

Features of the proposed RTL and chamber design are summarized here.

1. Inductance of the 3-m-long, 1-m-radius RTL transmission line is 15 nH out to 2 m radius where the gap is proportional to radius and is assumed to be 30 mm at 2 m.
2. All structures are protected by 1 m of flibe. This should result in long life structures and better economics due to reduced maintenance and downtime.
3. Guides or "bumps" in the RTL casting keep the spacing of 15 mm during insertion; gap = 0.015·r
4. The 1.5 mm gap near the target is created "on the fly" with the shot triggered when it is achieved. The inner and outer RTL cones are accelerated downward at 1 g (free fall) for 1.1 s or a distance of 5.6 m. When the RTL is 0.6 m above and 0.055 s before shot time and position the inner cone acceleration is increased to 2 g, which causes the gap to close from 15 mm to 1.5 mm at which time the transmission line is triggered.
5. The two 2-mm-thick shells making up the RTL have a mass 150 kg and assuming another 100 kg of stiffeners and electrode rings, 250 kg must be cooled from the liquid by about 400 K (heated back up by a shot) amounting to 238 MJ of lost useful yield (250 kg × 2380 J/kg·K × 400 K = 238 MJ), representing 8% yield loss. The energy conversion efficiency of the plant will be reduced by this amount. Said another way this amount of energy is not available to be converted to electricity. Clearly a lighter mass RTL cone set would be desirable. Would RTL cones of 1 mm wall thickness be practical?
6. The RTL inserter also serves as a nozzle for pulsed injection of flibe. The RTL will be moving at about 10 m/s at shot time and the liquid will be injected at about 15 m/s. The downward momentum of this liquid (60,000 Pa·s) overcomes the upward shot momentum or impulse.
7. Steady or pulsed jets protect the chamber sidewalls from neutrons and blast.
8. A mushroom jet protects the bottom of the chamber from neutrons and blast.
9. The gas in the chamber will be that of the vapor pressure of the flibe.

10. The inserter covers the 15 mm MITL opening about 1.5 ms after the shot and resurfaces or cleans the MITL electrode faces as it makes a two-way pass. The MITL cover covers the opening at all times except at shot time and a few ms afterwards. Since flibe vapor is condensable its pumping can be rapid. Very much non-condensable gas will preclude MITL operation as rapid pumping is difficult. Designs with gas fill may be unfeasible based on the inability to rapidly pump out the MITL and RTL.
11. The RTL shatters and is driven into downward moving liquid jets that carry them away. A worry is contamination of the interior of the MITL before closure by the inserter in 1.5 ms. Flibe vapor primarily from the transmission line current produced plasma will enter the MITL. This needs estimating.

4.9 Future Work

The frangible solid flibe RTL is the subject of considerable uncertainty. Can it be cast? Will it be strong enough to not fall apart during insertion? Will the current ramp up properly especially during the early part of the pulse? Will the MITL face be damaged by the prior current pulse? Experimental work will be needed to resolve these questions.

4.10 Inductance

The inductance of the RTL dominates the inductance of the entire circuit delivering power to the target load. This means the design of the RTL must consider low inductance to be one of the primary design goals. For this reason the inductance of a narrow gap coaxial transmission line is now derived.

Stored energy in an inductor $= \frac{1}{2} LI^2 = \int \frac{B^2}{2\mu_0} dV$

For a coaxial transmission line

$$B = \frac{\mu_0 I}{2\pi r}$$

$$dV = 2\pi r dA$$

Substituting we get the results:

$L = \frac{\int B dA}{I} = 2 \times 10^{-7} \int \frac{dA}{r}$ = inductance of a narrow gap coaxial transmission line.

As an example, take 12 nH inductance and 90 MA of current in a pulse. The energy in the 12 nH part of the line is 49 MJ and is lost. If the rise time of the 90 MA current is 100 ns, then the voltage across the transmission line is $dV = L\frac{dI}{dt}$ = 10.8 MV.

For the RTL shown above we now calculate the inductance. We assume the gap = w = $d_3 \frac{r}{r_3}$. The gap is assumed to be d_3 at position r_3. We take as an example at $r_3 = 2$ m, $d_3 = 30$ mm, $r_2 = 1$ m, $r_1 = 0.03$ m

dA = wdr

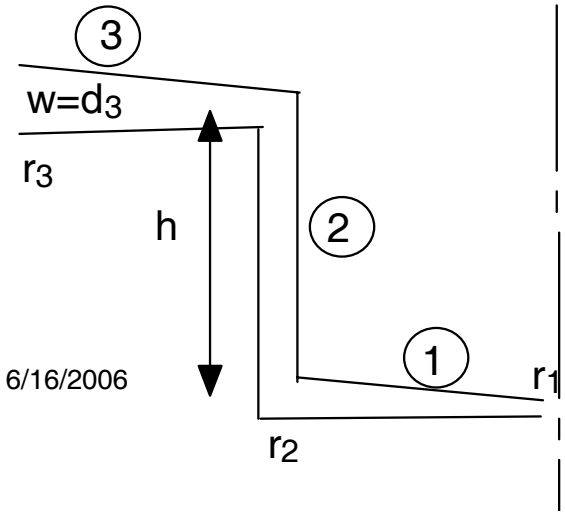

Figure 4.14: Three regions of RTL for inductance calculations.

We break the integral into three regions and calculate the inductance in each.

Region 3. The flat plate between 1 and 2 m radius,

$$L = \frac{\mu_0}{2\pi}\int \frac{dA}{r} = \frac{\mu_0}{2\pi}\int_{r_2}^{r_3} \frac{d_3 dr}{r_3} = \frac{\mu_0}{2\pi}\frac{d_3(r_3 - r_2)}{r_3} = 3 \text{ nH}$$

Region 2. The cylinder at radius 1 m and height, h, of 2 m.

$$dA = hw = \frac{d_3 h r_2}{r_3}$$

$$L = \frac{\mu_0}{2\pi}\int \frac{dA}{r} = \frac{\mu_0}{2\pi}\frac{d_3 h}{r_3} = 6 \text{ nH}.$$

Region 1. The flat plate between 0 and 1 m, actually the minimum gap would occur at or near the target of 1.5 mm at 0.1 m or less.

$$L = \frac{\mu_0}{2\pi}\int \frac{dA}{r} = \frac{\mu_0}{2\pi}\int_{r_1}^{r_2} \frac{d_3 dr}{r_3} = \frac{\mu_0}{2\pi}\frac{d_3(r_2 - r_1)}{r_3} = 3 \text{ nH}.$$

The total inductance of the 2-m transmission line inside of 2 m is 12 nH and for a 3-m high transmission line is 15 nH.

4.11 Shock Mitigation in Z-IFE

The fusion chamber in an IFE power plant must be design to contain repetitive fusion explosions. We describe here some initial estimates for the Z-IFE case based on prior but similar studies.

Inertial fusion yields of 3 GJ and 20 GJ cases are suggested as base cases for the Z-Pinch IFE power plant. The explosions are contained in a chamber whose walls are protected by jets of liquid flibe. The High Yield Lithium Injection Fusion Energy (HYLIFE) chamber was studied in great depth and extensively documented.[2] The reference case was for 1.8 GJ, but higher yields (4.8 GJ) were also considered. The fusion explosion was surrounded by an annular array of liquid lithium jets. The purpose of the liquid jets was to protect the steel vessel's walls from the strong shock and from cumulative damage by neutrons. An array of jets could attenuate the shock transmitted through gas to the walls to a low enough pressure leading to quite tolerable stresses. A series of published papers by Glenn[3] document this shock attenuation. An experiment by Liu, Peterson and Schrock[4] with a shock tube verified the idea with water jets. Liu wrote a 2-D computer hydro-code called TSUNAMI to calculate the gas shock attenuation and calculations were compared to experiment. The idea of shock mitigation with a porous media can be considered well established.

The shock results from the absorption of energetic particles of the target (called debris) and x-rays by liquid surfaces. The x-rays from the target cause ablative pressure that accelerates the liquid outward. The energy carried by debris and by the ablative material causes further evaporation of the liquid on a longer time scale that does not contribute significantly to acceleration of the liquid directly, but creates gas that must be vented. Because there is initially more gas pressure on the inside of the liquid jet array than the outside, there is an acceleration of the liquid outward until this gas is vented. Another important liquid acceleration mechanism is the sudden neutron heating of the liquid (i.e., faster than the liquid can expand). This isochoric heating pressurizes the liquid, which then hydrodynamically flies apart. According to an analysis by Glenn, breaking the liquid into jets or introducing bubbles or voids can cause 70% of the energy of this motion to dissipate. The outward momentum of this liquid must be stopped by the chamber wall without damage to its surface, and the stresses must be low enough to avoid damage. The vessel must be designed to be robust.

Using either jets or bubbles in liquids or porous media, the shock that would otherwise impact the wall with devastating consequences can be kept to tolerable limits[a]. We must be careful to fully consider the forces to the wall carried by the outward motion of the liquid used to attenuate neutrons and mitigate shocks. In HYLIFE-I, the average outward motion of the liquids was about 50 m/s.

---

[a] The fusion explosion results in x rays, debris from the target and neutrons. A bare chamber would see a large absorption of x rays and debris in the wall resulting in an ablative pressure that would destroy the wall by spallation and excessive stress as well as erosion. To mitigate these effects the wall is covered with a thin layer of liquid or a high-Z gas such as Xe is used to absorb the x rays and re-emit them over a longer time. Then the erosion becomes unimportant due to renewal of the liquid layer. The ablative pressure can still be excessive. Thick liquid walls eliminate the problem of x rays and debris on the wall.

Calculations Based on HYLIFE-II Analysis

A more recent design called HYLIFE-II[5] substituted flibe for lithium and was designed for a lower yield of 0.35 GJ. The average outward motion was predicted to 4 m/s. The liquid jets were injected downward with a speed of 12 m/s that dominated the outward motion so that the liquid strikes the chamber walls towards the bottom of the vessel.

Equilibrium Pressure in Chamber

The pressure in the chamber after the gas has equilibrated but before cooling by the liquid jets or walls is:

$P_c = (\gamma - 1)\frac{Y}{V}$, where γ is the ratio of specific heats (c_p/c_v) for dissociated flibe (1.2), Y is the non-neutron yield (0.3×3 GJ = 0.9 GJ) and V is the chamber volume assuming a 5 m radius by 7 m tall chamber. $V = \pi r^2 h = \pi 5^2 \cdot 7 = 550\ m^3$

In HYLIFE-II, the 0.35 GJ yield heated up and evaporated an estimated 5 kg of flibe. In the 3 GJ Z-IFE case this would be 40 kg. The 40 kg absorbs 2 MJ/kg on heating up to the boiling point and 5.3 kg/MJ evaporating.

Substituting these values gives:

$$P_c = (1.2-1)\frac{(0.9\cdot 10^9\ J - 40\ kg \times 7.3\ MJ/kg)}{550\ m^3} = 0.22\ MPa$$ (1.5 MPa for 20 GJ case.)

The chamber will come to an equilibrium pressure of about 2.2 atmospheres (15 atmospheres for the 20 GJ case) and drop to below one atmosphere in about one e-folding of cooling by condensation and other heat transfer processes. The chamber should be made somewhat larger for the 20 GJ case.

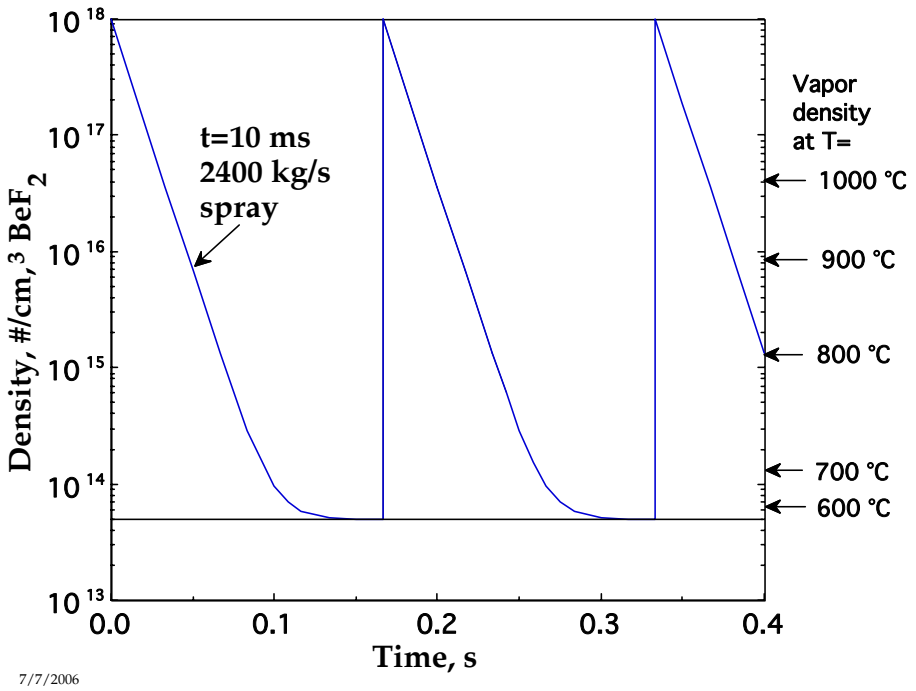

Figure 4.15: Condensation pumping for HYLIFE-II (Fig. 7, Ref.6), where τ ~10 ms. The base density depends on the temperature of the flibe (see Fig. B.4). The interpulse time for HYLIFE-II was 1/6 s where Z-IFE will be 2 s or more.

Suppose the liquid jets form a pocket of 1.1-m radius and 3.5 m high. The peak pressure inside the pocket would be:

$$V = \pi r^2 h = \pi 1.1^2 \cdot 3.5 = 13.3\, m^3$$

$$P_c = (\gamma - 1)\frac{Y}{V} = P_c = (1.2-1)\frac{(0.9\cdot 10^9\, J - 40\, kg \times 7.3\, MJ/kg)}{13.3\, m^3} = 9.1\, MPa$$

(60 MPa for the 20 GJ case). The assumed Z pocket volume of 13.3 m^3 could be increased to decrease this initial internal pressure. For the 20 GJ case let's assume we have a 2 m radius and a height of 7 m for 88 m^3. Using the same scaling, this results in a peak pocket pressure of 9.1 MPa.

Venting

In HYLIFE-II the gas vented in 0.47 ms to equalize the pressure across the jet array. During this 0.47 ms the jets are accelerated radially outward to ~1.7 m/s. The gas vents through the openings in the liquid array above the shot point and on the side of the liquid pocket. The total surface area of the inner pocket for the 3 GJ Z-IFE case is $\pi r^2 + 2\pi rh = \pi 1.1^2 + 2\pi 1.1 \cdot 3.5 = 28$ m^2. The venting area is a fraction of this area determined from the following schematic to be 8.3 m^2 (30% of total area).

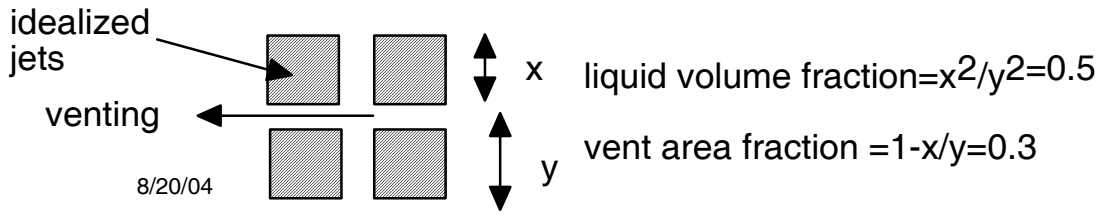

Figure 4.16: Simplified geometry of jets for venting calculations.

$A_1 = 0.3 \cdot (3.8\ m^2 + 24\ m^2) = 8.3 m^2$

C = thermal speed of dissociated flibe gas

$$\tau = \frac{V}{CA_1} = \frac{13.3 m^3}{1230 m/s \cdot 28 \cdot 0.3} = 1.3\ ms$$

$P_p \tau = \mathrm{v} \cdot \rho \Delta r$

$\mathrm{v} = \dfrac{8.8\ MPa \cdot 1.3 ms}{2000 kg/m^3 \cdot 1 m} = 5.7\ m/s$ is the average outward speed of 1- m equivalent of flibe accelerated during venting. The liquid above the shot is 2 m thick, so the upward speed would be 2.9 m/s. We should try to decrease this number. The velocity can be reduced by making the inner radius of the array greater that 1.1 m and by having more open area so the venting is faster than 1.s ms. Slots give higher venting area than cylinder jets, a larger pocket radius than 1.1 m, a larger stand off distance from the liquid.

For the 20 GJ case $A_1 = 0.3 \cdot (\pi \cdot 2^2\ m^2 + 2\pi \cdot 2 \cdot 7\ m^2) = 94 m^2$

$$\tau = \frac{V}{CA_1} = \frac{88 m^3}{1230 m/s \cdot 94 m^2} = 0.76\ ms$$

$$\mathrm{v} = \frac{9.1 MPa \cdot 0.76 ms}{2000 kg/m^3 \cdot 1 m} = 3.5\ m/s$$

The upward speed is 1.7 m/s.

Ablation

When the 3 GJ yield shot goes off the x ray and debris dose at 1.1 m on the flibe will be $\dfrac{3 \cdot 10^9 J \cdot 0.15}{4\pi 1.1^2 m^2} = 30 MJ/m^2$, from Ref. 6, Fig. 4-8 we see that about 60 μm of flibe is evaporated ablatively, that is suddenly. This is 0.12 kg/m^2 (2000 kg/m^2×60 μm) of material evaporated. From Ref. 5, Eqn. 13 we get:

$$v_{liquid} = \frac{(\frac{2 m_{vapor} E_{vapor}}{area \quad area})^{0.5}}{m_{liquid} \Big/ area} = \frac{(2 \cdot 0.12\, kg/m^2 \cdot 30 \times 10^6 J/m^2)^{0.5}}{2000\, kg/m^2} = 1.3\, m/s$$ outward motion of liquid jets located at 1.1-m distance for flibe of thickness equivalent to 1 m. The upward motion is 0.7 m/s.

For the 20 GJ case $\frac{20 \cdot 10^9 J \cdot 0.15}{4\pi 2^2 m^2} = 60\, MJ/m^2$ This is 0.14 kg/m^2 (2000 kg/m^2× 70 μm) of material evaporated.

$$v_{liquid} = \frac{(\frac{2 m_{vapor} E_{vapor}}{area \quad area})^{0.5}}{m_{liquid} \Big/ area} = \frac{(2 \cdot 0.14\, kg/m^2 \cdot 60 \times 10^6 J/m^2)^{0.5}}{2000\, kg/m^2} = 2.0\, m/s$$ (1 m/s upward)

Isochoric Heating

In HYLIFE-II the interior spallation speed was 82 m/s and an average outward speed of 1.7 m/s with the liquid at 0.5 m and 0.58 m thick radially. Scaling this to Z-IFE with the liquid located at 1.1 m:

$v_{liquid} = 82 \cdot \frac{3}{0.35}\left(\frac{0.5}{1.1}\right)^2\left(\frac{0.58\, m}{1 m}\right) = 84\, m/s$ This is dangerously high! For the 20 GJ case with a standoff distance of 2 m we get 300 m/s! The reason these numbers are dangerous is the possibility of jetting getting through the liquid to the wall and causing damage. This is an area for design changes to reduce the driver for jetting speed.

The average speed hitting the sidewall is reasonable

$v_{liquid} = 1.7 \cdot \frac{3}{0.35}\left(\frac{0.5}{1.1}\right)^2\left(\frac{0.58\, m}{1 m}\right) = 1.7\, m/s$

For the 20 GJ case $v_{liquid} = 1.7 \cdot \frac{20}{0.35}\left(\frac{0.5}{2}\right)^2\left(\frac{0.58\, m}{1 m}\right) = 3.5\ m/s$

From Ref. 6 on HYLIFE-II we get a heating of 250 J/g at 0.5 m for 350 MJ. Assuming the sound speed in molten salt is 3300 m/s and the Gruniesen parameter Γ is 1, we can compute the jump-off speed of spalled liquid.

$$v_{liquid} = \frac{\Gamma E}{Cm} = \frac{1 \times 250{,}000\, J/kg}{3300\, m/s} = 76\, m/s$$ for the 350 MJ case of HYLIFE-II.

This formula has excellent experimental verification.

An alternative analysis of isochoric heating is now presented rather than scaling from HLYLIFE-II analysis results.

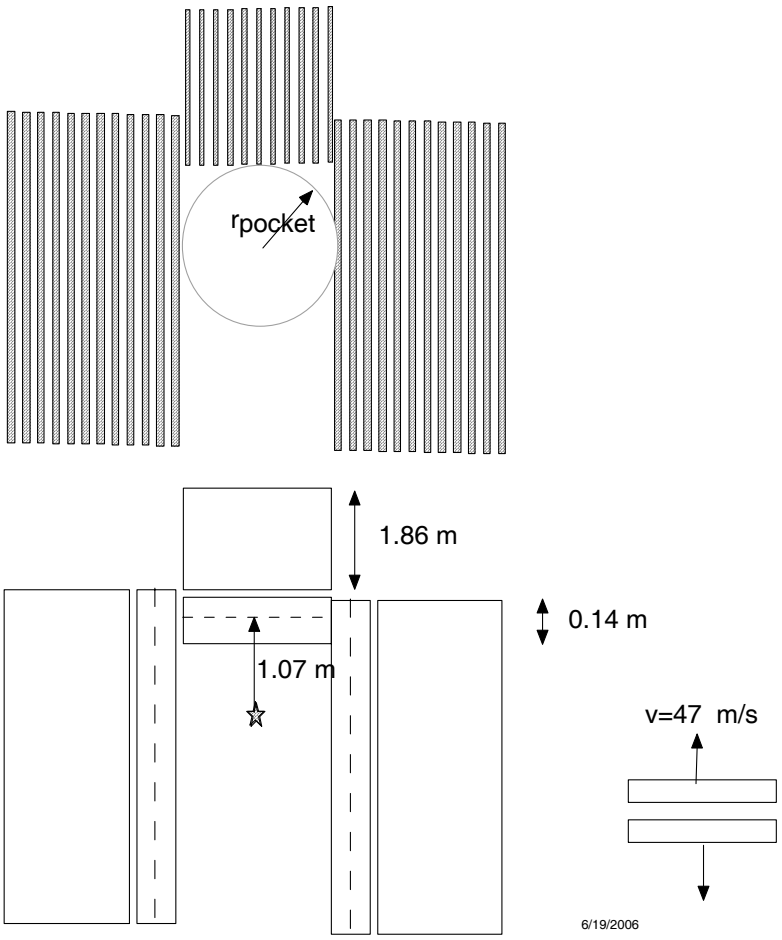

Figure 4.17: Showing the model problem for isochoric effects

Let us assume the neutron heating is 0.7 of the yield and all the deposition is in 0.14 m of flibe uniformly, that is 1 mean free path of neutrons.

$$E/m = \frac{3GJ \times 0.7}{4\pi(1.07\,m)^2 \times 0.14\,m \times \rho} = \frac{1.04 \times 10^9\,J/m^3}{\rho} = 5.2 \times 10^5\,J/kg$$

Following Glenn's assumption that 70% of the kinetic energy is absorbed in multiple collisions we get a downward and upward speed of the liquid in the two halves of 0.07 m thickness:

$$v_{liquid} = \frac{0.3\Gamma E}{Cm} = \frac{0.3 \times 1 \times 5.2 \times 10^5\,J/kg}{3300\,m/s} = 47\,m/s$$

The above factor of 0.3 or 70% of the energy dissipated seems reasonable and came from analysis but is not well verified by experiments.

When this upward moving liquid collides with the 1.86 m downward moving liquid that is assumed to be moving at a speed of 15 m/s its change in speed is:

$$\Delta v_{liquid} = 47\,m/s \times \frac{0.07\,m}{1.86\,m} = 1.7\,m/s$$

For the 20 GJ case with the same geometry the change in speed is:
$\Delta v_{liquid} = 1.7\,m/s \times \frac{20\,GJ}{3\,GJ} = 11.3\,m/s$ at 1 m stand-off distance up to the jets. This seems too high for the 15 m/s incoming liquid to overcome. For 2 m stand-off distance the change in speed is:
$\Delta v_{liquid} = 11.3\,m/s \times \left(\frac{1^2}{2^2}\right) = 2.8\,m/s$. This seems like an acceptably low value for the 15 m/s incoming liquid to overcome.

For the sideways case at 3 GJ, $\Delta v_{liquid} = 47\,m/s \times \left(\frac{0.07\,m}{0.86\,m}\right) = 3.8\,m/s$. For 20 GJ case

$\Delta v_{liquid} = 2.8\,m/s \times \left(\frac{1}{2}\right) = 1.4\,m/s$

Table 4.2: Parameters for Isochoric Heating Effect

	3 GJ case		20 GJ case	
r_{pocket}	1.1		2	
r_{vessel}, m	5		5	
h_{pocket}, m	3.5		7	
h_{vessel}, m	7		7	
$P_{0\ pocket}$, MPa	8.8		4.4	
$P_{0\ chamber}$, MPa	0.33		3.3	
	side	up	side	up
$v_{liquid,\ venting}$, m/s	5.7	2.9	3.5	1.7
$v_{liquid,\ ablation}$, m/s	1.3	0.7	2.0	1.0
$v_{liquid,\ isochoric}$, m/s	3.8	1.7	1.4	2.8
$v_{liquid,\ total}$, m/s	10.8	5.3	6.9	5.5

4.12 Blast Mitigation

The 2 m thick liquid moving downward at 15 m/s carries considerable momentum. The downward momentum per unit area is $\rho Vh = 2000 kg/m^3 \times 15 m/s \times 2m = 60{,}000 Pa \cdot s$. Can this mitigate the upward impulse due to the shot? From Table 1, we see the upward speed change is 5 m/s. Since this exceeds the downward liquid speed of 15 m/s, the jets height could be reduced and/or the speed could be reduced in future studies. The sideways speed of ~10 m/s seems acceptable because there are lots of jets to slow this down before hitting the walls.

4.13 Pumping Power

This section discusses pumping power for Z-IFE. The chamber configuration is given in Fig. 4.18. From the point of view of pumping power the important parameter here is the height, h.

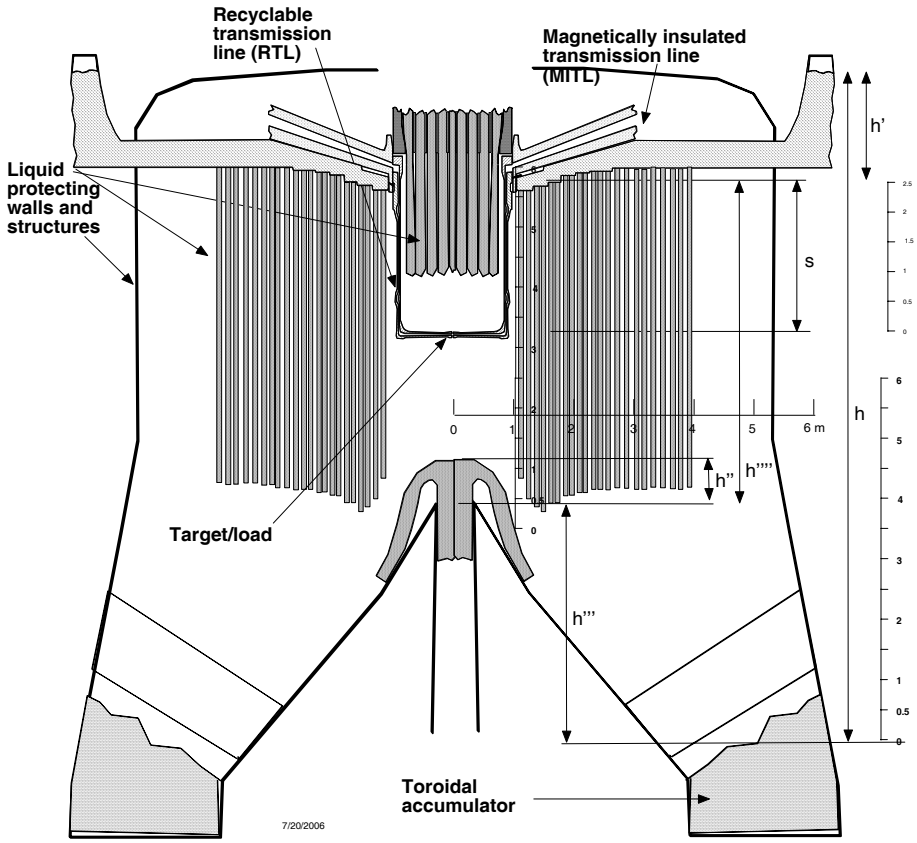

Figure 4.18: Chamber from pumping power point of view.

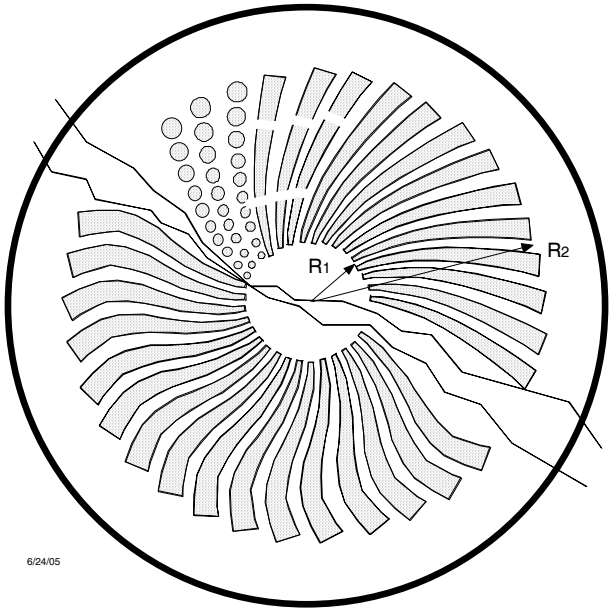

Figure 4.19: Cross-section of jets at the plane of the target. Curved slab jets ease venting while keeping a high packing fraction. Two versions are shown with partial coverage and three rows with rounds jets are shown.

Rapid venting is important to minimizing acceleration of liquid. Slab jets are much better than round jets from this point of view. The vent paths are designed to minimize neutron streaming. The above options are only examples to illustrate the idea. The important parameter in this figure for computing pumping power is the area of jets.

P = pumping power

h = height from pump inlet to nozzles + injection head, h'

h' = head above nozzles

v_o = jet speed at injection nozzles assuming, height h'

v = jet speed at horizontal plane of the target

g = acceleration of gravity = 10 m/s^2

ρ = flibe density = 2000 kg/m^3

$\dot{V}$ = flow rate, m^3/s

ε = jet packing fraction at the nozzles

L = areal liquid thickness

S = distance from nozzles to shot point = 2.5 m

η_p = pumping efficiency = 0.8

$\eta_{recovery}$ = head recovery efficiency = 0.5

R_1 and R_2 are the inner and outer radius of jets array at the plane of the target.

The power that has to be supplied to electric motors to pump the flibe to the reservoir assumed to be h' above the nozzles is:

$$P = \rho g h \dot{V} \left(\frac{1}{\eta_p} - \eta_{recovery} \right)$$

The areal thickness is:

$$L = (R_2 - R_1)\varepsilon_o \frac{v_o}{v}$$

$$\dot{V} = \pi (R_2^2 - R_1^2)\varepsilon v_o$$

$$v = \sqrt{v_o^2 + 2sg}$$

Example:

h' = 2 m

$$v_o = \sqrt{2sg} = \sqrt{2 \cdot 4 \cdot 10} = 6.32\ m/s$$

R_1 = 1 m

$R_2 = 4$ m

$\varepsilon = 0.55$

$v = \sqrt{v_o^2 + 2sg} = \sqrt{6.32^2 + 2 \cdot 2.5 \cdot 10} = 9.5\ m/s$ velocity at midplane

$$L = (R_2 - R_1)\varepsilon_o \frac{v_o}{v} = (4-1) \times 0.55 \frac{6.32}{9.5} = (4-1) \times 0.366 = 1.1\ m$$

This provides good neutron attenuation to protect the walls.

$$\dot{V} = \pi(R_2^2 - R_1^2)\varepsilon v_o = \pi(4^2 - 1^2)0.55 \cdot 6.32 = 25.9 m^2 \times 6.32 m/s = 164 m^3/s$$

Suppose the liquid height, h is 12 m including the head above the nozzle plate. Then the pumping power is:

$$P = \rho g h \dot{V}\left(\frac{1}{\eta_p} - \eta_{recovery}\right) = 2000 \cdot 10 \cdot 12 \cdot 164\left(\frac{1}{0.8} - 0.5\right) = 39MW(0.75) = 30MW$$

The pumping power supplied by electric motors for the jets is (39/0.8) 49 MWe without head recovery and 30 MWe with head recovery.

Suppose we decided to turn the liquid flow off to save pumping power during part of the interpulse time. In this case the flow could be turned off at the time the liquid arrives at the apex of the inverted cone diverter. From Fig. 4.18 we estimate this fall distance h to be about 5.5 m. The time fall t is:

$$t = \frac{-v_o + \sqrt{v_o^2 + 2h'''' g}}{g} = \frac{-6.32 + \sqrt{6.32^2 + 2 \cdot 5.5 \cdot 10}}{10} = 0.59\ s$$

for an interpulse time of 1.9 s from FY05 studies, the average flow rate, therefore average pumping power would be 0.59/1.9 = 0.31. The 30 MWe above would come down to 9.3 MWe.

The toroidal accumulator would have enough capacity to operate the pumps steadily. The jets would also have an accumulator tank so that it could be fed continuously but pulsed valves would supply the peak flow for 0.59 s.

Pulsed Jet

The volume in a 1 m radius, 1-m-high injected "slug" of liquid is 3.14 m^3 injected every 1.6 s. This pumping power is

$$P = \frac{\frac{1}{2}mv^2 + mg(h - h')}{\tau} = \frac{\frac{1}{2}6280\,kg \times (15\,m/s)^2 + 6280\,kg \times 10\,m/s^2(12.5\,m - 2\,m)}{1.9\,s}$$

$$= \frac{0.71\,MJ + 0.66\,MJ}{1.9s} = 0.72\,MW$$

$$P = \frac{0.72\,MW}{0.8} = 0.9\,MWe$$ = electrical pumping power without head recovery

$P = 0.9\,MWe\left(\frac{1}{0.8} - 0.5\right) = 0.7\,MWe$ = electrical pumping power with head recovery

This is a small pumping power compared to that of the side jets.

Mushroom Jet

R = 0.5 m
h'' = 1 m
h''' = 4 m

$$v = \left(\frac{2gh''}{\rho}\right)^{0.5} = \left(\frac{2\times 10\times 1}{2000}\right)^{0.5} = 0.1\,m/s$$

$$\dot{V} = \frac{\pi r^2 h}{\tau} = \frac{\pi \times (1m)^2 \times 1m}{1.6s} = 2m^3/s$$

$$P = \rho g(h''+h''')\dot{V} = 2000\cdot 10\cdot (1m+4m)\cdot 2m^3 = 0.2MW$$

The pumping power for the mushroom jet is small. This low power allows the option to enlarge this jet for more effective protection from neutrons.

LiPb Pumping Power

If we substitute LiPb at 9000 kg/m^3 for flibe with the same thickness of jet array, the pumping power of 30 MWe above for flibe would increase by the ratio of 9000/2000 to 135 MWe. However, LiPb is about half as effective at protection of the wall material from neutron damage at the same 1 m thickness. If the flow rate were stopped after 0.59 s in the above example of a 1.9 s interpulse time the 135 MW would drop to 42 MWe, which is still a large pumping power.

In conclusion, the jets should protect the walls (~1 m flibe thickness) and yet clear the chamber rapidly allowing a time between pulses of less than 2 second. Getting the target and recyclable transmission lines in place will be limiting rather than chamber clearing. The idea is to contain the fusion energy release with the aid of liquid jets without the liquid striking the side-walls, which is satisfied for the 3 GJ case but not the 20 GJ case.

4.14 Magnetic Stress on the RTL

During pulse power delivery the pressure inside the MITL will be magnetic and plasma pressure.

$$P = \frac{B^2}{2\mu_0}$$

$$B = \frac{\mu_0 L}{2\pi r}$$

$$P = \frac{\mu_0 I^2}{8\pi^2 r^2}$$

For 90 MA, r = 1 m and 0.1 μs pulse

P = 130 MPa

Pτ = 13 Pa·s

The 2 mm RTL will fly apart due to this magnetic impulse with a speed as follows.

$$v = \frac{P\tau}{\rho x} = \frac{13 Pa \cdot s}{2000 kg/m^3 \times 0.002 m} = 3.3 m/s$$

Plasma pressure might augment this some. The stiffeners of 20 mm thickness will travel at 0.3 m/s. Since the RTL is moving downward at 10 m/s, the debris will be headed mostly downward and should not enter the MITL.

4.15 Stresses in the Vessel Walls

The following section on steel and carbon composite vessels is taken primarily from the FY05 work and included here for completeness. The stress in the wall is caused mostly by the effects of the blast from the fusion explosion. The stress due to the chamber being evacuated is small as is the thermal stress with 1 m of flibe to reduce neutron heating. We assume the vessel is either made of ferritic steel or carbon composites. The advantage of steel is compatible with flibe in its reduced state up to the point it looses its strength at about 550 to 600 °C, it is low cost and fabricable. Its disadvantage is the temperature limitation. The advantage of carbon composites is the temperature can go over 1000 °C where Brayton cycles and hydrogen thermochemical cycles are possible and is chemically compatible with flibe including TF (see Fukuda and Peterson, reference 8). There are a number of disadvantages of carbon composite structures. High cost, difficulty of fabrication, joining and sealing, are problems needing solutions.

The ferritic steel example shown below is similar to that of HYLIFE-I except in its tritium containment. HYLIFE-I used lithium. Tritium permeation was not a problem because the lithium held tritium tightly as a hydride. With flibe in its reduced state tritium will be very diffusive and easily permeate through walls. We show double walls for tritium containment. The insulation region would have an inert gas that is processed for tritium removal. The lower temperature steel shroud will have reduced permeation to aid containment.

The carbon composite example shown in Fig. 4.21 can operate over 1000 °C. We suggest a silicon layer be applied during fabrication. Then the temperature would be raised over the silicon melt of 1400 °C where the Si reacts with C to form a layer of SiC. This layer holds the promise of hermetically sealing the chamber including greatly reduced tritium permeation. This same method might be successful for flat plate heat exchangers compatible with flibe and forming a tritium barrier. If the silicon and silicon carbide are in poor contact with the flibe, the combination might be compatible with flibe in its fluoridized state where tritium is largely in the form of TF. The reason is corrosion would take place largely by gas phase transport and hence through the not very porous media would be severely rate limited.

Applied research and development on carbon composites could resolve the issues mentioned above and result in a better, higher performing fusion chamber.

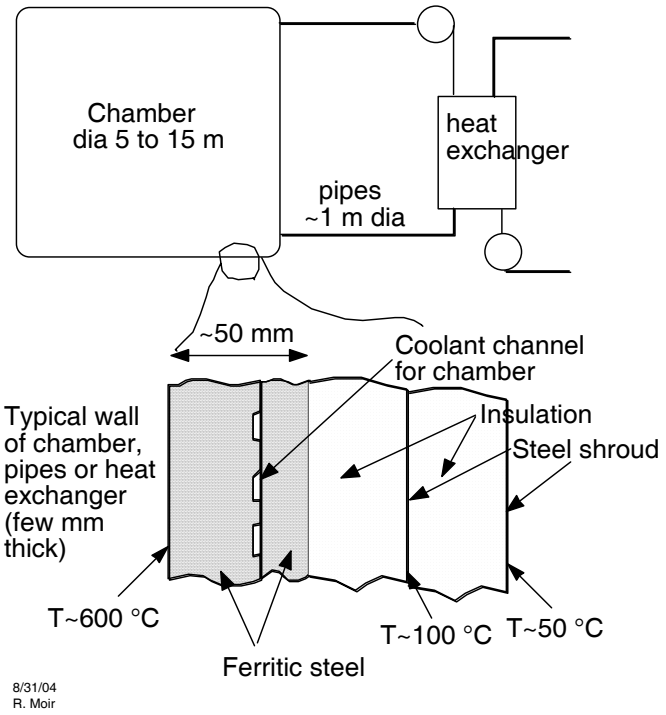

Figure 4.20: Ferritic steel chamber, pipe and heat exchanger walls.

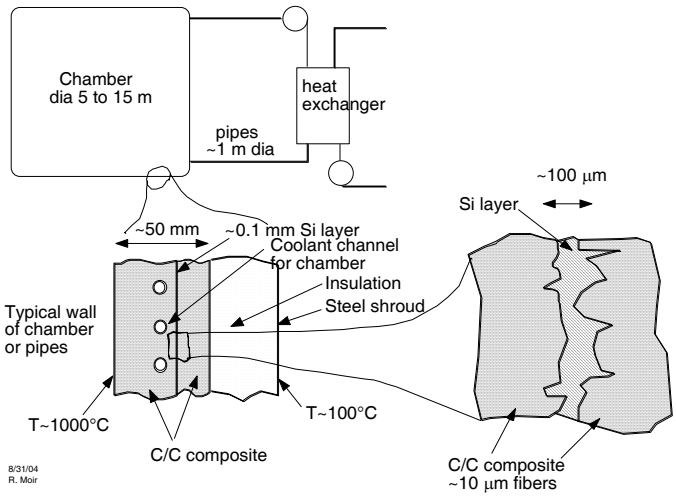

Figure 4.21: Carbon composite chamber, pipe and heat exchanger walls.

The peak stress in the chamber wall can be calculated from the following formula:

$\sigma = \frac{P\tau}{T}\sqrt{\frac{E}{2\rho(1-\nu^2)}}$ from Ref. 6, p 4-25 for a spherical vessel, where P is pressure, τ is duration of pressure, $P\tau$ is the impulse per unit area, T is wall thickness, ρ is density of the wall, E is

Young's modulus, ν is Poisson's ratio for the wall material. Here Pt is the pressure times time of the impulse on the wall. This is the same as the momentum per unit area on the wall. This formula assumes the impulse is delivered in a time short compared to the ring time of the vessel calculated below of a few ms. Let's take an example of liquid at 1-m radius, to 3-m radius with 50% void.

$m = \frac{4}{3}\pi(3^3 - 1^3)\cdot 2000 \cdot 0.5 = 1.09 \times 10^5 kg$. The momentum at 5 m/s is $5.4 \times 10^5\ kg\,m/s$ and this impacts an area = $4\pi 6^2 = 452\,m^2$. The specific impulse is $\frac{5.4 \times 10^5\ kg\,m/s}{452\,m^2} = 1190\,Pa \cdot s$.

Material parameters are given in the table for a ferritic steel and carbon composite vessel.

Table 4.3: Parameters for Vessel Walls

	Ferritic steel	Carbon composite
E, GPa	190	200
ρ , kg/m^2	7800	2000
ν	0.3	0.3

For this example the vessel wall stress is 87 MPa for steel and 176 MPa for carbon composite for a wall thickness of 50 mm. The above tensile stresses can be compared to the atmospheric compression stress of 12 MPa. We conclude a 10 m/s slug of liquid of 1-m equivalent thickness is somewhere near the margin of possible. A steel wall thickness similar to the 50 mm of HYLIFE-I seems reasonable but should be thicker for a carbon composite wall. Wall erosion will be a concern as well that must be considered.

The ring frequency of a long cylinder of radius r is

$f = \frac{1}{2\pi r}\sqrt{\frac{2}{\pi}}\sqrt{\frac{E}{\rho}}$ long cylindrical shell; $f = \frac{1}{2\pi r}\sqrt{\frac{E}{\rho}}$ spherical shell

For a 6-m-radius cylinder of steel this is 104 Hz or a period of 10 ms and for a carbon cylinder it is 210 Hz or a period of 4.7 ms.

4.16 Cost and development of the vessel

The HYLIFE-II vessel was assumed to be made of 304 SS because the nickel would make corrosion by TF less than in ferritic steel. The present suggestion is to use ferritic steel up to 550 or 600 °C and use carbon composites at ~1000°C. The mass of the 2GWe version with 4.75 m was 530 MT. The LLNL CAD model of the Z-IFE chamber completed for the FY05 had a chamber mass of 560 MT for the steel version with 5-cm-thick structures. These results are quite consistent despite the fact that detailed stress analysis has not been completed for the Z-IFE design. The cost of ferritic steel used in the systems model is $80/kg consistent with ARIES and other IFE studies. The cost of carbon composites is uncertain, but will be higher on a $/kg basis. At the same stress the carbon composites should be about 4 times lower mass. A carbon composite vessel at the same stress can cost about 80 × 3.9 = $312/kg.

If the radius of the Z-chamber is in fact set by impact stress, then the volume of steel and cost scales with yield as shown here.

$P\tau \propto Yield/4\pi r^2$ The specific impulse can be affected by design of the liquid jets.
Using the wall stress formula above we find:
$r^2 T \propto Yield$ at constant stress, and
cost $\propto r^2 T \propto Yield$.

For carbon composite construction to be practical we need to develop methods of hermetically sealing the porous C/C perhaps with chemical vapor deposition of carbon followed by silicon layering that is reacted at 1400 °C to form a SiC layer. We need to develop joining methods, perhaps bolted joints with "O-ring" seals. We need to develop methods to repair parts. We need pipes and heat exchanges to be developed of C/C. Finally, the cost must be in the range of $400/kg to be economical, at least not several or ten times that amounting to 10% of the plant cost.

4.17 Conclusions with Respect to RTL and Chamber Design

Design alternatives are suggested to improve feasibility and economics of the Z-IFE power plant. A solid RTL made of frozen flibe greatly eases its recycle and lowers its cost. Pulsed injection of liquid above the RTL protects the upper chamber structures so that from the point of view of neutron damage these structures could be considered life of the plant components. All structures are protected by 1 m of flibe equivalent. A time motion study results in an estimated 1.9 s between pulses. This rapid pulse rate should improve economics by allowing one chamber and one driver to power the entire plant rather than needing up to ten chambers and ten power supplies for the same total power. The chamber is kept under vacuum during the operation so as to keep non-condensable gases in the transmission line and RTL below the limiting value that will short out the transmission line. We recommend against tungsten for the high-Z components in the target in order to ease recovery and recycle and lower cost. The chamber material is steel. Carbon composite materials, while not practical today, might be developed in the foreseeable future allowing much higher operating temperature with its substantially increased efficiency of conversion of thermal energy to electricity or to other uses.

References for Section 4

1. C. L. Olson, "Z-pinch inertial fusion energy," Landollt-Boernstein Handbook on Energy Technologies, Vol. VIII/s Fusion Technologies, Edited by K. Heinloth, Springer-Verlag, Berlin (2004).
2. J. A. Blink, W. J. Hogan, J. Hovingh, W. R. Meier, and J. H. Pitts, "The high-yield lithium-injection fusion-energy (HYLIFE) reactor," LLNL Report UCRL-53559 (1985).
3. L. Glenn, references 17, 18, 19, 23 and 26 of Ref. 2.
4. J. C. Liu, P. F. Peterson, and V. E. Schrock, "Blast venting through blanket material in the HYLIFE ICF reactor," *Fusion Technology,* **21,** 1514 (1992).

5. R. W. Moir, R. L. Bieri, X. M. Chen, T. J. Dolan, M. A. Hoffman, P. A. House, R. L. Leber, J. D. Lee, Y. T. Lee, J. C. Liu, G. R. Longhurst, W. R. Meier, P. F. Peterson, R. W. Petzoldt, V. E. Schrock, M. T. Tobin, W. H. Williams, "HYLIFE-II: A Molten Salt Inertial Fusion Energy Power Plant Design-Final Report," *Fusion Technology,* **25**, 5-25 (1994).
6. R. W. Moir, "Chamber, target and final focus integrated design," *Nucl. Instr. and Methods in Physic Res.* **A 464,** 140-151 (2001).
7. R. W. Moir et al, "HYLIFE-II progress report," LLNL Report UCID-211816 (1991).
8. G. Fukuda and P. Peterson, "Carbon in fluoride systems" UC Berkeley, Department of Nuclear Engineering note (8/25/2004).
9. P. A. House, "HYLIFE-II reactor chamber design refinements," *Fusion Technology*, **26,** 1178-1195 (1994).

5. Potential Figures of Merit for Transmutation Technologies

The cost of electricity (COE) is normally used to evaluate and compare competing technologies for future electric power plants. Options for transmuting nuclear waste from fission power plants could also be evaluated in terms of how much the transmutation process adds to the COE. Using COE as the only figure of merit is, however, rather limited given 1) the large uncertainty in the cost of transmutation technologies and 2) the range of other considerations and motivations for transmutation. One such motivation is clear – to minimize the mass and heat load of material that needs to be sent to high level waste (HLW) storage facilities such as Yucca Mountain. Other figures of merit include technical maturity and proliferation risks of the proposed recovery, transmutation, recycling and disposal processes.

The National Academies of Sciences report, "Nuclear Wastes: Technologies for Separation and Transmutation," evaluated light water reactors (LWR), advanced liquid metal reactors (ALMR) and accelerator transmutation of waste (ATW) technologies.[1] Some of the findings and discussions, however, are relevant to fusion-based transmutation technologies, including the Z-pinch In-Zinerator. The report acknowledges that there is no one figure of merit for transmutation approaches and proposes a variety of measures by which to evaluate and compare systems. These include:

1) Rate and time for various percentage reductions in the transuranic (TRU) inventory
2) Flexibility and rate for reducing key fission product inventories
3) Safety issues for the reactor, fuel materials, and supporting fuel cycle
4) Development time, cost, feasibility, and risk through complete demonstration
5) Estimated time scale and costs for complete deployment, including overall fuel cycle economics; and
6) Comparative thermal and electrical efficiencies per net amount of waste transmuted.

Some comments about these measures with respect to In-Zinerator follow.

The first measure, rate and time to reduce the TRU inventory by a certain percent, addresses the fundamental goal of this application. It is important to evaluate the ***net*** decrease in TRUs versus time (likely for multiple fuel cycles) since different technologies produce additional TRUs in the burning process. The NAS study was focused on fixed or declining fission power scenarios and thus focused on destroying the existing inventory. In a growing economy, a corollary figure of merit could be the number fission reactors whose waste could be burned by a single transmutation plants (likely normalized in units of thermal power). This support ratio would vary by technology and would give a sense for the efficiency of the process (i.e., fusion neutrons versus fission neutrons). The neutronics calculations being carried out as part of the In-Zinerator study should be able to supply the information needed to evaluate these figures of merit.

The second measure, flexibility and rate for reducing key fission product inventories, is another measure that should be easy to evaluate for fusion-based systems. Cesium and strontium are important fission products since they are key contributors to the heat load of spent fuel for some 70 years. It is also advantageous to destroy technetium (^{99}Tc) and iodine (^{129}I), since the principal doses to humans after long periods of time are due mainly to these water-soluble fission products.[1] A low-energy neutron spectrum is more efficient for transmuting these. Again, the

effectiveness of the In-Zinerator to destroy key fission products can be evaluated based on neutronics analyses that include proper accounting for process flow over many cycles.

The next figure of merit (3) relating to safety is one in which the fusion-based transmutation systems can expect to have some advantage over fission reactors. The fact that the fusion system operates with K-effective less than one gives it an advantage. This was pointed out as the main advantage of fusion over fast fission reactors in the Fusion Energy Sciences Advisory Committee (FESAC) report on alternate applications of fusion.[2] In this regard, it will be important that other design features of the In-Zinerator do not lead to other safety issues that compromise the system. For example, inertial fusion chambers have a first wall that is subjected to intense and repetitive threats from the target. It is important that the integrity of the components containing the fission waste in the transmuter is not compromised by the possible failure of the first wall. The current In-Zinerator design with actinides contained in separate tubes is a good way to provide a secondary barrier. Eventually, accident analyses should be carried out for the design. With regard to the safety of the fuel materials and associated fuel cycle, there should be no difference compared to fission-based systems if comparable processes are used. If alternate fuel forms or reprocessing procedures are proposed (or required) for fusion-based transmutation, the relative advantages and disadvantages can be cited. While the In-Zinerator design concept is very preliminary, it is important to keep the overall safety considerations in mind in developing proposed chamber, blanket, fuel form, and processing concepts.

It is too early in the In-Zinerator study to make estimates related to the fourth and fifth items listed above, which have to do with development time, cost, risk, and overall fuel cycle economics. Clearly any fusion-based system will take longer and have higher development risk than LWRs and ALMR systems. Fusion is likely even more speculative than ATW, since the core fusion machine has not yet been demonstrated.

The final figure of merit mentioned by the NAS report, thermal and electric efficiency per net waste burned, is related to the support ratio and overall economics. Besides the fusion components, most of the plant costs will scale as either thermal power (e.g., hear exchangers, coolant pumps, etc.) or electric power (e.g., turbine plant equipment, electrical plant equipment). Since the transmutation plant is operated near K-effective of one, the thermal power is dominated by fission. Therefore, if we express the support ratio in terms of the total fission reactor thermal power serviced divided by the transmutation plant thermal power, the support ratio primarily depends on the fuel cycle, not the transmutation technology. The expected support ratio of the In-Zinerator is ~ 4-5. Efficient conversion to electric power is important since the sale of electric power by the transmutation plant will offset the cost of transmuting the waste. Again, due to the early stages of the In-Zinerator design, estimated capital and operating costs are not available or at best very preliminary. We can, however, evaluate transmutation costs parametrically. This approach is developed in more detail is the following paragraphs.

As an example of how we might evaluate the economic impact of the In-Zinerator (or any other transmutation technology), consider the following assumptions:

- The COE for the LWR includes the cost of full reprocessing (but without transmutation). That is, we are dealing with a closed fuel cycle for fission.

- The thermal support ratio (kW_{LWR}/kW_{trans}) equals the electric support ratio (kWe_{LWR}/kWe_{trans}) and is designated SR. (Basically this means the thermal-to-electric conversion efficiency is the same for the transmutation plant as the fission plants it supports. In fact, the fusion-based transmutation plant may operate at a higher temperature and have higher thermal conversion efficiency, but that will likely be offset by recirculated power needed for the driver.)
- The cost ratio, CR, is defined as the total annual operating cost of the transmutation plant per kW (thermal or electric) divided by the total annual operating cost per kW of the fission plant. Annual costs include both capital costs (return on capital investment) and operation and maintenance (O&M) cost.
- The transmutation plant is credited for the sale of electricity at the nominal LWR COE.

Under these assumptions, we can calculate the increase in the COE due to the transmutation process. This is shown in Fig. 5.1 as a function of the support ratio and cost ratio of the fusion-based transmutation plant. Note that this is the system average COE including the costs and electric production from the transmutation plant. As an example, if the transmutation plant annual costs are 1.5 times that of an LWR (CR = 1.5) and it has a support ratio of 4, the system average COE increases by ~10%.

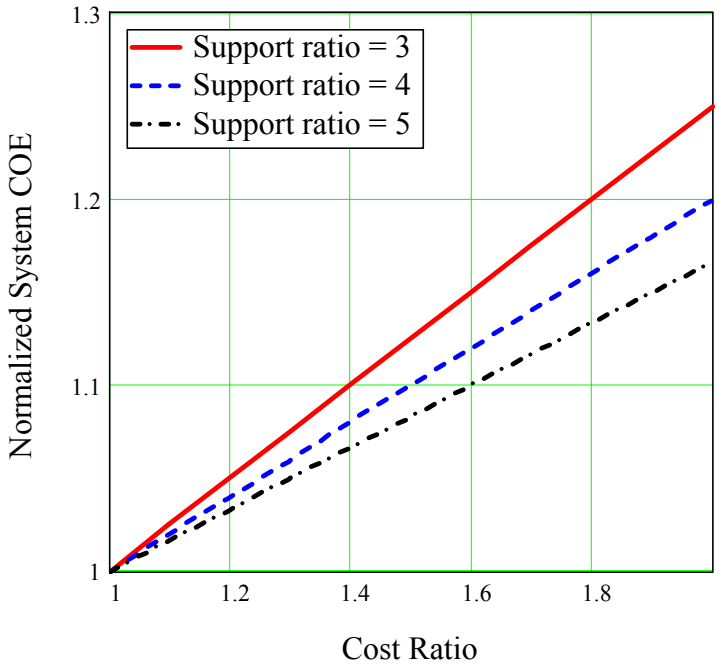

Figure 5.1: Normalized system average COE versus transmutation plant cost ratio for various support ratios.

If the net transmutation costs (total cost minus electricity sale credits at the reference LWR rate) are all attributed to the LWR fuel cycle, the impacts appear more significant. Figure 5.2 plots the normalized LWR fuel cycle cost as a function of transmutation plant cost ratio for support ratios ranging from 3-5. This figure assumes that the reference case fuel cycle without transmutation is

20% of the LWR COE. With a support ratio of 4 and cost ratio of 1.5, the LWR fuel cycle increases by 63%.

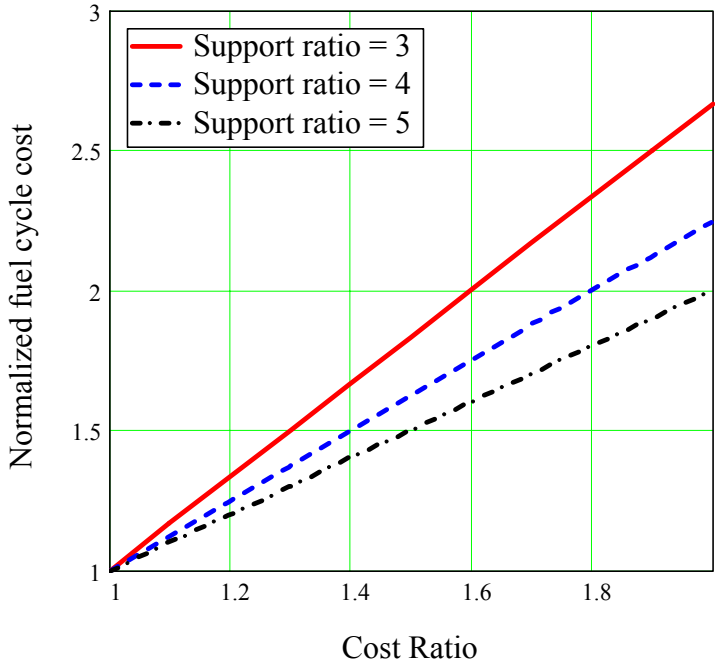

Figure 5.2: Normalized LWR fuel cycle cost versus transmutation plant cost ratio assuming all transmutation costs are attributed to the LWR fuel cycle.

These examples are only illustrative and need to be refined as design, cost, and performance details evolve for the In-Zinerator. In particular, the definition of support ratio will depend on exactly which TRU or fission products are targeted, since not all are consumed at the same rate. Differences in plant conversion efficiencies and the recirculating power for the fusion driver must also be accounted for. With more detailed information and analyses, this type of analysis can provide some sense of the potential of Z-pinch IFE for the transmutation application.

References for Section 5

1. *Nuclear Wastes: Technologies for Separations and Transmutation*, National Academy Press, Washington DC, ISBN: 0-309-56195-7 (1996).
2. "Non-Electric Applications of Fusion, Final Report to FESAC July 31, 2003," DOE report DOE/SC-076 (July 2003).

6. Suggested Improvements and Calculations for the In-Zinerator

As part of our work for SNL in FY06, we were asked to review the In-Zinerator design and provide feedback. This note documents some of the issues that were identified and suggests design improvements to address them. This note also includes several calculations related to the response of the chamber to fusion and fission energy pulses. Some of these calculations are based on scaling from calculations carried out for previous IFE chamber designs. As such they should be considered as rough estimates and verified with more detailed analyses for the In-Zinerator chamber.[1] The following topics are discussed in this section:

- Key issues with the present In-Zinerator design
- Ideas to improve the present design
- Stress on first wall
  - Impulse on first wall
  - Venting impulse
  - Thermal stress
- Neutron leakage out the top and bottom of the chamber
- Temperature and pressure rise after each pulse
- Need for materials assessment

6.1 Key Issues with the Present In-Zinerator Design

The In-Zinerator chamber is shown in Fig. 6.1 and 6.2. There are several design features that raise red flags:

1) The bare first wall will erode by ablation and suffer shock damage unless it is protected. This is a critical issue and must be resolved. The proposed use of a buffer gas may be adequate to reduce the peak heat load, but the potentially high debris fraction makes this approach difficult.
2) Without coverage at the top and bottom of the chamber, 20% of the source neutrons are lost and scattered neutron loss is increased as well. This is a lot of coverage area and performance to give up. It is not necessarily a feasibility issue, but will impact attractiveness in terms of overall transmutation rate and tritium breeding.
3) The first wall is much thicker (5 cm) than previous IFE chamber designs and will result in loss of available neutrons for transmutation and tritium breeding.

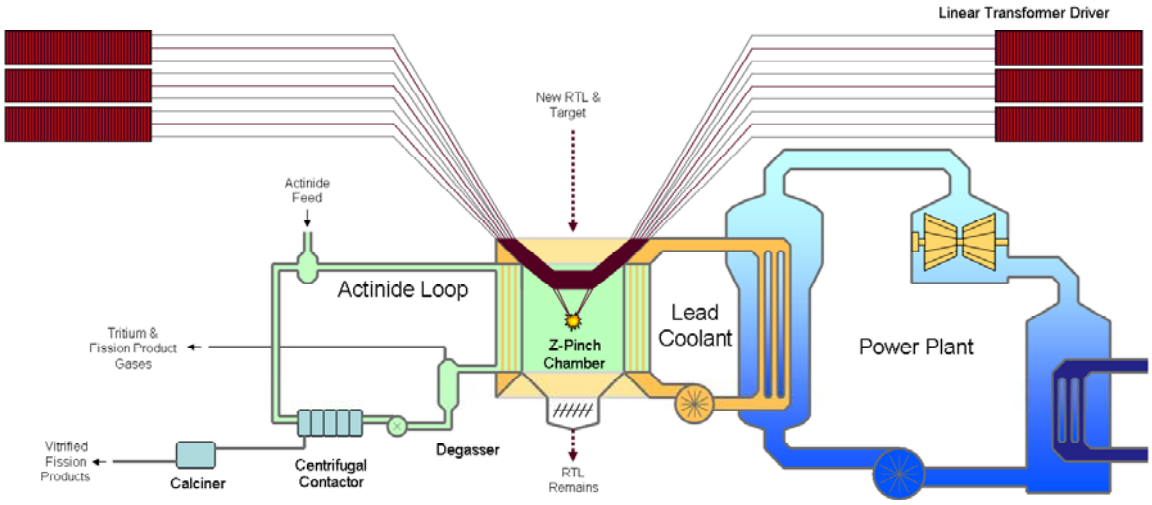

Figure 6.1: Present In-Zinerator design.

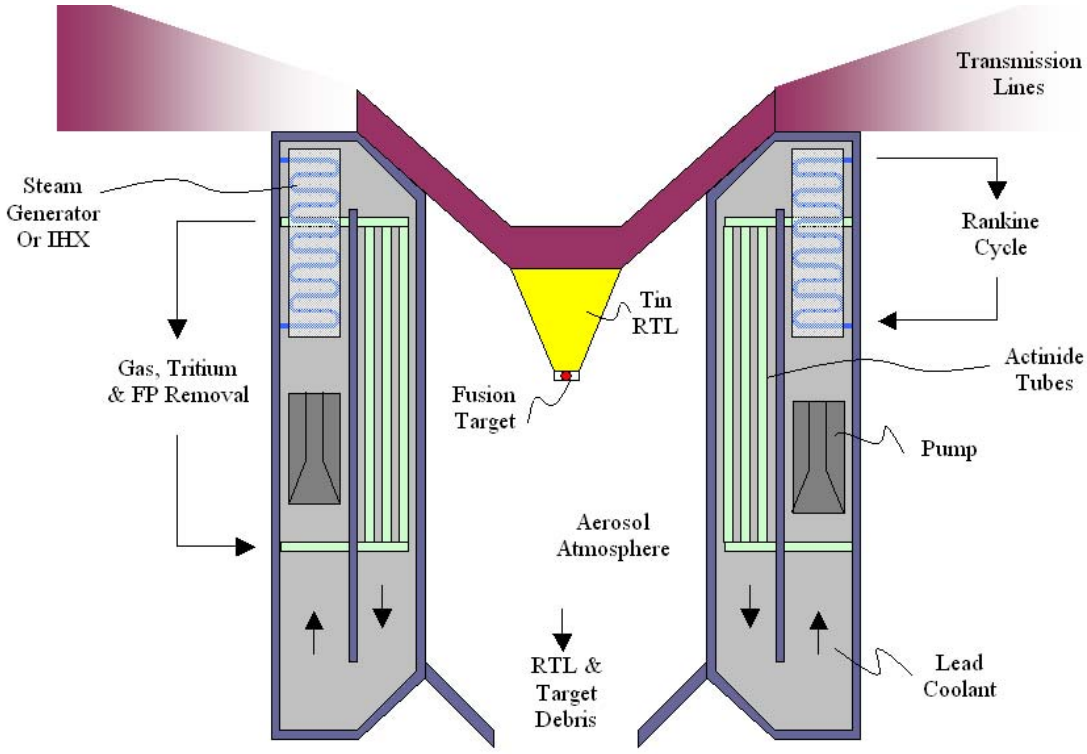

Figure 6.2: Expanded view of present chamber design.

6.2 Ideas to Improve the Present Design

In Fig. 6.3 we show schematically how top and bottom blankets can be added to improve the neutron economy. A wetted first wall of flowing liquid is added to protect against ablation. Finally we suggest using a thinner (< 5 cm) first wall if possible. (See stress calculations that follow.)

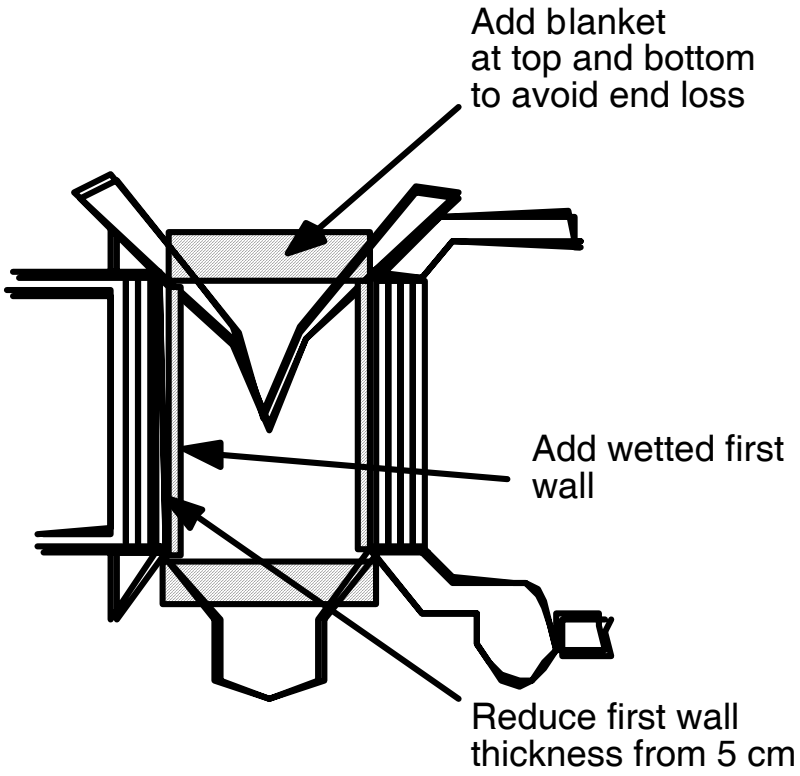

Figure 6.3: Modifications to present design.

It is easy to add the liquid wetted wall with lots of examples, for example the recent KOYO design.[2] A bottom blanket with provisions for venting and passage of RTL debris can also be added. Over 99% of the power is deposited in the flowing molten salt. An external heat exchanger would be less demanding than a heat exchanger to the lead coolant located inside the neutron flux region. These changes, i.e., adding top and bottom blankets and removing the heat exchanger from the blanket, are shown schematically in Fig. 6.4.

It is unclear how to add a blanket on top without interfering with the RTL except by the method suggested by LLNL for Z-IFE chamber. Our design for Z-IFE shown in Fig. 6.5 is a starting point for the morphed RTL. The flibe jets surrounding the target would be replaced by the tubular design of the In-Zinerator.

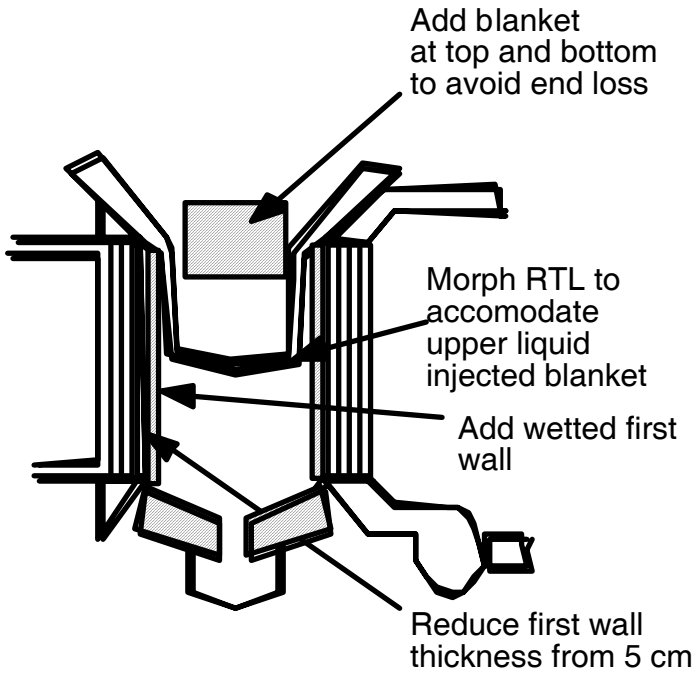

Fig. 6.4: Further modifications.

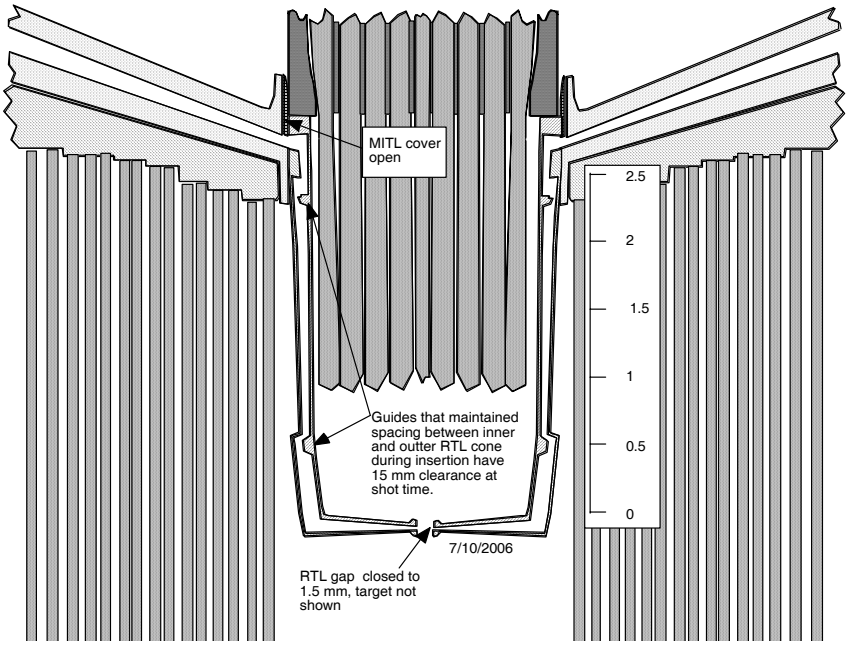

Fig. 6.5: Current LLNL Z-IFE chamber design.

6.3 Stress on the First Wall

We will calculate the impulse to the first wall and then calculate the resulting stress in the wall to see if 5 cm thickness is needed. Then we will calculate the thermal stress in the wall to see if the wall needs to be subdivided to reduce the thermal stress. The analysis is discussed in Ref. 3.

Impulse on First Wall

A yield of 200 MJ at 1.5 m from the steel wall would be about 60 MJ of x rays and debris. This is 2.1 MJ/m^2 with half coming in the first burst and half coming with the debris re-radiating in a later slower burst. This pulsed heat load exceeds the threshold of ablation by two orders of magnitude. Virtually any ablation is intolerable, and dry walls can only be used below the ablation threshold. If the wall is wetted by flibe, we estimate 15 μm will be ablated in these two pulses.[4] This amounts to (2000 kg/m^3 × 15×10^{-6} m =) 0.03 kg/m^2 and a total mass of ($4\pi 1.5^2$ × 15 μm × 2000 kg/m^3 =) 0.85 kg.

The resulting energy density in the vaporized flibe would be

$$\frac{E_{vapor}}{m^2} = 2.1\,MJ/m^2$$

$$\frac{E_{vapor}}{mass} = 2.1\,MJ/m^2 \div \frac{m^2}{0.03\,kg} = 71\,MJ/kg\,.$$

The representative vapor velocity is

$$E_{vapor} = \tfrac{1}{2}\,mass \cdot v_{vapor}^2$$

$$v_{vapor} = \sqrt{\left(\frac{2 \times E_{vapor}}{mass}\right)} = \sqrt{(2 \times 71\,MJ/kg)} = 12{,}000\,m/s,$$

and the ablative impulse to the first wall is

$$\frac{\text{Impulse}}{area} = \frac{mass}{area} \times v_{vapor} = 0.03kg/m^2 \times 12{,}000m/s = 360Pa \cdot s = \text{ablative impulse.}$$

Venting Impulse

The yield energy that is not in neutrons will fill the chamber in the form of hot gas. This gas will vent but before it does it exerts a pressure for a time on the first wall. The volume of the 4-m high 1.5 m radius chamber is $V = \pi \times 1.5^2 \times 4 = 28m^3$.

Scaling from HYLIFE-II with 350 MJ yield, a pocket of 2.1 m^3 and a pressure of 6.5 MPa gives the pressure in the In-Zinerator chamber as

$$P = 6.5\,MPa\frac{200\,MJ}{350\,MJ}\frac{2.1m^3}{28m^3} = 0.28\,MPa.$$

This is the pressure in chamber after shock waves bounce a few times but before venting out the bottom.

The time for the gas to vent out the open bottom is $\tau = \frac{V}{CA} = \frac{28\,m^3}{1230\,m/s \times \pi \times (1.5\,m)^2} = 3.3\,ms$,

where C is flibe vapor sound speed.

The impulse on the wall by the gas before it vents is

$I = P\tau = 0.28$ MPa × 3.3 ms = 920 Pa·s,

and the total impulse is from ablation and gas pressure is

$I_{total} = 360 + 920 = 1300$ Pa·s.

The resulting stress in the 5-cm-thick wall is

$$\sigma = \frac{P\tau}{T}\sqrt{\frac{E}{2\rho(1-\nu^2)}} = \frac{1300Pa \cdot s}{0.05m}\sqrt{\frac{190 \times 10^9\,Pa}{2 \times 7800kg/m^3(1-0.3^2)}} = 95MPa\,.$$

This is an acceptable stress for steel (14,000 psi).

The impulse per unit area scales as $1/r^2$. Increasing r from 1.5 m to 2 m would allow the wall to be thinned down from 5 cm to 2.8 cm at the same stress. This thinner wall would improve neutron economy.

Thermal Stress

In HYLIFE-II the first steel wall in the absence of a liquid wall diminishing the nuclear heating was 180 W/cm^3 at 3.2 m and 2.84 GW_{fusion}. Scaling this to 20 MW_{fusion} at 1.5 m gives 5.8 W/cm^3. Another way to compute the heating in iron is to divide the flux by the mean free path in iron of 7.1 cm for 14 MeV neutrons. Assuming 70% of the fusion power escapes the compressed capsule as neutrons, the heating is $= \frac{20\,MW_{fusion} \times 0.7}{4\pi(1.5m)^2 \times 0.07\,m} \approx 7\,MW/m^3 = 7\,W/cm^3$, to be compared with 5.8 W/cm^3 estimated above.

The temperature difference from the inside to the two surfaces if both are being cooled is

$$\Delta T = \frac{Qh^2}{8k} = \frac{5.8W/cm^3 \times (5cm)^2}{8 \times 0.45W/cm \cdot K} = 40K\,.$$

If the cooling were only from one side this would be 160 K. That is, suppose the wetted wall on the inside flowed so slowly that it did not remove much heat.

The resulting thermal stress for two-sided cooling would be

$$\sigma = \tfrac{2}{3}\frac{\alpha E \Delta T}{1-\nu} = \tfrac{2}{3}\frac{16.3\times10^{-6}\times190\times10^{9}\,Pa\times40\,K}{1-0.3} = 120\,MPa\ .$$

This seems to be a high but acceptable thermal stress. If the cooling were only from one side this would go up to 480 MPa. If we reduced the thickness as previously discussed to 2.8 cm and increase the radius to 2 m the thermal stress would drop to $120\,MPa\times\left(\frac{1.5}{2.0}\right)^2\left(\frac{2.8}{5.0}\right)^2 = 21\,MPa$ for two-sided cooling and 84 MPa for one-sided cooling. If we subdivide the 5 cm wall into two 2.5 cm walls each cooled from both sides the stress would drop by a factor of four.

6.4 Neutron Leakage Out the Top and Bottom of the Chamber

The idea of the In-Zinerator is to use the point source of neutrons to drive a subcritical assembly. It is a right circular cylinder of 4 m height and 1.5 m radius to the first wall. This gives an open hole at the top and bottom of 37° half angle. 20% of the source neutrons will stream out un-collided and more scattered leakage neutrons will be lost. A different kind of blanket could be placed on the top and bottom to utilize these neutrons. The neutron transport calculations should be to reviewed, especially to see if the assumptions on geometry of the upper and lower open regions are reasonable.

6.5 Temperature and Pressure Rise after Each Pulse

The first wall of the In-Zinerator chamber must be protected against the effects of ~60 MJ of x rays and debris (30% of 200 MJ) and the effects of 140 MJ of neutrons (70% of 200 MJ). 200 MJ is the equivalent energy of 48 kg of TNT. The energy multiplication of 150 in the fission blanket will give a yield of 30 GJ per pulse, the equivalent energy of 7 tons of TNT.

In HYLIFE-II we estimated a 350 MJ yield gave 250 J/g of heating in the flibe at the inner edge of the liquid pocket (at 0.5 m) resulting in 0.5 GPa pressure and a "jump off" speed of liquid spallation of 82 m/s. If a thin liquid wetted wall is added to protect the In-Zinerator chamber, the pressure and jump-off speed can be scaled from the HYLIFE-II results:

$P = 0.5GPa\times\frac{200}{350}\times\left(\frac{0.5}{1.5}\right)^2 = 0.032GPa$ = pressure in the wetted wall just after the shot, and

$v = 82m/s\times\frac{200}{350}\times\left(\frac{0.5}{1.5}\right)^2 = 5.2m/s$ = spallation speed.

The temperature rise in the actinide containing molten salt just beyond the first wall can be estimated based on HYLIFE-II results for flibe:

$$\Delta T \approx \frac{250{,}000 J/kg}{2380 J/kg \cdot K} \times \frac{30}{0.35} \times \left(\frac{0.5}{1.5}\right)^2 \approx 1000 K$$ = the temperature rise.

Assuming a starting temperature of 675 °C, the peak temperature after each shot is T = 675 + 1000 = 1675 °C. This will results in a cyclic fatigue problem in nearby structures in addition to the pressure pulse problems. The molten salt vapor pressure will be about 1 atmosphere. The second and third terms in the equation for ΔT give the scaling of 9.5 times that of HYLIFE-II.

The pressure in the actinide containing molten salt just after the shot is:

$$P = 0.5 GPa \times \frac{30}{0.35} \times \left(\frac{0.5}{1.5}\right)^2 = 4.8 GPa .$$

The spallation speed of this liquid if it were unconstrained is:

$$v = 82 m/s \times \frac{30}{0.35} \times \left(\frac{0.5}{1.5}\right)^2 = 780 m/s .$$

The effects of the 30 GJ of yield can be somewhat mitigated by injection or sparging with bubbles. Even considering use of bubbles, this pressure of 4.8 GPa and 780 m/s spallation speed amounts to a serious problem. Maybe there is experience and relevant data from burst reactors to get an idea of the effects to be expected. The isochoric pressures in the steel and lead will be two orders of magnitude lower because the heating is primarily in the molten salt and only indirectly in the lead and in the steel from the fission process.

6.6 Need for Materials Assessment

A materials assessment is needed. The chamber materials must be compatible both with lead and with molten salt. This molten salt is not in a reduced chemical state compared to flibe. It must be in a reasonably high oxidation state (fluoridation state) to keep from precipitating out metallic actinides on the walls. The melting point of actinides was mentioned to be 675 °C. Freeze-up and corrosion are important issues.

References for Section 6

1. B.B. Cipiti, “Fusion Transmutation of Waste and the Role of the In-Zinerator in the Nuclear Fuel Cycle,” SAND2006-3522, June 2006.
2. S. Nakai, et al., “Development of Laser Fusion Power Plant KOYO,” 16th IAEA Fusion Energy Conference IAEA-CN-64/G1-3/GP-17, Montreal, Canada, 7-11 Oct. 1996.
3. R. W. Moir, “Chamber, target and final focus integrated design,” *Nuclear Instruments and Methods in Physics Research A* **464,** 140-151 (2001).
4. R. W. Moir et al., "HYLIFE-II Progress Report," UCRL-ID-21816 (1991). Fig. 4-4, p.4-8.

Appendix A

Printout of Z-IFE Systems Code

The following PDF file is a printout of the complete Z-IFE systems code, which is written in Mathcad®.

Z-IFE Systems Model
September, 2006
Wayne Meier, LLNL (meier5@llnl.gov)

This preliminary systems model for a Z-pinch driven IFE power plants is based on the following primary sources of information:

- Target performance info is from C. Olson TOFE presentation (2004) and Roger Vesey presentation at Z-IFE project meetings (Aug, 2005).

- Most chamber and power plant scaling relationship are from OSIRIS heavy ion driven power plant study, which was a molten salt breeder and coolant. Also some info is from the HYLIFE-II thick liquid wall chamber design.

- Material costs (steel, etc.) are consistent with HAPL systems model for laser IFE.

- Target manufacture cost baseline is from SNL study. Flibe RTL is the base case here.

- Z-pinch driver cost evaluated parametrically. $15/J (re C. Olson) is base case value.

Target Gain - Based on Dynamic Hohlraum. Presentation (8/05) by Roger Vesey included points 1 and 3 below. Olson's 2005 TOFE paper gave info for the 3000 MJ yield design (point 2). Define target gain in terms of energy supplied by Z-pinch.

$i := 1, 2 .. 3$

Current	Absorbed , MJ	Pinch energy, MJ	Yield, MJ	Target Gain
$I_i :=$	$Ea_i :=$	$Epin_i :=$	$Y_i :=$	$Gp_i := \frac{Y_i}{Epin_i}$
56	2.4	14	530	$Gp_i =$ 37.9
86	6	32	3000	93.8
95	7.2	42	4600	109.5

Find gain scaling equation of form $G = a(E-b)^c$ that fits these three points. Fit yield point, i.e., G*E.

$a := 10$ $b := 10$ $c := 0.5$ guess values

Given

$a \cdot (14 - b)^c \cdot 14 = 530$ $a \cdot (32 - b)^c \cdot 32 = 3000$ $a \cdot (42 - b)^c \cdot 42 = 4600$

$\text{Find}(a, b, c) =$

30.04
12.17
0.38

This resulting target gain scaling with driver energy is weaker than Perkins finds for laser direct-drive target which go like ~ $E^{0.6}$. However, if we only consider the two high yield points, the scaling is ~ $E^{0.5}$.

$G(E) := 30.15 \cdot (E - 12.2)^{0.38}$ $G(14) = 37.7$ $G(32) = 93.8$ $G(42) = 109.5$

$Ed := 0, 1 .. 50$ Target gain vs Z-pinch energy

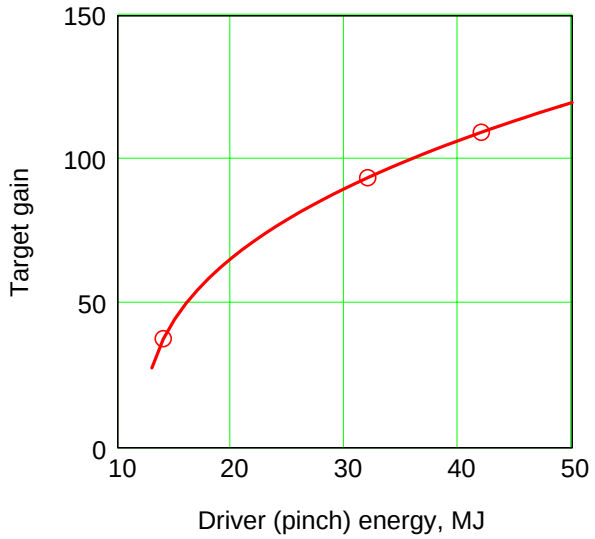

Target yield, MJ

$Y(E) := G(E) \cdot E$

$Y(14) = 528$

$Y(32) = 3000$

$Y(42) = 4600$

$Y_i =$

530.0
3000.0
4600.0

Good fit to reported gain points

Define a reference point for example calculations throught the code.

$Eo := 42$ $Y(Eo) = 4600$

Yield vs pinch energy
Calculated points shown

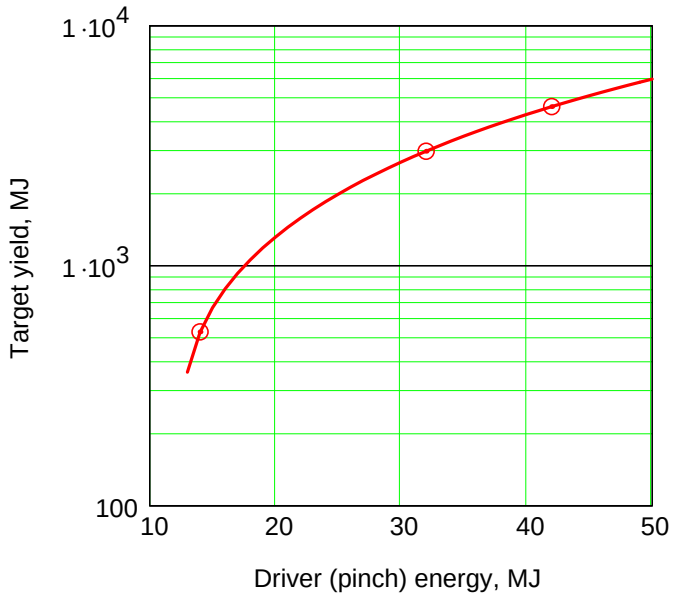

Power Balance:

RR = rep-rate, HZ $RRo := 0.5$ Baseline repetition rate for proposed LLNL design. This is higher than SNL 0.1 Hz base case and 0.3 Hz "stretch" case.

Energy multiplication factor (applied to total fusion power not just neutron fraction)

$M := 1.15$ UW 8/05 presentation: M = 1.115 for flibe, = 1.187 for PbLi
Meier 5/05 ISFNT paper: M = (16.73+3.53)/17.6 = 1.15 for flibe

Thermal-to-electric conversion efficiency (use 42% for steel chamber, 50% for C/C composite chamber).

$\eta e := 0.42$

Driver efficiency. For now assume it is fixed. It could be a function of rep-rate, so dependence is included but not used at this point.

$\eta d(RR) := 0.6$ Based on Tom Mehlhorn talk, 8/05 for dynamic hohlraum target and Linear Transformer Driver (LTD).

Fusion Power, MW

$Pf(E, RR) := Y(E) \cdot RR$ $\quad Pf(Eo, RRo) = 2299.9$

Thermal power, MWt

$Pth(E, RR) := Pf(E, RR) \cdot M$ $\quad Pth(Eo, RRo) = 2644.9$

Gross electric power, MWe

$Pg(E, RR) := Pth(E, RR) \cdot \eta e$ $\quad Pg(Eo, RRo) = 1110.9$

Driver power consumption, MWe

$Pd(E, RR) := \frac{E \cdot RR}{\eta d(RR)}$ $\quad Pd(Eo, RRo) = 35.0$

Auxiliary power for plant (4% of gross electric)

$Paux(E, RR) := 0.04 \cdot Pg(E, RR)$ $\quad Paux(Eo, RRo) = 44.4$

Flibe pumping power

Igor Sviatoslavsky presentation, 8/05 for flibe. Assume height scales with Y^0.5. Proposed intermittent flow, so assume scales directly with rep-rate.

$Ppump(E, RR) := 0.66 \cdot \frac{RR}{0.1} \cdot \left(\frac{Y(E)}{3000}\right)^{0.5}$ $\quad Ppump(Eo, RRo) = 4.1$

Moir result - Velocity set to maintain good liquid coverage at midplane (moderate thinning compared to packing fraction at the nozzle plate).

$Hc(E) := 8 \cdot \left(\frac{Y(E)}{4600}\right)^{0.5}$ LLNL chamber height from bottom of nozzle to collection vanes

$Hx := 4$ Extra height for flow collection at bottom plus 2 m head above nozzle plate.

LLNL FY06 report calculation based on total height of 12 m. Includes 50% velocity head recovery from flow at bottom of chamber.

$Ppump(E, RR) := 30 \cdot \frac{Hc(E) + Hx}{12}$ $\quad Ppump(Eo, RRo) = 30.0$

RTL factory power, MWe

$PRTLfo := 13.5$

$PRTLso := 184$

SNL study gave 13.5 MWe for flibe RTL and 184 MWe for steel RTL at 1 Hz (0.1 Hz per chamber times 10 chambers) and 3000 MJ yield target (pinch energy = 32 MJ). Assume this scales with rep-rate and driver energy (larger RTL for larger drivers). Use flibe as base case.
Since the calculation here are based on power per chamber, the RR term does not need to be multiplied by the number of chambers per power plant.

$$PRTL(E, RR) := PRTLfo \cdot \frac{RR}{1.0} \cdot \frac{E}{32} \qquad PRTL(Eo, RRo) = 8.9$$

Total recirculated power, MWe

$$Pcirc(E, RR) := Pd(E, RR) + Paux(E, RR) + Ppump(E, RR) + PRTL(E, RR)$$

$$Pcirc(Eo, RRo) = 118.3$$

Net electric power, MWe

$$Pnet(E, RR) := Pg(E, RR) - Pcirc(E, RR) \qquad Pnet(Eo, RRo) = 992.6$$

Thus the reference case parameters (4.6 GJ yield targets at 0.5 Hz) give ~ 1 GWe plant with a single chamber.

Net electric power vs driver energy if rep-rate is fixed at RRo $RRo = 0.5$

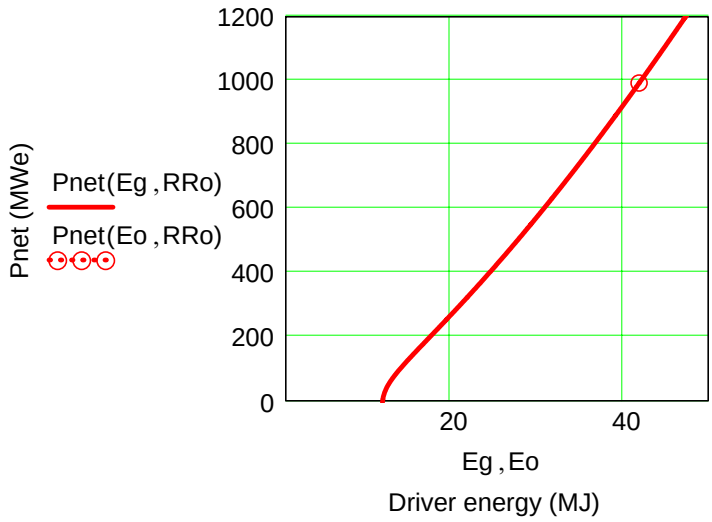

The 10 unit plant operating at 0.1 Hz per chamber with the same net power would be have a driver energy calculated here.

$Egv := 20$ guess value to start search

$$E10 := root(Pnet(Egv, 0.1) \cdot 10 - Pnet(Eo, RRo), Egv)$$

$E10 = 30.9$ $\quad Pnet(E10, 0.1) \cdot 10 = 992.6$ $\quad Pnet(Eo, RRo) = 992.6$

Most of the cost scaling equations are taken from the Osiris reactor study, which used molten salt coolant.

Inflation factor to convert from 1991$ (Osiris study) and 2005$ based on GDP Implicit Price Deflator. This is applied at end of costing.

$Inflate := 1.33$

The current SNL reference power plant design assumes multiple chambers supplied by a common RTL recyling/manufacturing system and common target factory. Each chamber, however, has its own pulsed power driver, heat transfer systems and power generation equipment. Thus, multiple, small power chambers suffer from significant economy of scale disadvantage compared to a single chamber and driver with the same net power. Nc is the number of chambers at the site.

$Nco := 1$ Reference case is a single chamber

20 Land and Land Rights

$CLLR := 11.6$

21 Structures and Site Facilities

21.1 Site improvements and Facilities (assume this scale as total site power)

$$CSI(E, RR, Nc) := 13.6 \cdot \left(\frac{Pg(E, RR) \cdot Nc}{1100} \right)^{0.5} \qquad CSI(Eo, RRo, Nco) = 13.7$$

21.2 Reactor Building

$$CRB(E, RR) := 32.1 \cdot \frac{Pg(E, RR)}{1100} \qquad CRB(Eo, RRo) = 32.4$$

21.3 Tubine and Controls Buildings

$$CTB(E, RR) := 29.0 \cdot \left(\frac{Pg(E, RR)}{1100} \right)^{0.5} \qquad CTB(Eo, RRo) = 29.1$$

21.4 Cooling System Structure

$$CCS(E, RR) := 5.1 \cdot \left(\frac{Pg(E, RR)}{1100} \right)^{0.5} \qquad CCS(Eo, RRo) = 5.1$$

21.5 Driver Building - Assume the driver (pulsed power) doubles the cost of the reactor building

$$CDB(E, RR) := CRB(E, RR) \qquad CDB(Eo, RRo) = 32.4$$

21.6 Miscellaneous Buildings (assume this scales with total site power)

$$CMB(E, RR, Nc) := 26.9 \cdot \left(\frac{Pg(E, RR) \cdot Nc}{1100} \right)^{0.5} \qquad CMB(Eo, RRo, Nco) = 27.0$$

Total Structures and Facilities

$$CSSF(E, RR, Nc) := CSI(E, RR, Nc) + CRB(E, RR)\cdot Nc + CTB(E, RR)\cdot Nc + CCS(E, RR)\cdot Nc \ldots + CDB(E, RR)\cdot Nc + CMB(E, RR, Nc)$$

$$CSSF(Eo, RRo, Nco) = 139.8$$

Sanity check: Osiris base case with yield of 432 MJ and thermal power of 2505 MWt had total structures and site facilities cost of $137.6M. Compare to above scaling.

$Y(13.4) = 433.0$

$Pth(13.4, 5.03) = 2504.6$

$CSSF(13.4, 5.03, 1) = 134.3$ Result is consistent

Reactor Plant Equipment

22.1 Fist wall, blanket and vacuum vessel

Here we use the cost data from the HAPL ferritic steel chamber

From 8/05 SNL meeting, UW talk by El Guebaly gave
3 GJ, 0.1 Hz per chamber
Flibe volume:
in chamber vol = 800 m^3/10
total volume = 1600 m^3/10
unit cost = 43/kg

Steel wall thickness = 30 cm (UW value)
10 m diameter
6 m high (ellipsoidal)
Replacement volume = 150/10 m^3 (6-20 FPY)
Permanent = 630/10 m3
Total = 780/10 = 78m^3
Cipeti used 15 cm

$\rho st := 7800$ Ferritic steel density, kg/m^3

$\rho flibe := 2000$ Flibe density, kg/m^3

$\rho car := 1700$ Density of carbon composite, kg/m^3

Unit costs, $/kg (Personal communication with L. Wagner, all in 2003$ scaled from ARIES docs)

$UCbst := 76.23$ Reduce Activation FS - blanket structures, from ARIES AT 2003$

$UCvvst := 31.53$ RA FS for vacuum vessel, from ARIES AT 2003$

$UCcar := 10\cdot 23.63$ Assume cost of carbon composite = 10x cost of graphite
cost from Waganer in 2003 $

For the UW elliptical chamber:

$$Rw(E) := 5 \cdot \left(\frac{Y(E)}{3000} \right)^{0.5}$$

Elliptical chamber had 5 m radius, 3 m half height. Assume these scale with square root of target yield.

$$Hw(E) := 3 \cdot \left(\frac{Y(E)}{3000} \right)^{0.5}$$

Wall thickness, m

$$\Delta w := 0.3$$

Outer radius and height

$$Rwo(E) := Rw(E) + \Delta w$$

$$Hwo(E) := Hw(E) + \Delta w$$

Volume of steel wall (equation for elliptical shell)

$$Vw(E) := \frac{4 \cdot \pi}{3} \cdot \left(Rwo(E)^2 \cdot Hwo(E) - Rw(E)^2 \cdot Hw(E) \right)$$

Check result - UW quoted 78 m3 for their 3000 MJ reference case

$Y(33) = 3152.6$ $Vw(32) = 74.1$ This scaling result is slightly less.

Cost of chamber, $M 2003$

$$Cch03(E) := UCbst \cdot Vw(E) \cdot \rho st \cdot 10^{-6}$$ $Cch03(Eo) = 66.7$

Put in 1991$ to be consistent with other plant costs (2003$ = 1.27*1991$)

$$Cch(E) := \frac{Cch03(E)}{1.27}$$ $Cch(Eo) = 52.5$

Also include LLNL chamber example. This chamber is more cylindrical and is designed to handle the large flow being directed into flow return channels. Could consider both steel and C/C versions.

$$Vch(E) := 108 \cdot \left(\frac{Y(E)}{4600} \right)$$

LLNL CAD drawing from FY05 report has total structure volume of 215m^3 for C-C version with 10-cm-thick walls. Steel chamber (base case) would be ~1/2 that amount (= 108 m^3). Assume it scales as of yield since area and thickness both scale as Y^1.2.

For a carbon composite chamber (put in 1991$ to be consistent with other costs before escalation)

$$Cch(E) := UCcar \cdot Vch(E) \cdot 2 \cdot \rho car \cdot 10^{-6} \cdot \frac{1}{1.27} \qquad Cch(Eo) = 68.3$$

For the steel chamber (in 1991$) Note that 107 m^3 includes flow diffuser at bottom of chamber. This accounts for ~36 of 108 m^3)

$$Cch(E) := UCbst \cdot Vch(E) \cdot \rho st \cdot 10^{-6} \cdot \frac{1}{1.27} \qquad Cch(Eo) = 50.6$$

22.2 Breeding Material (also coolant). Sum of head above nozzle, liquid in chamber, liquid in collection region at bottom and liquid in recirculating pumps and pipes. Assume 4m outer and 1 m inner radius for nozzle and jet array. Assume return flow at 5 m/s.

Vol in head

$$Vhead := \pi\left(4^2 - 1^2\right) \cdot 2 \qquad Vhead = 94.2$$

Vol in chamber

$$Hch(E) := Hc(E)$$

Set chamber height: = Hc for LLNL design, = 2*Hw for UW design

$$Vinch(E) := \pi \cdot \left(4^2 - 1^2\right) \cdot 0.33 \cdot Hc(E) \qquad Vinch(Eo) = 124.4$$

At lower yield of 3000 MJ: $Vinch(32) = 100.5$ Compared to UW result of 80 m^3 per chamber

Vol in collection region (or pool)

$$Vcol := Vhead$$

Vol in return pipes = (flow rate/flow velocity) * return height

$$Vpipes(E, RR) := Vinch(E) \cdot RR \cdot \frac{1}{5} \cdot Hc(E) \qquad Vpipes(Eo, RRo) = 99.5$$

Total volume of flibe

$$Vflibe(E, RR) := Vhead + Vinch(E) + Vcol + Vpipes(E, RR) \qquad Vflibe(Eo, RRo) = 412.4$$

Cost of breeding material (flibe) at $43/kg (UW talk 8/05). Convert to 1991 dollars.

$$CBM(E, RR) := Vflibe(E, RR) \cdot \rho flibe \cdot 43 \cdot 10^{-6} \cdot \frac{1}{Inflate} \qquad CBM(Eo, RRo) = 26.7$$

22.3 Vacuum system

$$CVAC := 5$$

22.4 Target systems

Here we consider the RTL as part of the target. There are two main parts of the target cost: the RTL and the fuel capsule. SNL estimate RTL plant direct capital cost for both steel and flibe RTLs. They also calculated power consumption, which is significant especially for the steel RTL plant.

SNL RTL factory direct capital cost ($M). Ref 8/05 workshop presentations by Cipiti.

For Fe RTL $CRTLo := 623$ $M

For Flibe RTL $CRTLo := 124$

Assume capital costs scale as production rate to the 0.7 power and directly proportional to the drive energy. Assume that power is proportional to RR and E. Using E=32MJ, Y= 3000 MJ, RR = 10*0.1 Hz = 1.0 Hz (i.e., one factory for 10 unit plant) as reference cost point.
Probably need better determination of how mass of RTL and cost scale with driver energy
Here I divide by 1991-2005 inflation factory (1.33) to put on same basis as other costs. Inflation then applied at end.

Here I include the possibility that the RTL and target factory are shared by Nc chamber. All other subsystems are dedicated to a single chamber (driver, heat exchangers, turbines, etc.)

$$CRTL(E, RR, Nc) := CRTLo \cdot \left(\frac{RR \cdot Nc}{1.0}\right)^{0.7} \cdot \left(\frac{E}{32}\right) \cdot \frac{1}{1.33}$$

For Flibe:

$CRTL(Eo, RRo, Nco) = 75.3$ $CRTL(E10, 0.1, 10) = 90.0$

Also must include the cost of fuel capsules. Here we use the same cost scaling relationship as direct driver capsules for laser IFE (from the HAPL Program systems code) and increase it by 100% to account for more complex indirect drive design.

Target Factory Equipment and Buildings
Scaling of GA study results
$64.7 M in 2002$ for GA reference case (5.8 Hz, 350 MJ, 2030 MWfusion)

$$CTF02(E, RR, Nc) := 2 \cdot 64.7 \cdot \left[0.14 + 0.73 \cdot \left(\frac{RR \cdot Nc}{5.8}\right)^{0.57} \dots + 0.13 \cdot \left(\frac{Pf(E, RR \cdot Nc)}{2030}\right)^{0.67} \right]$$

Convert to 1991$ to put on same basis as other costs
(GNP IPD ratio = 1.03552/0.83623 = 1.24)

$$CTF(E, RR, Nc) := \frac{CTF02(E, RR, Nc)}{1.24}$$ $CTF(Eo, RRo, Nco) = 48.2$

Total Target Systems = RTL factory plus target factory

$$CTS(E, RR, Nc) := CRTL(E, RR, Nc) + CTF(E, RR, Nc)$$

$Pnet(Eo, RRo) = 992.6$ $\quad CTS(Eo, RRo, Nco) = 123.5$ for 1 chamber, 1.0 GWe

$Pnet(E10, 0.1)\cdot 10 = 992.6$ $\quad CTS(E10, 0.1, 10) = 149.6$ for 10 chambers, 100 MWe each

22.5 Tritium recovery

$$CTR(E, RR) := 41\cdot\left(\frac{Pth(E, RR)}{3300}\right)$$

Possibly could be a shared system for multiple chambers but since scaling is linear, there is little difference if we multiply single chamber by Nc or scale with thermal power of NC chambers.

22.7 Heat Transport System

Primary coolant piping

$$CPP(E, RR) := 27.0\cdot\left(\frac{Pth(E, RR)}{2450}\right)^{0.5} \qquad CPP(Eo, RRo) = 28.1$$

Primary (Flibe) pumps and motors

Osiris flibe flow rate through the chamber was equal to flow rate to the IHX and was set by power removal needs, whereas Z-IFE flow rate is set by need to establish thick liquid wall. Osiris had 150 C ΔT in heat exchanger for reference 2450 MWt corresponding to
2450E6 W / (150 K * 2380 J/kg-K * 2000kg/m^3) = 3.4 m^3/s. Use this to scale Z-IFE pumps and pipes. Chamber flow rate (min) = Vol of flibe in chamber * RR. Scale as square root of flow rate.

$$CPRP(E, RR) := 22.1\cdot\left(\frac{Vinch(E)\cdot RR}{3.4}\right)^{0.5} \qquad CPRP(Eo, RRo) = 94.5$$

IHX

$$CIHX(E, RR) := 97.8\cdot\left(\frac{Pth(E, RR)}{2450}\right) \qquad CIHX(Eo, RRo) = 105.6$$

Secondary Loop Piping

$$CSP(E, RR) := 14.6\cdot\left(\frac{Pth(E, RR)}{2450}\right)^{0.5} \qquad CSP(Eo, RRo) = 15.2$$

Secondary Coolant Pumps and Motors

$$CSPM(E, RR) := 25.2\cdot\left(\frac{Pth(E, RR)}{2450}\right)^{0.74} \qquad CSPM(Eo, RRo) = 26.7$$

Secondary coolant clean-up

$$CSCU(E, RR) := 4.0 \cdot \left(\frac{Pth(E, RR)}{2450} \right)^{1.5} \qquad CSCU(Eo, RRo) = 4.5$$

Steam Generators

$$CSG(E, RR) := 58 \cdot \left(\frac{Pth(E, RR)}{2450} \right)^{0.89} \qquad CSG(Eo, RRo) = 62.1$$

Total HTS cost

$$CHTS(E, RR) := CPP(E, RR) + CPRP(E, RR) + CIHX(E, RR) \ ... \\ + CSP(E, RR) + CSPM(E, RR) + CSCU(E, RR) \ ... \\ + CSG(E, RR)$$

$$CHTS(Eo, RRo) = 336.6$$

Remote maintenance equipment
Bechtel's allowance (assume this can be shared by all chambers in the case of multi-chamber plants, i.e., it is somewhat mobile)

$$CRM := 100$$

Total reactor plant equipment

$$CRPE(E, RR, Nc) := Cch(E) \cdot Nc + CBM(E, RR) \cdot Nc + CVAC \cdot Nc \ ... \\ + CTS(E, RR, Nc) + CTR(E, RR) \cdot Nc + CHTS(E, RR) \cdot Nc + CRM$$

1 chamber, 0.5 Hz/chamber plant $CRPE(Eo, RRo, Nco) = 675.2$

10 chamber, 0.1 Hz/chamber plant $CRPE(E10, 0.1, 10) = 1655.8$

Turbine Plant Equipment

Recall that $Pg(Eo, RRo) = 1110.9$

$$CTPE(E, RR) := 221.5 \cdot \left(\frac{Pg(E, RR)}{1100} \right)^{0.8} \qquad CTPE(Eo, RRo) = 223.2$$

Electrical Plant Equipment

$$CEPE(E, RR) := 65.6 \cdot \left(\frac{Pg(E, RR)}{1100} \right)^{0.4} \qquad CEPE(Eo, RRo) = 65.9$$

Miscellaneous Plant Equipment

$$CMPE(E, RR) := 18.4 \cdot \left(\frac{Pg(E, RR)}{1100} \right)^{0.3} \qquad CMPE(Eo, RRo) = 18.5$$

Heat Rejection Equipment (assume this is shared by Nc chambers)

$$CHRE(E, RR, Nc) := 44.0 \cdot \left(\frac{Pth(E, RR) \cdot Nc - Pg(E, RR) \cdot Nc}{1350} \right)^{0.8}$$

$$CHRE(Eo, RRo, Nco) = 48.7$$

Total Reactor and BOP (includes target factory)

$$CR1(E, RR, Nc) := CLLR + CSSF(E, RR, Nc) + CRPE(E, RR, Nc) + CTPE(E, RR) \ ... \\ + CEPE(E, RR) + CMPE(E, RR) + CHRE(E, RR, Nc)$$

Inflate from 1991$ to 2005$ $\qquad CR1(Eo, RRo, Nco) = 1182.9$

$Inflate = 1.33$

$CR(E, RR, Nc) := Inflate \cdot CR1(E, RR, Nc)$

1 chamber, 0.5 Hz/chamber plant $\qquad CR(Eo, RRo, Nco) = 1573.2$

10 chamber, 0.1 Hz/chamber plant $\qquad CR(E10, 0.1, 10) = 2727.1$

Driver (Z-pinch) Cost - for now just using $/J

$UCdo := 15$ Base case assumes $15/J. C. Olson's 12/04 FPA talk quotes $30/J demonstrated on Z and states that LTD could be 1/2 the cost. Assume this is 2005$.

$Cd(E, UCd) := UCd \cdot E \qquad Cd(Eo, UCdo) = 630.0$

Total Direct Capital Cost

$$CTDC(E, RR, Nc, UCd) := CR(E, RR, Nc) + Cd(E, UCd) \cdot Nc$$

$$CTDC(Eo, RRo, Nco, UCdo) = 2203.2$$

Cost of Electricity Calculation

Total Capital Cost. Indirect cost multiplier is based on LSA-2. This is same assumption as used in other IFE and most MFE plant studies.

$$TCC(E, RR, Nc, UCd) := 1.936 \cdot CTDC(E, RR, Nc, UCd)$$

$$TCC(Eo, RRo, Nco, UCdo) = 4265.5$$

Annual O&M Cost for Plant
Based on LSA-2

$$OMP(E, RR, Nc) := 66.4 \cdot \left(\frac{Pg(E, RR) \cdot Nc}{1200} \right)^{0.5} \cdot Inflate$$

$$OMP(Eo, RRo, Nco) = 85.0$$

Target factory O&M (From General Atomics study)

$$OMTF02(E, RR, Nc) := 17.1 \cdot \left(\frac{CTF02(E, RR, Nc)}{64.7} \right) + 1.7 \cdot \frac{RR \cdot Y(E) \cdot Nc}{5.8 \cdot 350}$$

Convert to 2005$ (GNP IPD for 2002 to 2005 = 110.89/103.552 = 1.071

$$OMTF(E, RR, Nc) := OMTF02(E, RR, Nc) \cdot 1.071$$

Total O&M

$$OMTF(Eo, RRo, Nco) = 19.0$$

$$OM(E, RR, Nc) := OMP(E, RR, Nc) + OMTF(E, RR, Nc)$$

$$OM(Eo, RRo, Nco) = 103.9$$

$$OM(E10, 0.1, 10) = 117.8$$

Decommissioning - from guidelines

$$COED := 0.05$$

Constant Dollar Cost of Electricity, cents/kWeh

$CF := 0.85$ Plant capacity factor

$$COE(E, RR, Nc, UCd) := \frac{0.0966 \cdot TCC(E, RR, Nc, UCd) + OM(E, RR, Nc)}{0.0876 \cdot CF \cdot Pnet(E, RR) \cdot Nc} + COED$$

$$COE(Eo, RRo, Nco, UCdo) = 7.0$$

$$COE(E10, 0.1, 10, UCdo) = 20.3$$

$RRg := 0.1, 0.15 .. 0.5$

Cost of electricity vs chamber rep-rate for different driver cost assumptions
(+/- factor of two around base case of $15/J)
Ed = 42 MJ, Y = 4600 MJ, 1 chamber plant

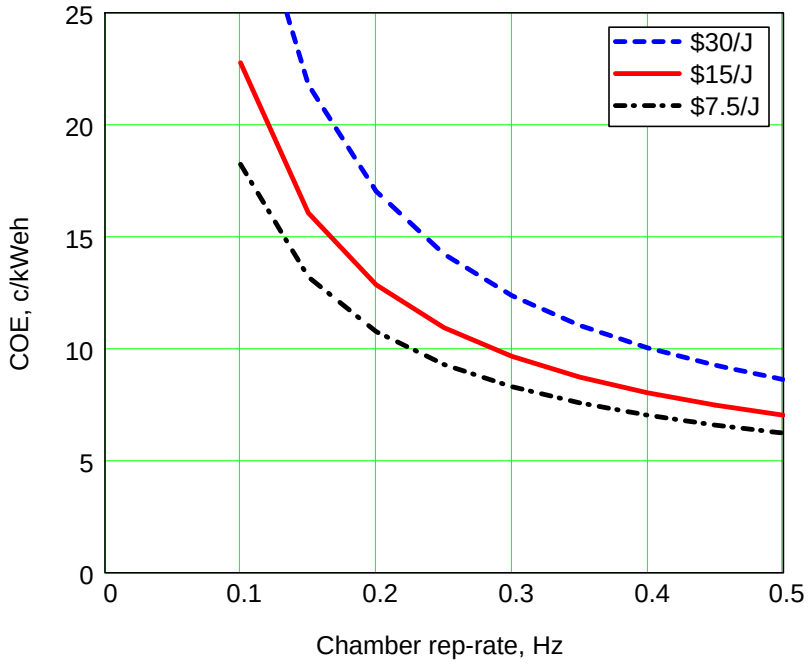

Calculate the driver enegy for a fixed net power, Pfo

$Pfo := 1000$ Fixed 1000 MWe

$Edgv := 3$ guess value

$RRg := 0.1, 0.2 .. 0.5$ Evaluate for range of rep-rates

$Edf(RR, Nc, Pfix) := root(Pnet(Edgv, RR) \cdot Nc - Pfix, Edgv)$

1 chamber 2 chambers

$$RRg = \begin{pmatrix} 0.1 \\ 0.2 \\ 0.3 \\ 0.4 \\ 0.5 \end{pmatrix} \quad Edf(RRg, 1, Pfo) = \begin{pmatrix} 127.4 \\ 78.2 \\ 59.2 \\ 48.8 \\ 42.2 \end{pmatrix} \quad Edf(RRg, 2, Pfo) = \begin{pmatrix} 80.4 \\ 49.9 \\ 38.2 \\ 31.9 \\ 27.8 \end{pmatrix}$$

5 chambers 10 chambers

$$RRg = \begin{pmatrix} 0.1 \\ 0.2 \\ 0.3 \\ 0.4 \\ 0.5 \end{pmatrix} \quad Edf(RRg, 5, Pfo) = \begin{pmatrix} 45.5 \\ 29.0 \\ 22.9 \\ 19.7 \\ 17.8 \end{pmatrix} \quad Edf(RRg, 10, Pfo) = \begin{pmatrix} 31.0 \\ 20.6 \\ 17.0 \\ 15.3 \\ 14.3 \end{pmatrix}$$

RRq := 0.1 , 0.15 .. 0.5

Driver energy required for fixed net power vs chamber rep-rate for various number of chambers per plant

Pfo = 1000.0 MWe

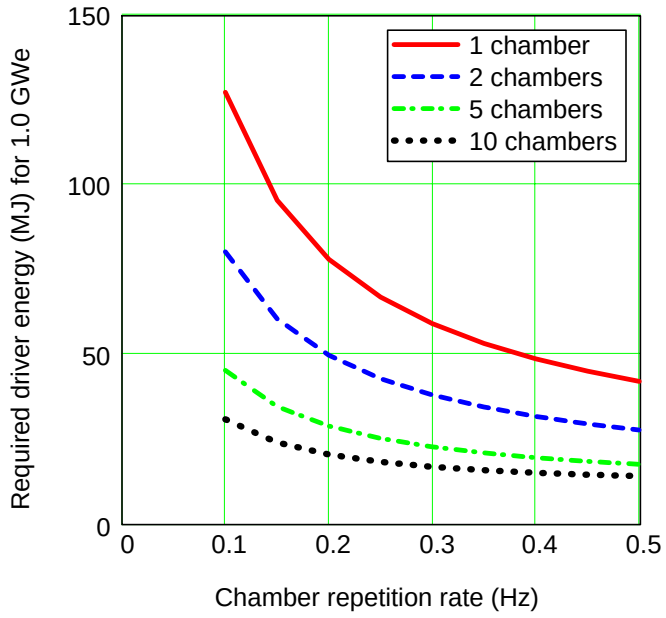

COE vs chamber rep-rate for various number of chambers per plant. Driver cost = $15/J.

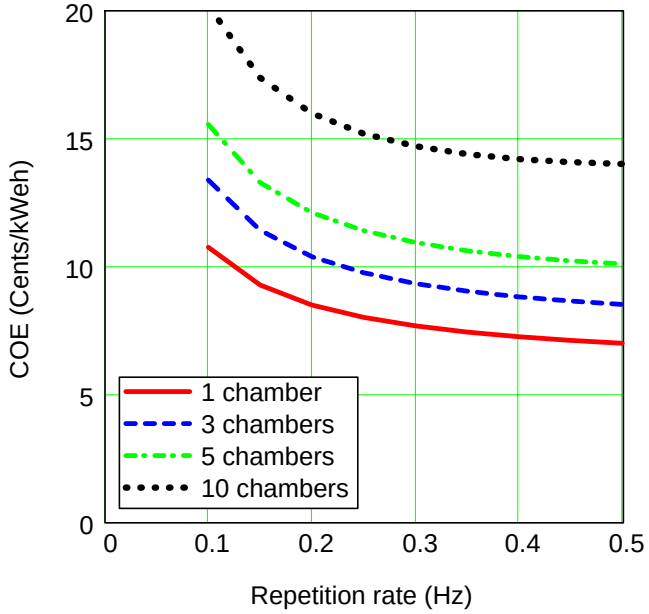

Calculate required rep-rate for fixed net power of plant

RRgv := 0 guess value

RRf(Ed, Nc, Pfix) := root(Pnet(Ed, RRgv)·Nc − Pfix, RRgv)

RRf(Eo, 1, Pfo) = 0.5

RRf(E10, 10, Pfo) = 0.101

Pfg := 100, 200 .. 1000 range of net powers for graph

Chamber rep-rate vs plant net power for various driver energies
Single chamber plant: Nc = 1.

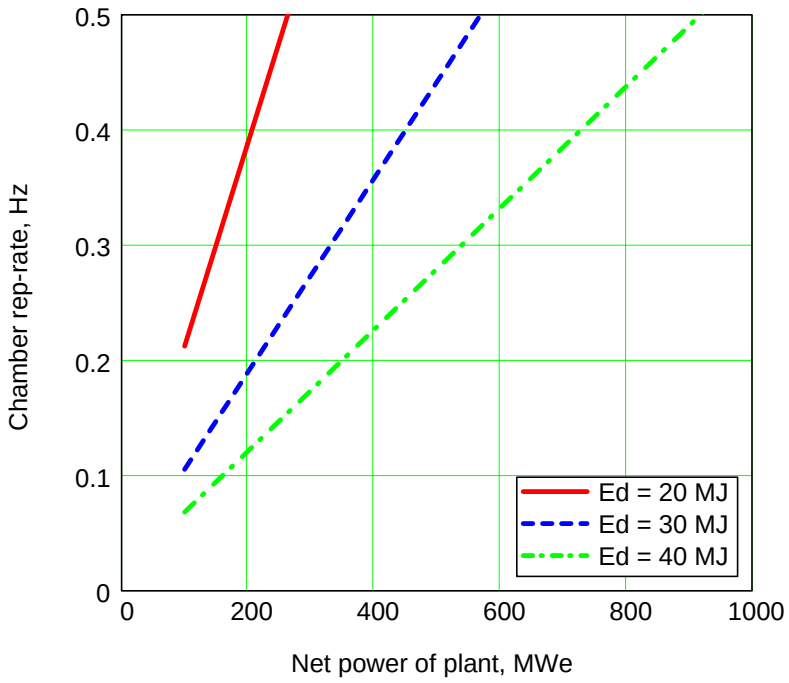

Chamber rep-rate vs plant net power for various driver energies
Two chamber plant: Nc = 2.

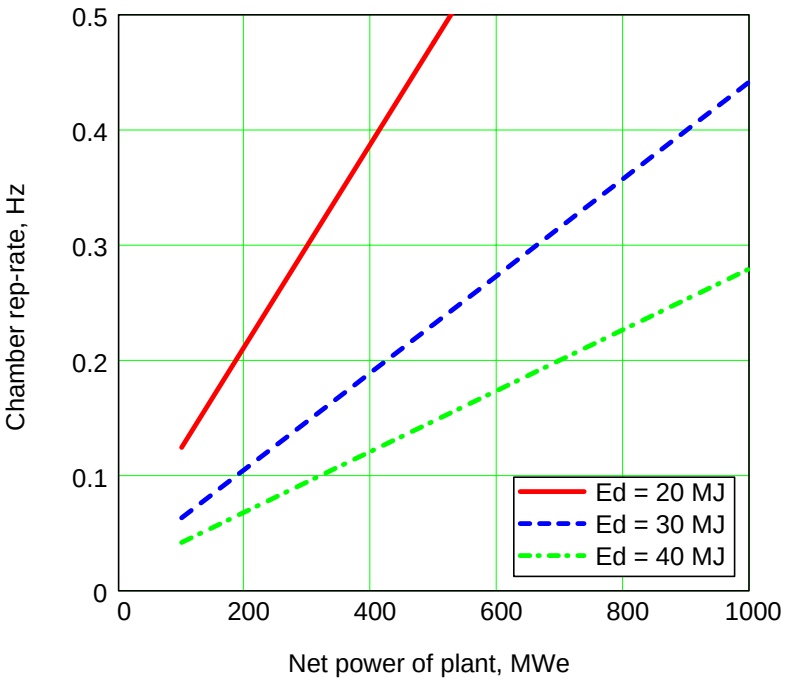

Chamber rep-rate vs plant net power for various driver energies
Five chamber plant: Nc = 5.

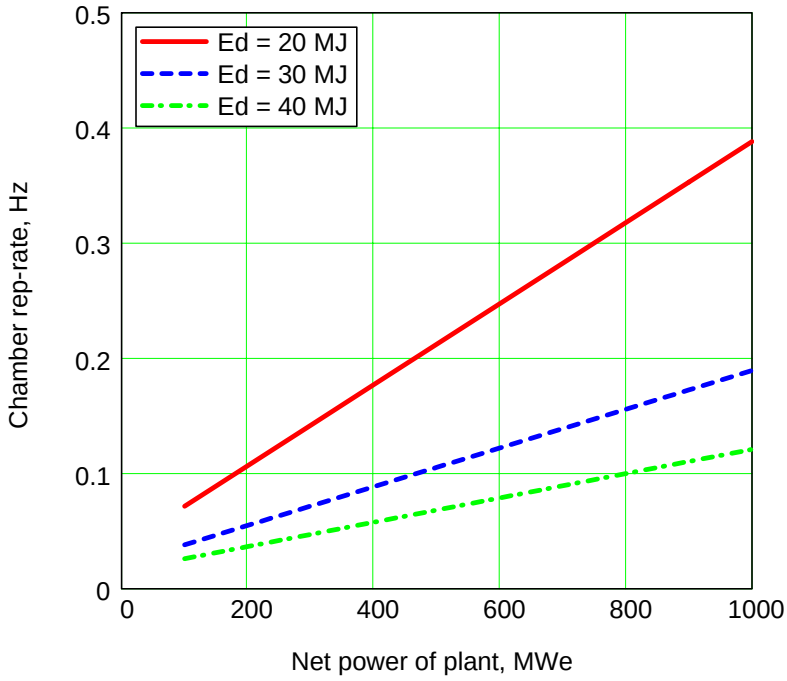

Edg := 13 , 14 .. 60

COE vs driver energy with rep-rate that gives constant 1000 MWe power for entire plant.

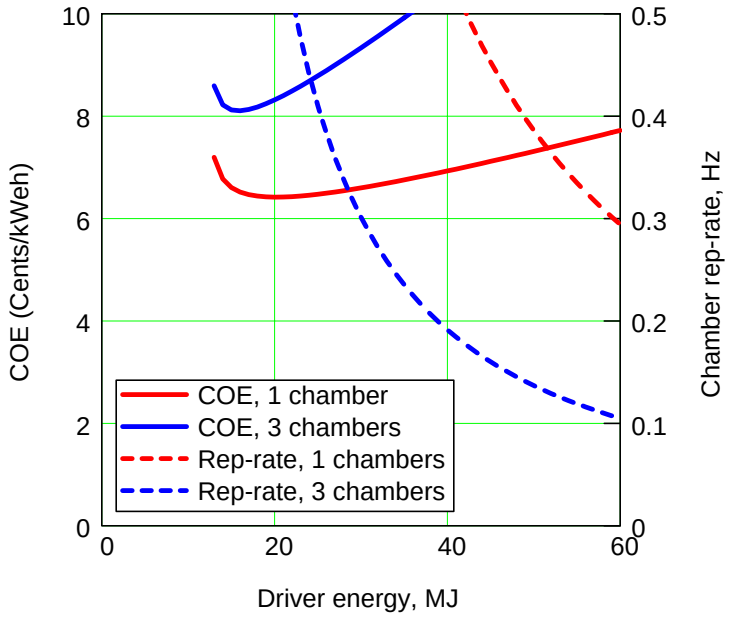

Z pinch IFE plants have minimum COE at E<20 MJ, but this corresponds to chamber rep-rates greater than 0.5 Hz (likely maximum based on replacing RTL after each shot) even for a 10 unit plant.

COE vs chamber rep-rate for various net powers (500, 1000 and 2000 MWe) for a single chamber plant

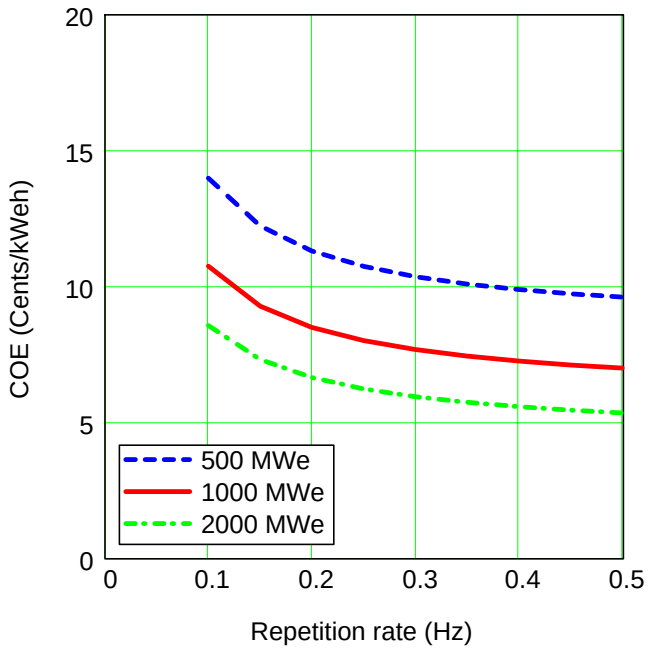

COE vs chamber rep-rate for various net powers (500, 1000 and 2000 MWe) for a two chamber plant

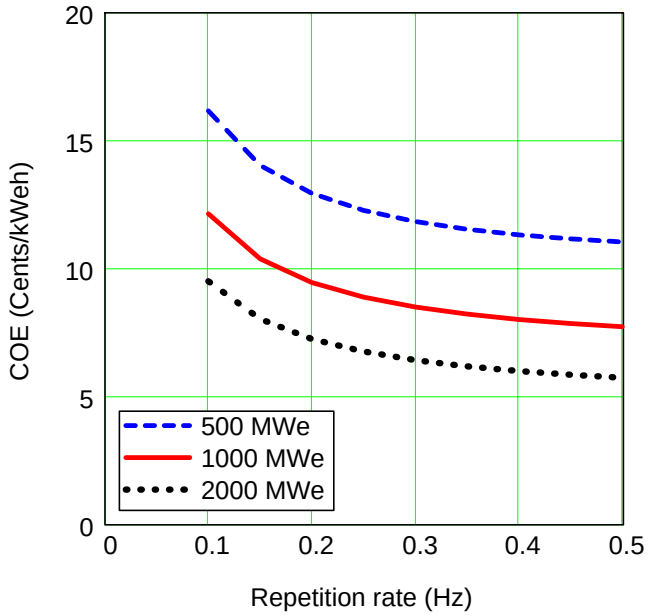

Results for max rep-rate of 0.1, 0.3 and 0.5 Hz are tabulated here for 1, 2 and 5 chambers per plant.

Range for number of chambers

$Nc_i :=$

1
2
5

RRmax = 0.1

Required driver energy and resulting COE for 1, 2 and 5 chamber plants with max rep-rate of **0.1 Hz per chamber**.

$Edf(0.1, Nc_i, Pfo) =$

127.4
80.4
45.5

$COE(Edf(0.1, Nc_i, Pfo), 0.1, Nc_i, UCdo) =$

10.8
12.1
15.6

RRmax = 0.3

Required driver energy and resulting COE for 1, 2 and 5 chamber plants with max rep-rate of **0.3 Hz per chamber**.

$Edf(0.3, Nc_i, Pfo) =$

59.2
38.2
22.9

$COE(Edf(0.3, Nc_i, Pfo), 0.3, Nc_i, UCdo) =$

7.7
8.5
10.9

RRmax = 0.5

Required driver energy and resulting COE for 1, 2 and 5 chamber plants with max rep-rate of **0.5 Hz per chamber**.

$Edf(0.5, Nc_i, Pfo) =$

42.2
27.8
17.8

$COE(Edf(0.5, Nc_i, Pfo), 0.5, Nc_i, UCdo) =$

7.0
7.7
10.1

As shown in the plots above, lowest COE correspond to fewest chambers and rep-rates as high as possible.

Appendix B

Additional Information Relevant to RTL and Chamber Design

B.1 Why have 10 to 20 Torr of inert gas in the chamber?

Inert gas, Xe or Kr is often suggested to protect walls from x rays. The gas absorbs the x rays and re-emits over a longer time. The longer x-ray pulse length allows conduction to reduce the peak surface temperature and hence reduces the peak stress. Liquid jets protect the walls from neutrons and at the same time from x rays. The inert gas is a non-condensable gas that interferes with condensation. We should avoid inert gas or minimize it. If we have no inert gas, avoiding the rush of gas up the transmission lines should make keeping them clean easier. The RTL inserter closes the MITL opening 1.5 ms after a shot and a slide valve keeps the MITL opening closed until the inserter returns to again protect the MITL from gas entry.

The ZIFE project continues to invoke gas in the chamber. Unless there is a feasible way to pump down the MITL and RTL interiors in the inter-shot time, the use of inert gas should be dropped.

B.2 Vapor Pressure of Flibe and Evaporation (Condensation) Rates

The vapor pressure and evaporation rates are calculated from the following equations and plotted in Fig. B.1 through B.4. (These were previously reported in FY05, but are included here for completeness.) The mass density ρ has been added since FY05 work and is shown in Fig. B.5.

$P(Pa)=e^{A-B/T}$

$$J = \frac{n\bar{v}}{4} = \frac{p}{(2\pi mkT)^{0.5}} = CT^{-0.5}e^{(A-B/T)}$$

$$n = \frac{p}{kT}$$

$$\rho = nm = \frac{mP}{kT}$$

Here, A = 26.59, B =25,390, C = 3.828×10^{23} for BeF_2 evaporation, k = 1.3807×10^{-23} J/K and m = 7.8058×10^{-26} kg. The flibe vapor pressure used was $\log_{10} P_{torr} = 9.424 - 11026.208/T(K)$ and was converted to pascals.[1,2] As seen in Fig. B.3, this latest estimate of vapor pressure (and therefore evaporation rates) is about a factor of three lower than previous estimates in the region of 500 °C but the same at the 1000 °C region.

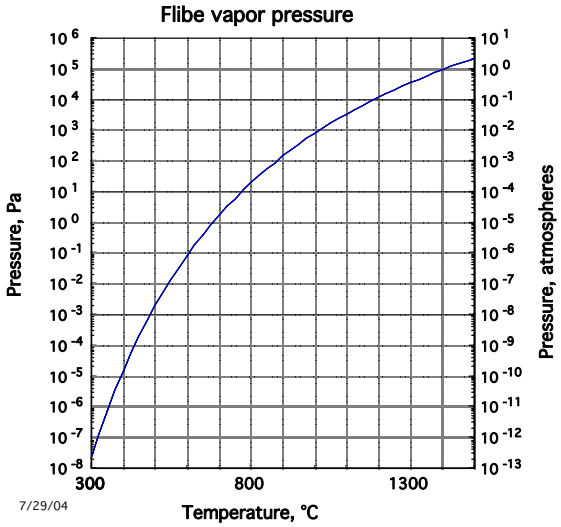

Figure B.1: Vapor pressure for flibe. To convert to units of Torr use P(Torr)=P(Pa)/133.3.

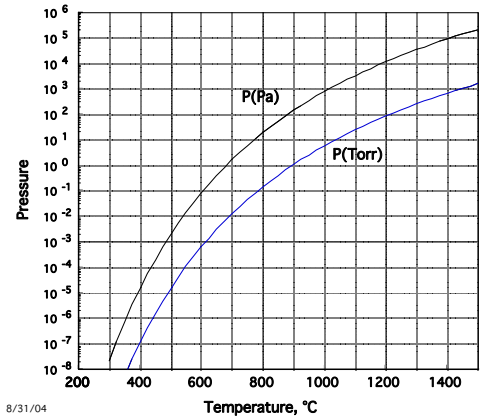

Figure B.2: Flibe vapor pressure in Pa and Torr.

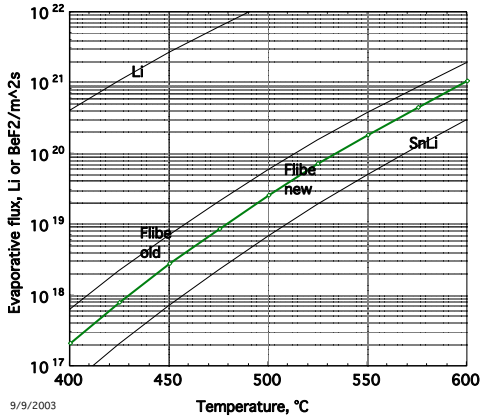

Figure B.3: Evaporation (and condensation) rates into vacuum for candidate liquids. At equilibrium $J_{evaporation} = J_{condensation}$.

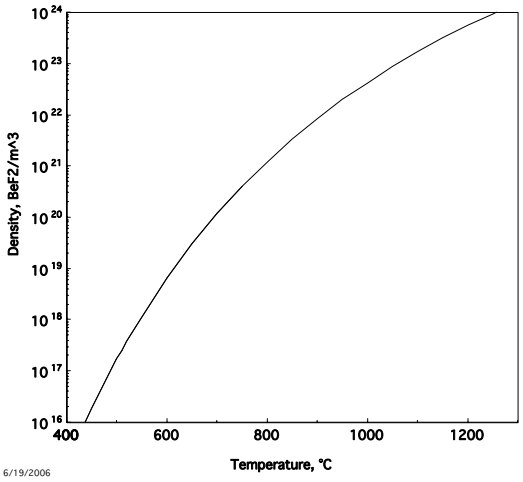

Figure B.4: Particle density versus temperature at equilibrium.

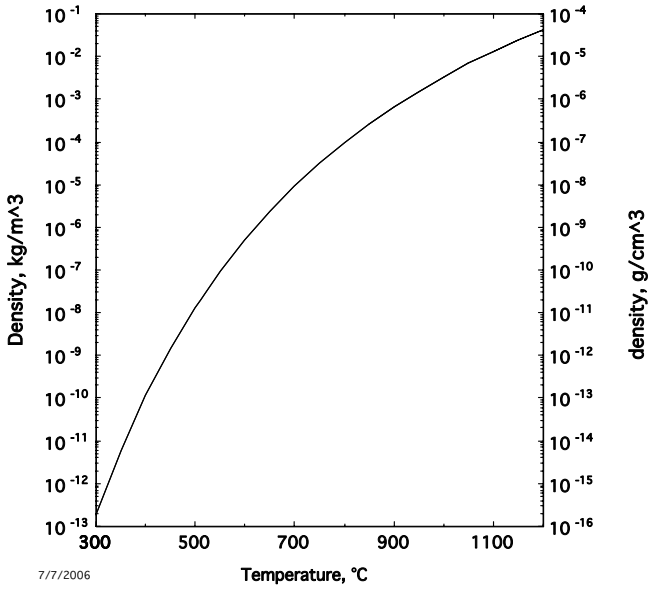

Figure B.5: Mass density versus temperature at equilibrium.

B.3 Alternatives to Tungsten Wires

The problem with tungsten wires is recovery from flibe. Tungsten will form finely divided solids in the salt. Although Remy Gallix at General Atomics has shown a chemical process to extract tungsten from flibe it must be costly including recycle and its feasibility is questionable. Alternatively, lead, bismuth or mercury could be considered. Perhaps other materials would work. Lead and bismuth are liquids and can be recovered by centrifuging. The problem is attack of metal surfaces. Also Bi results in ^{210}Po, which is a hazard and a waste disposal problem. Mercury is a solid at low temperatures but a vapor under operating conditions and evaporative separation is straightforward. The mercury can be recovered with ppm levels remaining. Corrosion at these low levels is probably negligible. Safety under accident conditions of course must be weighed but safety is enhanced by the low inventory of Hg. The FY05 report discusses the strength of cryogenic Hg wires.

B.4 Alternatives to Steel RTL

In the HYLIFE-CT we considered frozen flibe for a double conical coaxial transmission line of about 2.5-m length similar to the ZIFE transmission line. The inner surface could be coated with a conductor, for example lead or mercury to aid surface conduction. Recovery seems straightforward as opposed to recovery and reuse of steel.

B.5 When do we melt flibe?

In HYLIFE-II the energy deposited in the jets at 0.5 m radius is 250 J/g. The heat capacity is 2380 J/kg·K. Suppose frozen flibe were used at 60 °C. Flibe melts at 460 °C. A ΔT=400 K will cause melting. In HYLIFE-II the nearest jets increased in temperature by

$$\frac{250\times10^3\ J}{kg}\ \frac{kg\,K}{2380\ J}=105\ K\ .$$

Scaling to Z, this is $\frac{3}{0.35}105=900\ K$ at 0.5 m distance. At 0.75 m, the frozen flibe in Z will just melt. This means the RTL portions further away than 0.75 m will be blown apart as solid pieces. These pieces could be troublesome by erosion of impeller blades.

Shattered pieces of solid flibe will travel in the coolant for a time $\tau=\frac{x^2}{\alpha}$,

$$\alpha=\frac{k}{\rho c}=\frac{1W/mK}{2000kg/m^3\times2380J/kgK}=2\times10^{-7}\ m^2/s\ .$$

Two millimeter thick (1 mm radius) will travel for of order 5 s before melting, whereas 20-mm-thick pieces will travel in the coolant circuit for minutes. A typical time for the flibe to pass through pumps was about 10 s or less. The time to melt could be worked out more accurately, however it is not a simple problem.

B.6 Flibe Volume

Most of the flibe at any one time is in the piping system flowing to and from pumps, vacuum disengagers, and heat exchangers. Less than 10% is in the chamber at any one time. It follows that the volume will be insensitive to yield. In HYLIFE-II the volume estimated was approximately 1200 m^3.

$$V_{flibe}(m^3)=5.6\cdot P_{thermal}(MW)^{0.5}+310\cdot\frac{P_{thermal}(MW)}{1100\,MW}$$

The idea was that many of the components scale with square root of power, meaning larger units are utilize flibe better. The heat exchangers, however, will be built in approximately 1100 MW_{th} size, and higher power will add more units.

References for Appendix B

1. D. R. Olander, G. T. Fukuda, and C. F. Baes,, Jr., "Equilibrium pressure over BeF2/LiF (Flibe) molten mixtures," *Fusion Technology,* **41**, 141 (2002).
2. M. R. Zaghloul, D, D. Sze and A. R. Raffray, "Thermo-physical properties and equilibrium vapor-composition of lithium fluoride-beryllium fluoride ($2LiF/BeF_2$) molten salt," *Fusion Science and Technology,* **44,** 344-350 (2003).